Aus dem Zentrum Physiologie und Pathophysiologie
der Universität zu Köln
Institut für Vegetative Physiologie
Geschäftsführende Direktorin:
Universitätsprofessorin Dr. rer. nat. T. Korotkova

Role of age, sex, and telokin ablation on murine urethral smooth muscle contractility

Inaugural-Dissertation zur Erlangung der zahnärztlichen Doktorwürde
der Medizinischen Fakultät
der Universität zu Köln

vorgelegt von
Jens Jonas Jagdfeld
aus Frechen

promoviert am 11. Oktober 2024

Gedruckt mit Genehmigung der Medizinischen Fakultät der Universität zu Köln
2024

Dekan: Universitätsprofessor Dr. med. G. R. Fink
1. Gutachterin: Professorin Dr. med. G. Pfitzer
2. Gutachter: Privatdozent Dr. med. T. H. Kuru

Erklärung

Ich erkläre hiermit, dass ich die vorliegende Dissertationsschrift ohne unzulässige Hilfe Dritter und ohne Benutzung anderer als der angegebenen Hilfsmittel angefertigt habe; die aus fremden Quellen direkt oder indirekt übernommenen Gedanken sind als solche kenntlich gemacht.

Bei der Auswahl und Auswertung des Materials sowie bei der Herstellung des Manuskriptes habe ich Unterstützungsleistungen von folgenden Personen erhalten:

Frau Universitätsprofessor Dr. med. Gabriele Pfitzer

Weitere Personen waren an der Erstellung der vorliegenden Arbeit nicht beteiligt. Insbesondere habe ich nicht die Hilfe einer Promotionsberaterin/eines Promotionsberaters in Anspruch genommen. Dritte haben von mir weder unmittelbar noch mittelbar geldwerte Leistungen für Arbeiten erhalten, die im Zusammenhang mit dem Inhalt der vorgelegten Dissertationsschrift stehen.

Die Dissertationsschrift wurde von mir bisher weder im Inland noch im Ausland in gleicher oder ähnlicher Form einer anderen Prüfungsbehörde vorgelegt.

Die dieser Arbeit zugrundeliegenden Experimente wurden, soweit nicht anders angegeben, von mir selbst nach den entsprechenden Anweisungen von Prof. Dr. G. Pfitzer, Dr. L. Lubomirov und D. Metzler durchgeführt. A. Kahl hat alle Verfahren zur Herstellung der histologischen Präparate durchgeführt, einschließlich Einbettung, Mikropräparation, Färbung und Scannen der Proben, die ich ihr zur Verfügung gestellt habe. D. Metzler hat mir vorgewogene Portionen von Pulvern zur Verfügung gestellt, die bei der Herstellung von physiologischen Kochsalzlösungen verwendet wurden. Keine weiteren Personen waren an der intellektuellen Produktion dieser Arbeit beteiligt. Die Daten wurden von mir selbst mit der Software Graphpad Prism ausgewertet.

Erklärung zur guten wissenschaftlichen Praxis:

Ich erkläre hiermit, dass ich die Ordnung zur Sicherung guter wissenschaftlicher Praxis und zum Umgang mit wissenschaftlichem Fehlverhalten (Amtliche Mitteilung der Universität zu Köln AM 132/2020) der Universität zu Köln gelesen habe und verpflichte mich hiermit, die dort genannten Vorgaben bei allen wissenschaftlichen Tätigkeiten zu beachten und umzusetzen.

Köln, den 30.04.2024

Jens Jonas Jagdfeld

Danksagung

In erster Linie bin ich Frau Dr. Pfitzer für ihre unschätzbare Beratung, ihre unerschütterliche Unterstützung und ihr aufschlussreiches Feedback während meiner gesamten Promotionszeit zu großem Dank verpflichtet. Ihr Fachwissen, ihre Geduld und ihre Unterstützung waren für den erfolgreichen Abschluss dieser Arbeit von entscheidender Bedeutung.

Ich möchte auch Frau Metzler meinen herzlichen Dank für ihre unschätzbare Anleitung und Hilfestellung im Labor aussprechen. Ihre Expertise im Umgang mit Mäusen und ihre geduldige Unterweisung haben maßgeblich zu meiner Entwicklung praktischer Laborfertigkeiten beigetragen.

Mein herzlicher Dank gilt auch Dr. Lubomirov für die angenehme Zusammenarbeit im Labor, die Einweisung in das Laborequipment und die Software.

Für Bärbel

Table of Contents

Abbreviations

ACh	Acetylcholine
ANS	Autonomic nervous system
AR	Adrenergic receptor
ATP	Adenosine 5′-triphosphate
AVP	Vasopressin
CaM	Calmodulin
cAMP	Cyclic adenosine monophosphate
CaP	Calponin
cGMP	Cyclic guanosine monophosphate
CM	Caldesmon
CNS	Central nervous system
COPD	Chronic obstructive pulmonary disease
CRC	Concentration-response curve
DSM	Detrusor smooth muscle
EDTA	Ethylenediaminetetraacetic acid
EMLC	Essential myosin light chain
eNOS	Endothelial nitric oxide synthase
EUS	External urethral sphincter
F-actin	Filamentous actin
G-actin	Globular actin
GEF	Guanosine nucleotide exchange factor
GPCR	G-protein coupled receptor
ILK	Integrin linked kinase
iNOS	Inducible nitric oxide synthase
IP3	Inositol trisphosphate
IUS	Internal urethral sphincter
KO	Knock-out
L-NAME	N(gamma)-nitro-L-arginine methyl ester
LUTS	Lower urinary tract symptoms
MHC	Myosin heavy chain
MLC	Myosin light chain
MLCK	Myosin light chain kinase
MLCP	Myosin light chain phosphatase
MYPT1	Myosin phosphatase targeting subunit 1
NANC	Non adrenergic non cholinergic
NE	Noradrenaline
nNOS	Neuronal nitric oxide synthase
NO	Nitric oxide
NOS	Nitric oxide synthase
PE	Phenylephrine

P_i	Inorganic phosphate
PKC	Protein kinase C
PLC	Phospholipase C
PNS	Peripheral nervous system
PSS	Physiologic saline solution
RMLC	Regulatory myosin light chain
ROK	Rho-associated protein kinase
RT	Room temperature
sGC	Soluble guanylyl cyclase
SM	Smooth muscle
SR	Sarcoplasmic reticulum
TM	Tropomyosin
VOC	Voltage operated calcium channel
WT	Wild type

1. Zusammenfassung

Um die zwei Phasen der Tätigkeit des unteren Harntrakts, Befüllen und Leeren der Blase, zu steuern, gehen Urethra und Harnblase komplementäre Funktionen ein: Während der Füll-Phase erschlafft die Muskulatur der Blase, sie kann sich ausdehnen und dient als Reservoir für den Urin. Zeitgleich schließen die internen urethralen Sphinktere, um Harnkontinenz zu gewährleisten. Wird die Blase entleert, so kontrahiert die Blasenmuskulatur und die Sphinktere relaxieren, der Urin kann somit ausgeschieden werden. In einem höchst-komplexen Zusammenspiel verschiedener Signalkaskaden wird so das Ausscheiden von Urin reguliert. Dieses komplexe System ist anfällig für Fehler. Viele Menschen, vor allem ältere, leiden unter verschiedenen Funktionsstörungen des unteren Harntrakts, zusammengefasst unter dem Namen LUTS (lower urinary tract symptoms).

Einer der Akteure dieses Systems ist das 17 kDa Protein Telokin. Fehlen dieses Proteins beeinträchtigt die cGMP-induzierte Relaxation und erhöht die Kontraktionskraft. Als Modulator der glattmuskulären Relaxation reduziert es die Ca^{2+} Sensitivität. Zu den verschiedenen vorgeschlagenen Wirkungsmechanismen zählen Hemmung der MLCK (myosin light chain kinase) und gesteigerte Aktivität der MLCP (myosin light chain phosphatase) durch Telokin.

Durch unsere Arbeit mit Professor A. Somlyo standen unserem Institut telokin-defiziente Mäuse zur Verfügung. Diese Mäuse wiesen häufig massiv vergrößerte Blasen und Harnverhalt auf. Die daraus resultierenden Fragestellungen zur Rolle von Telokin in der Kontraktion sowie Relaxation der Urethra sollen in dieser Arbeit beleuchtet werden. Die Reaktion von urethralen Ring-Präparaten auf verschiedene kontrahierende sowie relaxierende Agonisten und elektrische Feldstimulation wurde mit Hilfe von Myographen erforscht. Mäuse für diese Experimente wiesen die Parameter Wildtyp oder Telokin KO (knock-out), weiblich oder männlich und jung oder alt auf.

In meinen Experimenten konnte ich zeigen, dass junge und alte KO Weibchen sowie alte KO Männchen eine signifikante Linksverschiebung der Dosis-Wirkungs-Kurve von AVP gegenüber WT Mäusen aufweisen. In jungen Männchen wurde kein signifikanter Unterschied zwischen telokin-defizienten und WT Mäusen als Reaktion auf AVP (Arginin-vasopressin), PE (Phenylephrin) oder KCl (Kaliumchlorid) sichtbar.

Die Relaxation von vorkontrahierten Urethrapräparaten war bei telokin-defizienten Weibchen, im Vergleich zu den Wildtypen, signifikant abgeschwächt in Reaktion auf einen NO-Donor sowie auf elektrische Feldstimulation. Männchen wiesen diesen Unterschied ebenfalls auf, jedoch nur bei Vorkontraktion der Urethras durch PE, nicht durch AVP.

Zusammengefasst konnte ich in dieser Dissertation erstmals zeigen, dass Telokindefizienz zu erhöhter Kontraktion und abgeschwächter Relaxation der Urethra von weiblichen Mäusen führt. Weiterführende Experimente sind notwendig, um dieses Thema weiter zu erforschen.

2. Introduction

2.1. Clinical Background

Modern medicine faces many challenges, the increasing life expectancy and thus an aging population certainly being one of them. Cardiovascular diseases, malignant neoplasms and chronic obstructive pulmonary disease (COPD) are classified as the leading contributors to disease burden in older people (Prince et al. 2015). However, there is another cluster of symptoms that correlates to widely encountered dysfunctions with concomitant reduction in quality of life. Lower urinary tract symptoms (LUTS) are very widespread among older people in western countries. According to a survey, over 70 % of people above the age of 40 experience some form of LUTS at least occasionally, with the severity and incidence increasing with age (Coyne et al. 2009). LUTS refers to a group of symptoms related to micturition. These can occur during the storage phase, during or after micturition (urination) and range from increased urination frequency to urinary incontinence or urinary retention.

The causes for these symptoms are numerous. In order to treat these diseases, it is important to understand the complex underlying physiological systems that regulate the processes of storage and voiding of urine.

2.2. The lower urinary tract

The urinary system experiences two phases, filling and voiding. During the filling phase, urine produced by the kidneys is transported to the bladder by the ureters. There the urine is collected and stored, expanding the bladder in the process. The bladder acts like a reservoir, preventing urine from leaking by relaxing the muscles of the bladder wall and contracting the circular muscles of the urethra. During voiding, the bladder contracts, the urethral muscles relax, allowing urine to flow out through the urethra in a process called urination. In adults, voiding is under voluntary control (Yang 2003).

2.2.1 The bladder

The bladder lies at the base of the pelvis. Macroscopically it can be divided into four distinct parts: The apex and the fundus refer to the anterosuperior and posteroinferior part of the bladder, respectively. The body comprises the large part between apex and fundus. The neck is located anteriorly of the fundus on the bladder floor and is the area where the bladder is connected to the urethra via the urethral opening (Shermadou et al. 2023). The ureters connect posterolaterally of the neck at the ureteric orifices. Together with the bladder outlet these ureteric orifices circumscribe a triangular region of the bladder called the trigone. During filling it contracts to keep the ureteric orifices open and the neck closed. It relaxes during micturition to ensure proper voiding and help prevent ureteric reflux (Fry et al. 2010).

The bladder wall consists of urothelium, three layers of smooth muscle and an outer adventitia. The urothelium is a kind of stratified epithelium with three distinct cell layers that lines the renal pelvis, ureters, bladder and proximal urethra (Dalghi et al. 2020). The smooth muscle layers are called detrusor muscle and include a medial layer with circular smooth muscle orientation, and an inner and outer, longitudinally arranged smooth muscle layer.

2.2.2. The urethra

The urethra is a hollow tube, connecting the bladder to the external surface of the body. It is sexually dimorphic and its anatomy differs between males and females. In males, it passes through the prostate and along the penis. In females, the urethra is shorter, passing through the perineal membrane and exiting in a gap between clitoris and vaginal opening (Ferreira et al. 2021).

The proximal urethra is continuous with the bladder, sharing the same structure of urothelium, lamina propria and smooth muscle. Distally however, the lining changes from the distinct urothelium to stratified squamous epithelium (Carlile et al. 1987, Holstein et al. 1991).

Continence is achieved through contraction of the urethra by two distinct sphincters, the external and internal urethral sphincter (EUS and IUS, respectively). The IUS is considered to be a continuation of the detrusor smooth muscle. It is located between the neck of the bladder and the proximal end of the urethra. It consists of an inner, mostly longitudinally aligned layer, and an outer, circular layer. Because it is made of smooth muscle it is not under voluntary control, but rather innervated by the autonomous nervous system. During the filling phase, sympathetic fibres maintain a tonic contraction. During voiding, parasympathetic fibres elicit a relaxation, allowing urine to travel through the urethra (Keller et al. 2018, Jung et al. 2012).

While passing through the deep perineal pouch, a region just above the peritoneal membrane, the urethra is surrounded by striated muscles in a circular arrangement. This structure is referred to as the EUS. Unlike the IUS it is under voluntary control, being innervated by the deep perineal branch of the pudendal nerve (Bolla et al. 2023).

2.3. Innervation of the lower urinary tract

The complementary function of detrusor smooth muscle, and internal and external urethral requires a high level of coordination, which depends on the interaction of the central nervous system (CNS) and the peripheral nervous system (PNS). The PNS consists of the somatic nervous system, which is responsible for voluntary movements, and the autonomic nervous system (ANS), which regulates unconscious functions and responses of the body. The two subsystems of the ANS, namely the sympathetic and parasympathetic nervous systems, work in an antagonistic fashion: While sympathetic innervation typically leads to heightened bodily awareness and physical capabilities, i.e. fight or flight response, the parasympathetic response

mainly aims to lower the blood pressure and heart rate and facilitates digestion, i.e. rest and digest. The fibres of each PNS-division exhibit differences in the pathways they follow and the neurotransmitters they use (Waxenbaum et al. 2023).

Somatic innervation is supplied by the pudendal nerve, which originates from the convergence of three rami from S2-S4. By releasing acetylcholine (ACh), which acts on nicotinic acetylcholine receptors of the motor end plate, it causes contraction of the EUS (Bortolini et al. 2014).

Also from S2-S4 exit neurons that form the pelvic nerve which provides parasympathetic innervation. After synapsing in either the pelvic or the intramural ganglia in the bladder, this nerve stimulates the DSM to contract during the voiding phase. Its neurotransmitter ACh acts on nicotinic receptors in the postganglionic fibres and on muscarinic receptors on bladder smooth muscle (Bortolini et al. 2014). Apart from the cholinergic stimulation, the bladder is susceptible to non-cholinergic stimulation by adenosine 5'-triphosphate (ATP), which acts on $P2X_1$ receptors (Vial et al. 2000). Apart from parasympathetic fibres, ATP is also released by bladder urothelium upon distension (Andersson 2015).

Finally, sympathetic stimulation with consequential urethral contraction and relaxation of the DSM during the storage phase is mediated by the hypogastric nerve, which originates from T10-T12. This nerve uses ACh in the ganglionic synapse and NE in the post-ganglionic fibres (Bortolini et al. 2014). Upon stimulation by noradrenaline (NE), α-AR in the urethra elicit contraction and β_3-receptors relaxation of the DSM (Michel et al. 2006, Yamaguchi 2002).

2.3.1. The receptors of the lower urinary tract

Upon activation, receptors trigger certain events in one of two ways, depending on their type: Ionotropic receptors such as the nicotinic ACh receptor open ion channels, as is the case in the skeletal muscles of the EUS (Lee et al. 2021). In contrast, metabotropic receptors, or G protein-coupled receptors (GPCR), that are present in smooth muscle, activate intracellular G proteins.

Adrenergic receptors (AR) are GPCR and respond to adrenaline or noradrenaline. They can be divided into two categories, α-and β-AR (Cicarelli et al. 2017). Generally speaking, the stimulation of α-AR leads to vasoconstriction and smooth muscle contraction, while the activation of β-AR results in increased myocardial contractility and smooth muscle relaxation. Of the six subtypes (α_{1A}, α_{1B}, α_{1D}, α_{2A}, α_{2B}, α_{2C}) only α_{1A} and α_{2A} appear to play a role in regulation of LUT (Bortolini et al. 2014). The α_{1a} receptors are present in the urethra and mediate contraction during the storage phase. α_{2A} receptors take a part in prejunctional inhibition of neurotransmitter release (Michel et al. 2006).

There are three subtypes of the β-AR, namely β_1, β_2 and β_3. Only β_2 and β_3 are expressed in the bladder, with β_3-adreno receptors being the primary mediator of relaxation (Takeda et al. 1999).

Cholinergic transmission involves the neurotransmitter ACh stimulating muscarinic and nicotinic receptors. Muscarinic receptors are GPCR. Of the 5 muscarinic receptor subtypes known (M1-M5), only M2 and M3 are expressed in DSM (Chess-Williams 2002). Although M2 is three to nine times more abundant, studies show that M3 is the decisive receptor for excitatory stimulation (Matsui et al. 2000). Nicotinic receptors are ionotropic receptors found on the motor endplate and ganglia of the ANS, that open cation channels upon activation (Unwin 2013).

Apart from these “classic” neurotransmitters of the ANS there are also non-adrenergic non-cholinergic (NANC) neurons that play a role in modulating smooth muscle tone in the LUT. They are present in the parasympathetic division of the pelvic nerve (Bortolini et al. 2014).

Purinergic transmission involves the use of ATP as a neurotransmitter. This hypothesis was first proposed in 1972 (Burnstock 1972), and was later augmented with the proposition that ATP acts as a cotransmitter in cholinergic and adrenergic transmission (Burnstock 1976). ATPs role as cotransmitter in most nerves is now widely accepted (Burnstock 2007). There are three types of receptors that ATP can activate. P1, P2Y and P2X, with the two former being GPCR and the latter being a ligand-gated ion channel. In the human bladder, parasympathetic fibres activate P2X receptors on the DSM during bladder voiding (Burnstock 2013).

In the 1990s, nitric oxide (NO) was recognized as a neurotransmitter that mediates NANC inhibitory responses (Rand 1992). NO seems to play a key role in urethral relaxation (Andersson et al. 1992). NO is synthesized from the amino acid L-arginine and molecular oxygen by nitric oxide synthase (NOS), which exists in 3 isoforms. Neuronal NOS (nNOS) is present in neurons of CNS, PNS and some other cell types. Its role is to centrally regulate blood pressure, smooth muscle relaxation and vasodilatation. Inducible NOS (iNOS) is involved in defence of bacteria and parasites. Endothelial NOS (eNOS) is most common in epithelial cells and regulates vasodilation (Förstermann et al. 2011). Further, eNOS and nNOS rely on the presence of Ca^{2+} for NO synthesis, and are also considered to be constitutively active (Winder et al. 2014). Urothelial cells can produce NO via all three isoforms, and various disorders can heavily alter their expression levels (Sancho et al. 2014).

2.4. Smooth muscle

With the exception of the heart, smooth muscle tissue is present in the walls of all internal organs and blood vessels. It regulates blood pressure, modulates the resistance in the airways and is essential in the gastrointestinal and urogenital systems. Although the fundamental mechanism of muscle contraction is the same for both smooth and skeletal muscle, i.e. sliding

filament theory involving thick and thin myofilaments, smooth muscle differs in many significant key aspects from their striated counterparts (Pfitzer 2014).

Skeletal muscles exhibit distinct striations under polarized light microscopy, which is the reason it is also called striated muscle. These eponymous striations stem from the highly organized repetition of the fundamental contractile unit, the sarcomere. In the sarcomere the dark A-bands, containing both thick and thin filaments, alternate with the light I-bands, which only contain the thin filaments (Shadrin et al. 2016).

Smooth muscle cells lack these striations as their filaments are not as regularly aligned. The cells are fusiform and have a centrally located nucleus. Smooth muscle tissue can be classified in various ways:

1) By the duration of contraction: Phasic smooth muscles enable the peristalsis in the gastrointestinal tract, while tonic smooth muscles are present in sphincters.

2) By the way of innervation: SM cells of the single-unit-type are electrically linked via gap junctions and form a functional syncytium. This type of SM is spontaneously active due to the presence of pacemaker cells. The detrusor is a typical example of a single-unit SM. In contrast, the multi-unit-type of smooth muscle shows no spontaneous activity and the cells contract independently from one another.

3) By their proliferation rate: While adult smooth muscle is of the contractile phenotype, the proliferative type is mostly present during embryonic development (Pfitzer 2014).

The myofilaments form a crosslinked network. The thin filaments are obliquely arranged and are connected to the cell wall by dense bands, and within the cell by dense bodies. Both contain the protein alpha-actinin, an actin-binding protein, present also in the Z-discs of striated muscle, indicating that they are analogues of Z-discs. Thick filaments are surrounded by the thin filaments. This arrangement mimics the sarcomere in striated muscles and is referred to as mini-sarcomere (Somlyo et al. 2012). In smooth muscle tissue, the thin filaments outnumber the thick filaments in a 13:1 ratio, a stark difference to the 6:1 ratio in striated muscle (Brandes et al. 2019).

2.4.1. Myofilaments of the contractile system

2.4.1.1. Actin

The thin filaments are comprised of filamentous actin (F-actin) and actin associated proteins. F-actin is formed by polymerization of globular (G-) actin monomers into a two-stranded, helical filament. Along the groove lie two long fibrous proteins tropomyosin (TM) and caldesmon (CM) as well as calponin (CaP). Modulation of the contractile mechanism is attributed to these proteins (Somlyo et al. 2012).

In striated muscles, the troponin-C of the heterotrimeric troponin complex acts as the Ca^{2+} sensor. In smooth muscle, in which troponin is not expressed, the cytoplasmic protein

calmodulin is the Ca^{2+}-sensor. Calmodulin is a dumbbell shaped molecule, whose globular ends can each bind two Ca^{2+} ions with high affinity (Pfitzer 2014).

2.4.1.2. Myosin

Every thick filament is made up of hundreds of myosin molecules in a side-polar arrangement. A myosin molecule consists of two myosin heavy chains (MHC) and four myosin light chains (MLC). The MHC typically have an N-terminal head domain, a C-terminal tail domain and a neck domain connecting the two. The globular head domain contains the catalytic site for ATP-hydrolysis and a binding site for actin, the tail domain is an α-coil and facilitates association of myosin molecules to antiparallelly oriented dimers, which then assemble into filaments (Pfitzer 2014). The four light chains, that are located at the neck domain, can be further subdivided. Each MHC binds one essential myosin light chain (EMLC) and one regulatory myosin light chain (RMLC), the latter of which capable of being reversibly phosphorylated. The total amount of myosin in SM is ~5 fold less compared to skeletal muscle. Nevertheless, SM is capable of generating equivalent maximum force/myocyte cross-section. This is due to the longer length of SM myosin compared to striated muscle as well as the side polar and antiparallel arrangement (Ashton et al. 1975, Murphy et al. 1974).

2.4.1.3. Intermediate filaments

Intermediate filaments mostly contain the proteins vimentin and desmin. They connect dense bands and dense bodies, binding sites for actin filaments and the equivalent of Z-discs, to each other, forming a network that provides mechanical integrity to the cell and play a role in smooth muscle force development (Wang et al. 2006, Tang 2008).

2.5. The contractile mechanism in smooth muscle

Due to the side polar arrangement of the myosin filaments and their length, which is larger than that of striated muscles, smooth muscle tissue can be passively stretched to a significantly higher degree compared to striated muscle, without forfeiting the ability of active contraction. This is especially important for organs with a reservoir function like the urinary bladder and the stomach (Pfitzer 2014).

2.5.1. Cross-bridge cycling in smooth muscle

Contraction in smooth muscle is, like in striated muscle, based upon the sliding filament mechanism. During contraction as well as passive stretching, myosin filaments glide along actin filaments without shortening the lengths of the individual filaments (Pfitzer 2014). Active contraction involves shortening of the mini sarcomeres due to a process called cross-bridge cycling which is driven by the hydrolysis of ATP. By binding to myosin heads, ATP forces the

myosin head to detach from actin. ATP is then hydrolysed by the myosin ATPase into ADP and phosphate (P_i). This allows the myosin head to bind to actin. The available energy from dissipating the free inorganic phosphate P_i is used in tilting of the myosin head, causing contraction. The sarcomere remains in this force generating arrangement until ADP disassociates from myosin, allowing a new ATP molecule to bind and starting the cycle over. In smooth muscle tissue, ADP disassociates from myosin 100-1000-fold slower than in striated muscle, presumably because of the higher affinity of smooth muscle myosin for ADP. This leads to a much slower contraction speed and very high efficiency of force generation in smooth muscle tissue. In fact, ATP use per force/cross-section area is 100-500-fold less than in striated muscle (VanBuren et al. 1994). Smooth muscle tissue is capable of additionally lowering its energy turnover: In a state termed “latch”, smooth muscle tissue is capable of holding the cross-bridge for a longer period of time in the force-generating state, drastically lowering ATP and O_2 consumption (Hai et al. 1988).

A prerequisite for the activation of the cross-bridge cycle is the phosphorylation of the RMLC at serine 19. Without this phosphorylation, one myosin head attaches itself to the other, resulting in both heads being incapable of binding to actin (Pfitzer 2014). Phosphorylation of RMLC at serine 19 causes a conformational change, disentangling the myosin heads and freeing them up to start the cross-bridge cycle. The degree of RMLC phosphorylation is determined by the opposing enzymes, myosin light chain kinase (MLCK) and myosin light chain phosphatase (MLCP). MLCP is constitutively active while MLCK is auto-inhibited, requiring binding of Ca^{2+}-calmodulin to the regulatory domain of MLCK to activate the enzyme (see chapter 2.5.3).

2.5.2. Excitation-contraction-coupling

The initiation of the contractile process in smooth muscle can be prompted by various stimuli, including electrical, mechanical and chemical signals. The regulatory mechanisms in play are very complex and overlap, forming a network of contractile and relaxing stimuli, the balance of which determines smooth muscle tone. As a result, SM are almost never maximally contracted or relaxed (Pfitzer 2014).

2.5.2.1. Electrical stimulation

Like in striated muscle, eliciting a contraction in SM involves the depolarisation of the cell membrane, which causes voltage operated calcium channels (VOC) to open. In phasic smooth muscle, like the bladder detrusor, depolarization can occur spontaneously: Special pacemaker cells (Cajal cells) trigger local depolarisations, which propagate via gap junctions to neighbouring muscle cells and can initiate an action potential (spikes). The high extracellular Ca^{2+} concentrations of 1,5 mmol/l compared to the very low cytosolic concentration in SM of

0,1 µmol/l, together with the resting potential of the SM cell membrane of 40 – 70 mV, results in a very high electromechanical gradient for Ca^{2+}. This enables a very rapid influx of Ca^{2+} ions after opening of VOCs (Pfitzer 2014).

2.5.2.2. Mechanical stimulation

VOC on the membrane of SM cells can also be opened by stretching of the cells. In what is known as the myogenic tone, pressure-sensitive non-selective cation channels open in response to stretching of the sarcolemma, causing a depolarisation and, in turn, opening of the VOC (Pfitzer 2014). While such channels have not yet been detected in urethral tissues, the stretch-sensitive TRPV4-channel was reported in urothelial cells of the bladder (Wu et al. 2020).

2.5.2.3. Chemical stimulation

Contraction of SM can be elicited by neurotransmitters and hormones. They can cause an influx of Ca^{2+} by binding to receptor operated calcium channels (ROC) and, by activation of G_q-coupled receptors, they trigger the formation of IP_3 from PIP_3, which releases Ca^{2+} from the sarcoplasmic reticulum into the cytosol. Contraction of both the internal and the external urethral sphincters is mediated by chemical stimulation (Pfitzer 2014).

2.5.3. Calcium-dependent contraction

Contraction in SM typically requires a rise in intracellular calcium concentration. Due to mechanical, electrical or chemical stimulation, Ca^{2+} ions enter the cytoplasm from the extracellular space via opening of ion channels as well as from the sarcoplasmic reticulum (SR) upon activation of the inositol triphosphate receptor (IP_3R), a downstream target of $G_{q/11}$-IP_3 (Webb 2003). At concentrations above ~10^{-7} mol/l Ca^{2+} binds to the intracellular protein calmodulin (CM). This $(Ca^{2+})_4$-calmodulin-complex binds to the autoinhibitory domain of MLCK, causing a conformational change and unblocking the catalytic domain. This allows the $(Ca^{2+})_4$-calmodulin-MLCK-holoenzyme-complex to bind to, and phosphorylate, RMLC (Figure 1).

MLCK is encoded by the *mylk1* gene and occurs in three isoforms, which appear to have largely redundant functions. The short 130 kDa isoform is the primary isoform expressed in smooth muscle. MLCK is an elongated protein with an N-terminal binding site for actin and a C-terminal binding site for myosin. Located C-terminally of the catalytic domain is the autoinhibitory domain, which is a pseudosubstrate for RMLC. At low intracellular Ca^{2+} concentrations (<10^{-7} mol/l) it shields the catalytic domain of MLCK, prohibiting it from binding to myosin (Pfitzer 2014).

A drop in Ca^{2+} concentration to below 10^{-7} mol/l results in the disassociation of the $(Ca^{2+})_4$-calmodulin-MLCK-holoenzyme-complex, but not yet in relaxation. The cross-bridge cycle continues as long as the RMLC is phosphorylated. Only after dephosphorylation of the RMLC by MLCP is the inhibitory myosin head conformation restored and relaxation occurs (Webb 2003).

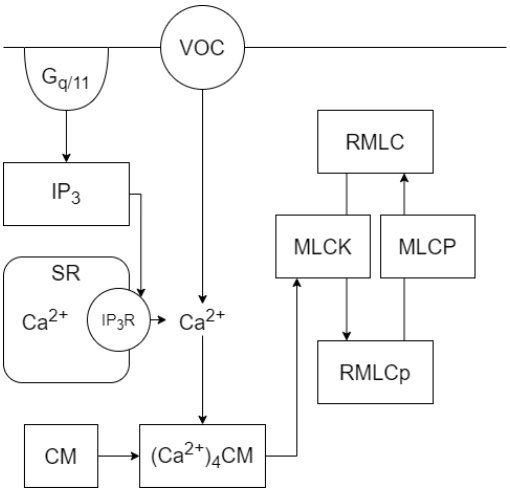

Figure 1: Scheme of the calcium-dependent phosphorylation of RMLC in smooth muscle
Simplified schematic representation of contraction in smooth muscle cells upon influx of calcium. VOC: voltage operated calcium channel, IP_3: inositol triphosphate, IP_3R: inositol triphosphate receptor, SR: sarcoplasmic reticulum, CM: Calmodulin, RMLC/RMLCp: regulatory myosin light chain unphosphorylated and phosphorylated, respectively, MLCK: myosin light chain kinase, MLCP: myosin light chain phosphatase

Relaxation of smooth muscle can occur passively and actively. Smooth muscle relaxes passively after the excitatory stimulation ceases and the Ca^{2+} levels revert back to normal and RMLC are dephosphorylated. Active relaxation is mediated by certain hormones and neurotransmitters that increase cyclic AMP and cyclic GMP concentrations in the smooth muscle cells, which then lead to a decrease in the Ca^{2+} concentration and increase in the MLCP activity (Webb 2003).

2.5.4. Calcium-independent modulation of myosin phosphorylation

The $[Ca^2]_i$ and thus the ratio of MLCK/MLCP activity constitutes the number of phosphorylated RMLC and in turn the contractile strength. However, certain mediators and pathways exist that influence the degree RMLC phosphorylation at a constant $[Ca^2]_i$, shifting the balance either toward RMLC phosphorylation (Ca^{2+} sensitization) or RMLC dephosphorylation (Ca^{2+} desensitization) (Webb 2003).

2.5.4.1. Calcium sensitization

Calcium sensitization relies on G-protein induced inhibition of MLCP. MLCP is a trimeric complex, consisting of the 110 kDa regulatory subunit (myosin phosphatase targeting subunit, MYPT), the 38 kDa catalytic subunit PP1 and the third subunit M20, with as of yet unknown function. The regulatory subunit MYPT harbours several phosphorylation sites, including Thr696 and Thr853, which are phosphorylated by a number of protein kinases causing inhibition of MLCP activity (Pfitzer 2001).

One of these kinases is Rho-associated protein kinase (ROK), which is a downstream target of $G_{12/13}$-RhoA signalling. It phosphorylates Thr696 and Thr853, thereby inhibiting MLCP. $G_{12/13}$ activates guanine nucleotide exchange factors (GEFs), causing transformation of inactive, GDP-bound RhoA into active, GTP-bound RhoA. After translocating towards the cell membrane, RhoA activates ROK (Pütz et al. 2009).

After stimulation, $G_{q/11}$ activates phospholipase C (PLC), which activates diacylglycerol (DAG). DAG in turn activates protein kinase C (PKC), which facilitates the phosphorylation of the protein kinase C potentiated inhibitor (CPI-17). After phosphorylation, CPI-17 is a potent MLCP inhibitor, facilitating phosphorylation of RMLC (Pfitzer 2001).

Although the influx of Ca^{2+} ions from ROC is relatively low compared to VOCs, contractions elicited via stimulation by neurotransmitters are no less potent than those caused by electromechanical coupling. Through G-protein facilitated calcium sensitization, even a minimal rise in intracellular Ca^{2+} concentration can cause a contraction (Pfitzer 2014).

2.5.4.2. Calcium desensitization

Opposing the ROK and PKC pathways are mechanisms, which increase or disinhibit MLCP activity by impeding its inhibition by ROK. Nitric oxide (NO) activates guanylyl cyclase (GC), which raises the levels of intracellular cyclic guanosine monophosphate (cGMP). This second messenger molecule in turn activates protein kinase G (PKG), which directly interferes with RhoA signalling. Furthermore, it phosphorylates MYPT at Ser-965 without affecting its functional ability but prohibiting further inhibitory phosphorylation at Thr-696 (Pütz et al. 2009, Wirth et al. 2012). In addition, it interferes with the inhibitory phosphorylation of MYPT by CPI-17 by activation of protein phosphatase 2a (PP2a), which promotes dephosphorylation of CPI-17 (Vetterkind et al. 2012).

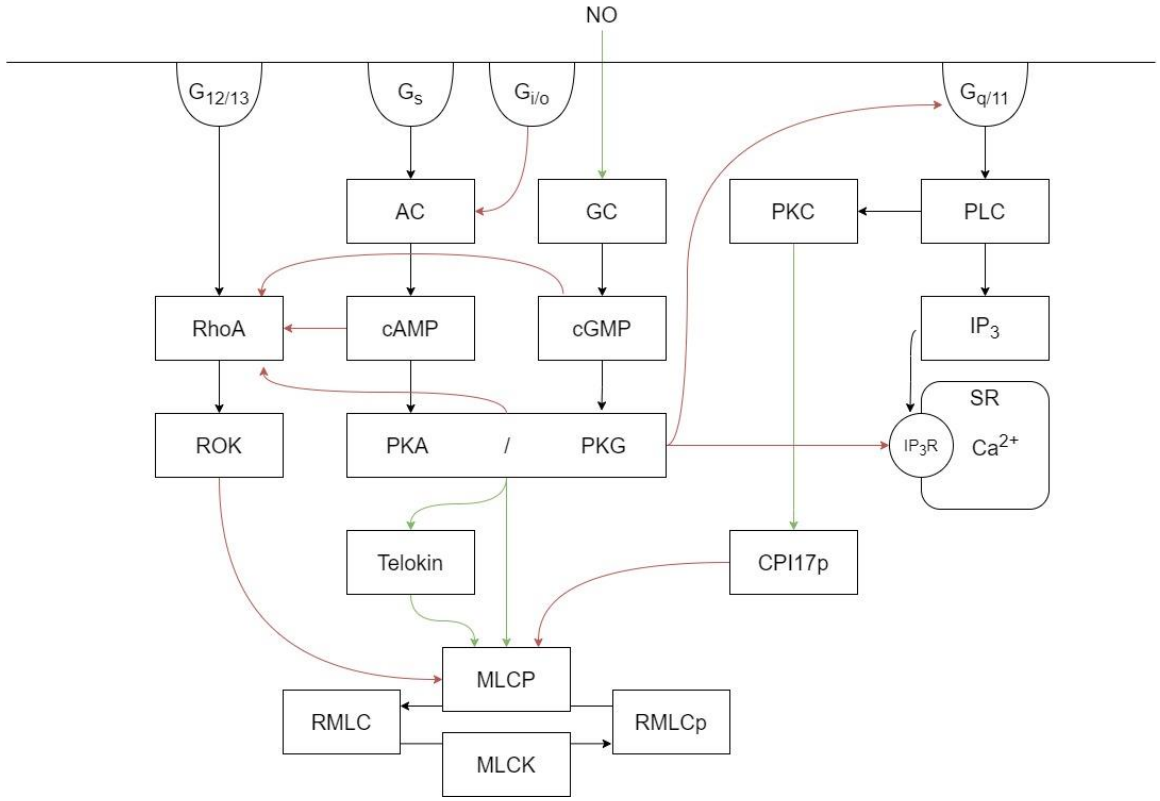

Figure 2: Schematic of GPCR-mediated modulation of RMLC phosphorylation in smooth muscle
Simplified illustration of pathways of GPCR and their influence on RMLC phosphorylation and, hence, muscle contraction. AC: adenylyl cyclase, cAMP: cyclic adenosine monophosphate, RhoA: Ras homolog family member A, ROK: Rho associated kinase, PKA/PKG: Protein kinase A/G, CPI17p: phosphorylated form of protein kinase C potentiated inhibitor, RMLC/RMLCp: (phosphorylated) regulatory myosin light chain, MLCP: myosin light chain phosphatase, MLCK: myosin light chain kinase, PLC: phospholipase C, PKC: protein kinase C, IP_3: Inositol triphosphate, IP_3R: Inositol triphosphate receptor, SR: sarcoplasmic reticulum. Red arrows illustrate attenuation, green arrows illustrate enhancing.

Stimulation of G_s induces activation of adenylyl cyclase, a membrane bound enzyme that catalyses the formation of ATP to cyclic adenosine monophosphate (cAMP), another second messenger, which exerts its action through activation of PKA. Like PKG, PKA inhibits the activation of the ROK cascade (Wirth et al. 2012).

Furthermore, both PKA and PKG phosphorylate telokin, a small acidic protein, which is thought to promote relaxation by increasing MLCP activity (Khromov et al. 2012; see chapter 2.5.5).

2.5.5. Telokin

Telokin is a 17 kDa acidic protein, which is specific to SM. First described in 1989 (Ito et al. 1989), it was later discovered to be identical with the C-terminus of MLCK. Like MLCK, it is encoded by the *mylk1* gene and is expressed abundantly in phasic SM of the intestinal and urinary tracts. Telokin lacks MLCKs binding sites for calmodulin, as well as its catalytic domain. It can bind to the S1/S2 region of unphosphorylated myosin. N-terminally it harbours several phosphorylation sites: A PKA/PKG site at Ser-13 and a mitogen-activated protein kinase (MAPK) site at Ser-19 (Wu et al. 1998).

Telokins physiological function in vivo remains unclear. In a telokin-deficient mouse model, lack of telokin impaired cGMP mediated ileal smooth muscle relaxation (Khromov et al. 2012) and increased resting tone of gastric smooth muscle (An et al 2015). Its role in the smooth muscle of the lower urinary tract has not yet been explored. In vitro telokin decreases Ca^{2+}-sensitivity and various hypotheses exist that aim to explain by which mechanism telokin procures its relaxing effect.

Somlyo et al proposed that telokin induces an increase in MLCP activity, based on the findings, that telokin increased the rate of dephosphorylation of the RMLC (Khromov et al. 2006, Khromov et al. 2012). The researchers also observed an augmented relaxing effect of telokin when phosphorylated at Ser-13 by PKA/PKG (Wu et al. 1998).

There is also well-established evidence for the hypothesis of telokin decreasing the rate of phosphorylation of RMLCK by MLCK. Based on the finding, that telokin only attenuates K_m but not V_{max}, a role of telokin as a competitive antagonist of MLCK for the S1-S2 binding site on myosin was proposed in 1997. Thus, by binding to myosin, it shields the nearby RMLC from phosphorylation by MLCK and also by non-canonical Ca^{2+}-independent MLC-kinases, thereby inhibiting contraction (Sherbakova et al. 2010).

Through our collaboration with Professor Avril Somlyo, our institute had access to a Bl6 telokin$^{-/-}$ (TKO) strain of mice. In prior studies conducted with these TKO mice, our researchers observed, that (i) some aged mice exhibited a dilated bladder as well as urinary retention and (ii) the TKO strain seemed to be more often affected than wild type (WT) mice. Consequently, the question of telokins role in urethral contraction and relaxation comes to mind. In previous studies the regulation of force and relaxation of murine urethra has been assessed both functionally and immunohistochemically in regards to NO-sensitive guanylyl cyclase and PKG, which are upstream of telokin (Lies et al. 2013). The impaired relaxation of urethra and its internal sphincter in telokin deficient mice has not been studied

Figure 3: A severely enlarged bladder of a ~24-month-old female TKO mouse.
Enlarged bladders are a common sight in older TKO mice. The bladder of the pictured specimen had a dry weight of 280 mg, or 0,74 % of the bodyweight, and contained 8,5 ml of urine. The diameter was ~26 mm.

Source: Photo by Jens Jagdfeld

2.6. The objective of the present study

In this study, I tested the following two hypotheses:

1. Contraction of urethra ex vivo to two agonists, vasopressin and phenylephrine, is augmented in telokin$^{-/-}$ mice.
2. NO- and EFS-mediated relaxation of urethra ex vivo is impaired in telokin$^{-/-}$ mice.

Since sex and age affect urethral function I performed these investigations in young and aged female and male mice.

3. Materials and Methods

3.1. Animal origin

The telokin$^{-/-}$ founder mice were obtained from Professor A. Somlyo, University of Virginia, and were backcrossed into the C57BL/6N background (Khromov et al. 2006). The C57BL/6N WT mice were obtained from Charles River. They were bred and housed in the Center for Molecular Medicine Cologne in standard mouse cages with wood chippings and paper tissues as nesting material at constant temperature and humidity levels with a 12h day/night cycle. They received nitrosamine deficient maintenance diet in dry pellet form by altromin (https://altromin.com/products/standarddiets/rats/1320) and water ad libitum. The animals were sacrificed at age 17,2±3,2 weeks or 108±8,7 weeks (median ± SD) quickly and painlessly by cervical dislocation, in accordance with the legislation (AZ8.87-50.10.47.09 and 84-02.05.20.12.147, Tierschutzgesetz & Tierschutz-Versuchstierverordnung). A total of 243 animals were used.

3.2. Physiologic saline solution

Force recording was carried out in physiologic saline solution (PSS), which was freshly prepared every day. The compounds were dissolved in water to 80 % of the final volume and stirred for a minimum of 30 minutes, after which $CaCl_2$ as stock solution was added drop by drop to pre-empt calcium phosphate salt precipitation. The pH was adjusted to 7,1 at room temperature (RT, 22 °C) using 1 M HCl. The PSS was heated to 37 °C using a water bath and bubbled with carbogen (95 % O_2, 5 % CO_2) at a pH of 7.4. Before commencing the force recording experiments, the pH was measured and adjusted to 7,4 at 37 °C. For studying potassium-induced contractions, a PSS high in potassium was used, in which the NaCl was replaced with KCl in equimolar concentration (K-PSS, Table 1). For dissection a PSS without glucose was prepared and adjusted to pH 7,4 at RT (Table 1).

	Dissection PSS	**PSS**	**125mM K-PSS**
NaCl	130	130	10
KCl	4,7	4,7	125
KH_2PO_4	1,18	1,18	1,18
$MgSO_4$ $7H_2O$	1,17	1,17	1,17
$NaHCO_3$	14,9	14,9	14,9
Glucose	-	5,5	5,5
EGTA	0,026	0,026	0,026
$CaCl_2$	1,6	1,6	1,6
pH	7,4	7,4	7,4
temperature	22 °C	37 °C	37 °C

Table 1: Physiologic saline solutions
Composition of the different physiologic saline solutions used. All concentrations are given in mM.

3.3. Preparation of urethral smooth muscle

The animals were sacrificed by cervical dislocation. A priorly weighed paper towel was used to capture and measure eventual urine loss. The mice were weighed and then fixed on a preparation board in supine position by their extremities. The skin of the abdomen was cut transversely and opened by pulling on the adjacent skin in cranial and caudal direction. The abdominal muscles were cut open. Using a syringe, urine was taken from the bladder and measured. In females, the bladder was lifted up and carefully separated from the vagina wall with a pair of fine scissors. The urethra was cut off distally enough to ensure a sufficient length of the preparation. The extracted tissues were transferred into a preparation dish containing RT dissection PSS. Using a microscope and fine preparation tools, fat and connective tissue were trimmed from the urethra and separated from the bladder neck. The remaining urethra was cut so to obtain two ~1mm long ring preparations.

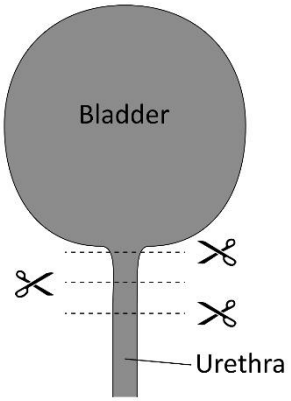

Figure 4: Dissection of urethral ring preparations
The bladder and distal end of the urethra were pinned down onto Sylgard coated dishes. Using fine scissors, a section of urethra was cut free approximately 1 mm in length. The section was to be as proximal as possible, to ensure (i) good comparability between preparations and (ii) enough distance from the striated muscles of the external urethral sphincter.

In males, the urethra was cut distally of the ventral prostate and the ducti deferentes were severed. Lifting the bladder up and using a large pair of scissors, the bladder, ventral prostate and urethra were cut free. The extracted tissues were transferred into a preparation dish containing dissection PSS. Fat and connective tissue were trimmed from the urethra and the ventral prostate. Two ~ 1mm long sections of urethra were cut free from the preparation very proximally to the bladder (Figure 4).

The bladder was transported onto a priorly weighed paper towel and squeezed empty, capturing and measuring eventual residual urine. The empty bladder was then dabbed dry and weighed.

3.4. Functional assays

3.4.1. Force recording

The force was recorded using the Myograph System 610A by Danish Myo Technology (DMT). This system allowed using four myograph chamber units simultaneously (Figure 5)

Each individual chamber unit contained a central chamber made of stainless steel. When connecting the chamber units to the interface, the system featured individually controlled gas inflow and suction as well as heating. The urethral ring preparation was suspended by two wires, which were attached to the tissue supports, or jaws. One jaw was connected to a force transducer and the other one to a micrometre.

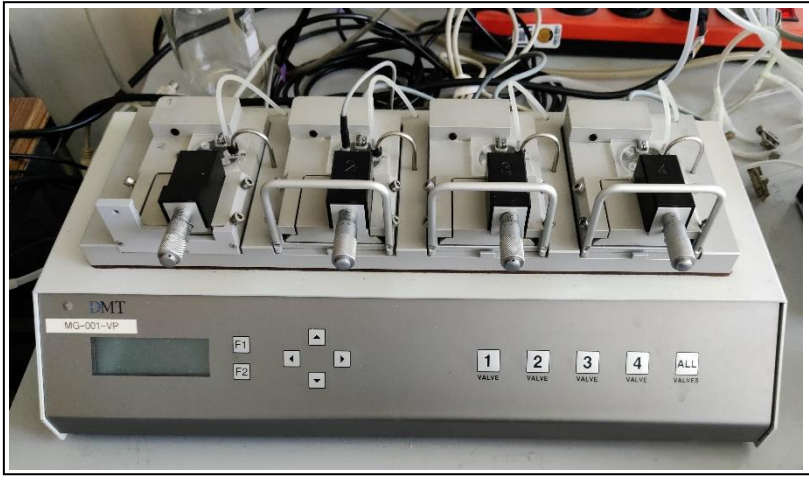

Figure 5: The myograph 610A by Danish Myo Technology
The four chamber units are in place in their corresponding slots of the interface, their wires connected to the interface and the suction and bubbling arms are in place.

Source: Photo by Jens Jagdfeld

Contraction of the urethral ring preparations displaced the transducer unit and was transformed into an electrical signal, which was proportional to the force generated by the sample. This signal was recorded by a data acquisition system (PowerLab 4/30 by AD Instruments) and displayed using Labchart by AD Instruments.

The myograph chamber units, suction and gas tubes were thoroughly cleaned every day with distilled water and acetone. Calibration was performed regularly using the calibration kit supplied by the manufacturer: After fixing a wire on the mounting jaws of the transducer, the chamber was filled with distilled water and the temperature increased to 37 °C. Afterwards, a bridge and balance were placed on top of the chamber unit, ensuring that the pin of the balance reaches into the mounting jaws of the transducer without touching the wire. After an equilibration period, a 2 g weight was placed on the balance (Figure 6).

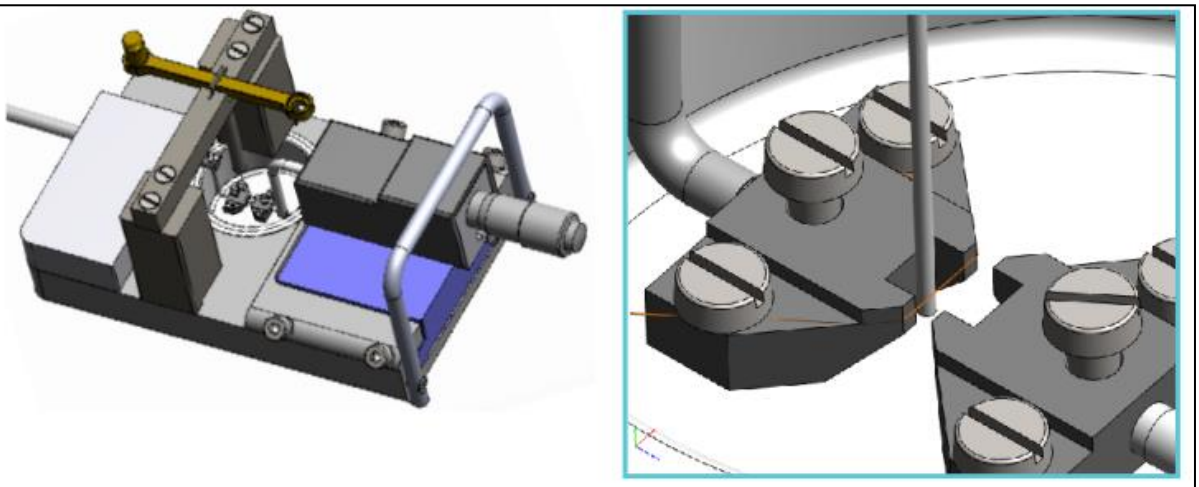

Figure 6: Calibration of the myograph
Calibrating the myograph unit using the calibration kit (bridge, balance and 2 g weight) supplied by the manufacturer DMT. Left: The balance is placed on the bridge, the 2 g weight placed on the side of the transducer. Right: The pin of the bridge exerts a force on the wire of the transducer

Modified from: USER MANUAL, VOL.2.0 by DMT

3.4.2. Mounting the preparations into the myograph unit

The urethral sections were transferred into the chamber of the myograph unit containing RT dissection PSS. Using a microscope, two 40 µm thick wires were threaded through the urethral lumen and fixed on either side of the myograph jaws with screws (Figure 7)

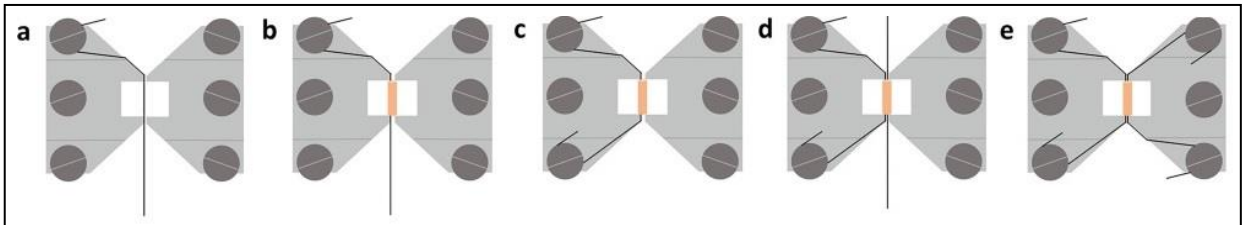

Figure 7: Mounting of urethral ring preparations into the myograph unit
a: Attaching the first wire to the jaw by screwing it in place with the top left screw, then fixing the wire by pinning it in between the jaws. b: Threading the preparation onto the first wire and placing it in the space between the jaws. c: Fixing the first wire using the bottom left screw. d: Opening the jaws slightly to thread the second wire through the preparation. Afterwards fixing the wire in place by closing the jaws again, pinning the wire between them. e: Screwing the second wire in place using the top right screw first, then opening the jaws slightly and fixing the wire to the bottom right screw.

Modified from: The Use of Wire Myography to Investigate Vascular Tone and Function by Kayleigh Griffiths & Melanie Madhani (2022).

After measuring the dimensions of the preparation and setting the distance of the two wires to ~0,1mm, the myograph units were then placed onto their corresponding position on the myograph interface. The suction and bubbling arm were placed into the bath, the chamber was closed with a lid and the data wires were connected.

3.4.3. Stretching and reference contraction

After mounting of the preparation into the myograph unit, the organ chamber was washed once with PSS at room temperature bubbled with carbogen (95 % O_2, 5 % CO_2) and allowed to rest for one hour while raising the temperature to 37 °C. Simultaneously the PSS and K-PSS bottles were similarly bubbled and heated in a water bath to 37 °C.

After one hour the pH of both PSS was adjusted to 7,4 at 37 °C and each chamber was washed once with PSS and force recording was started. The preparations were stretched in 100 µm steps until a steady resting tension of ~1 mN was reached. Afterwards, the organ bath was washed once more and allowed to rest for another hour.

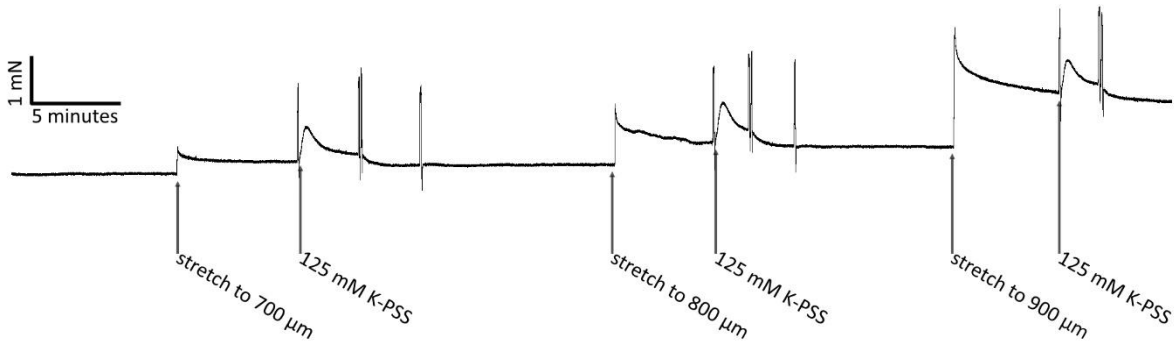

Figure 9: Original force tracing of a length – force relationship
Shown above is an excerpt of an original force tracing of a length – force relationship experiment. Urethral ring preparations (n=9) were stretched in 100 µm steps. After an equilibration period of 5 minutes a contraction using 125 mM K-PSS was elicited after each stretch. The artifacts (vertical lines) stem from the changing of PSS in the test chamber.

The resting force used in this study was based on force-length relations for optimal KCl-induced contractions: For this, urethral ring preparations were stretched in steps of 100 µm, and, after an equilibration period of 5 minutes at each step, a contraction was induced by 125 mM K-PSS. Stretching resulted in a rapid force increase followed by partial relaxation (stress relaxation) to a lower steady state force. The amplitude of the KCl induced contractions

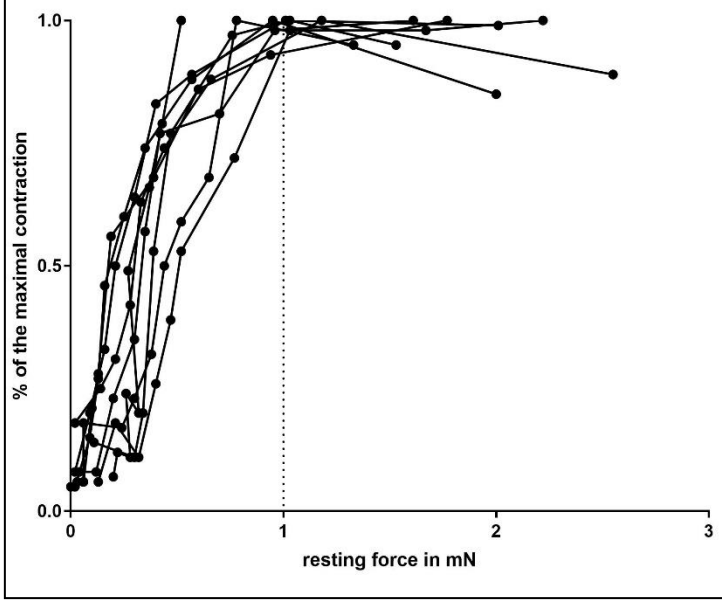

Figure 8: Optimal resting force of urethral ring preparations
The maximal force of each 125 mM K-PSS induced contraction (after subtracting the resting force), is expressed in % of the strongest contraction achieved by that specimen (y axis), and plotted against the corresponding resting force (x axis).

increased with increasing prestretches and was maximal at a resting force of 1 mN (Figure 8, 9).

The results show, that almost all specimens exhibited a maximal contraction at a resting tension of ~ 1 mN, and that contractions performed at higher resting tensions often resulted in a decrease of generated force (Figure 9).

The resting force of 1 mN used in this study differs from the oftentimes used 2 mN (Alexandre et al. 2016, Triguero et al. 2014). A possible explanation might be that the researchers in those studies used longer sections of urethra (2-4 mm).

To verify their contractile ability, all preparations were stimulated three times with 125 mM K-PSS for 3 minutes each. Between stimulations, the preparations were washed with PSS twice with a 3-minute pause in between the washes. After 10 minutes, this stimulation process was repeated (Figure 10).

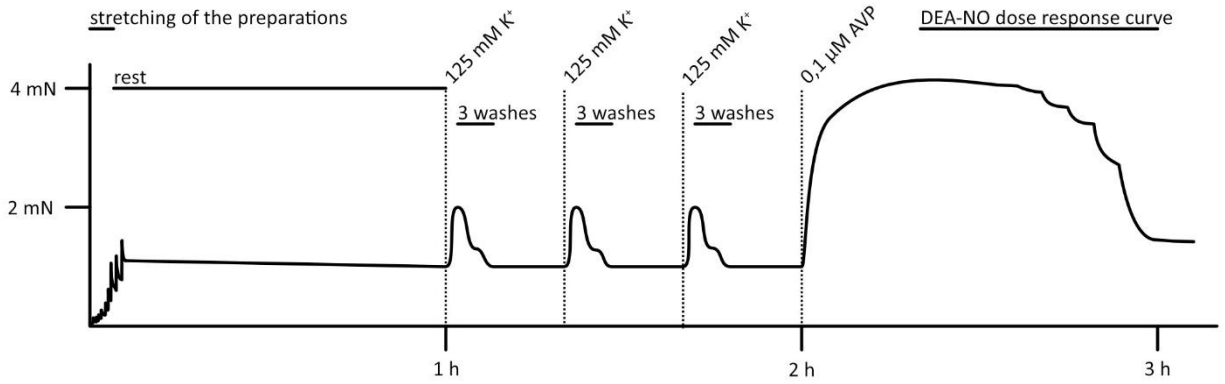

Figure 10: Experimental protocol
After letting the preparations warm up to 37 °C for one hour the recording was started. The preparations were stretched to a resting force of 1 mN, after which they were left to rest for one hour. Then three reference contractions were elicited using high K-PSS. Various experiments were then carried out. Exemplary, a DEA-NO dose-response curve after prior contraction by AVP is shown above.

3.4.4. Effect of contractile agonists

Concentration response curves were obtained by incubating the preparations with cumulatively increasing concentrations of PE (2 minutes at each concentration, concentration range 0,1 µM – 30 µM), and vasopressin (AVP, 3 minutes at each concentration, concentration range 1 nM – 1 µM).

3.4.5. DEA-NO induced relaxation

The relaxing effect of DEA-NO, an NO donor, was assayed in preparations precontracted by either PE or AVP.

The AVP experiments were done in the presence of 1 µM atropine and 100 µM L-NAME to inhibit muscarinic acetylcholine receptors and NO synthase, respectively. The preparations

were incubated with 0,1 µM AVP for 5 minutes after which DEA-NO was added every 3 minutes in cumulatively increasing concentrations ranging from 0,1 µM to 300 µM.
The effect of DEA-NO on preparations precontracted by PE was done on males only, as females did not respond to stimulation by PE. The contraction was induced using 10 µM PE for 5 minutes, after which preparations were treated with 10 µM and then with 310 µM DEA-NO for 3 minutes each.

3.4.6. DEA-NO effect on KCl induced contraction

The preparations were contracted twice with 125 mM KCl as reference baseline. Then two successive KCl induced contractions were performed in the presence of 30 µM and 100 µM DEA-NO, respectively. Finally, a last KCl induced contraction without DEA-NO was obtained.

3.4.7. Electric Field Stimulation (EFS)

The relaxing effect of NANC-neurons was assayed using electric field stimulation (EFS). Special myograph units were used for EFS experiments: First, an electrode was screwed in place in the chamber. After the preparation was mounted, the second electrode was screwed on top, sandwiching the preparation between the two electrodes. Rising bath temperature to 37 °C, equilibration and reference contractions were performed as described in chapter 3.4.2 & 3.4.3. “NANC conditions” were achieved by adding an inhibitor cocktail containing 1 µM each of atropine (a competitive antagonist of M1-M5 cholinergic receptors), phentolamine (unspecific α-adrenoreceptor antagonist), indomethacin (inhibitor of cyclooxygenase 1 & 2) and propranolol (nonselective β blocker). Precontraction was elicited by 0,1 µM AVP. After 5 minutes, EFS was applied at 0,5ms pulse width (bipolar), 5s train duration, 40 V and frequencies of 8 Hz, 16 Hz and 32 Hz and 5-minute pauses between stimulations. EFS was done using a CS8 Stimulator by Danish Myo Technology (DMT). The stimulator was controlled using the MyoPULSE software by DMT.

3.5. Fixation with PFA

Preservation of tissues for histological analysis was performed using 4 % Paraformaldehyde (PFA) dissolved in phosphate-buffered saline (PBS). At the end of the experiment, the PSS was suctioned off and the chamber was filled with PFA. The myograph tray was placed in a Styrofoam container along with cool packs on a vibrating plate overnight. The next day the wires holding the preparations were carefully cut, the urethral rings slid off and stored in Eppendorf tubes containing PFA at 4 °C until further processing by Anja Kahl as in Pütz et al. 2021.

3.6. Statistics

EC_{50} & IC_{50} values as well as the Hill slope were calculated for every sample group by fitting the data with a sigmoidal regression curve. Statistical evaluation was done using unpaired, two tailed t-test as well as one-way and two-way-ANOVA as appropriate. A value of $p<0,05$ was determined to be significant. All presented data are mean ± SD of the indicated number of animals n unless stated otherwise. Animal age is presented as median ± SD.

All data obtained were collected and processed using Excel (Microsoft Office 2003) and GraphPad Prism 7.04. Graphics and diagrams were produced using Affinity Photo and draw.io, respectively.

4. Results

4.1. Cryoconservation and staining

Of the many urethral ring preparations used in the experiments, some were fixed in PFA in the myograph immediately after the experiments were concluded. They were further processed by Anja Kahl: Figure 11 displays three examples of thus obtained histologic preparations. The urethras seen stem from mice with different ages, sex and genotypes. The previously performed functional assay using a wire myograph system explains the ellipsoid form of these sections.

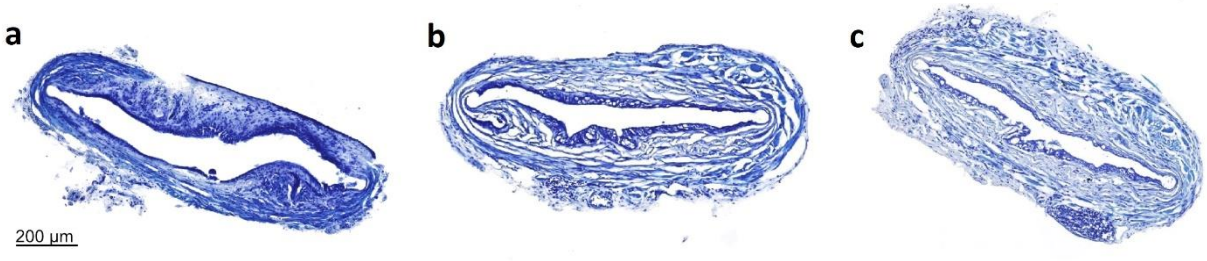

Figure 11: Histological images of urethral ring preparations
Three exemplary histological images of Nissl-stained urethral tissue under 40-times magnification. The preparations stem from a, a ~ 20-week-old KO male, b a ~ 2-year-old WT female, and c, a ~ 2-year-old KO female. All preparations were previously subject to myograph experiments, explaining their ellipsoid appearance. Histological sections and staining were done by Anja Kahl.

4.2. Animal and bladder weight

Animals were weighed immediately after sacrificing and eventual urination was measured using a previously weighed tissue. At the time of death, the animals had an age of 17,2±3,2 weeks (median ± SD; n=123) in the young, and 108±8,7 weeks (median ± SD; n=120) in the old age group. Old animals had a significantly higher body weight compared to young animals. Body weight of mice did not differ significantly between WT and telokin$^{-/-}$ animals in the young and old age group (Figure 12 A&B). Across both age groups and both genotypes, males displayed a significantly higher body weight compared to females (Figure 12).

After separating the bladder from the urethra, the bladder was dabbed dry and weighed. Any residual urine was captured and measured using a previously weighed tissue. For this dissertation, I assumed a urine density of 1000 kg/m^3. In young animals, total urine volume (urination during sacrificing + residual urine in bladder) did not differ between genotypes. In aged animals, urine volume showed a higher variability. It was significantly higher in old KO compared to old WT as well as young KO males. In old females, the mean urinary volume

tended to be higher in KO mice but did not reach the level of significance because of the high variations (Figure 12 C&D, Table 2).

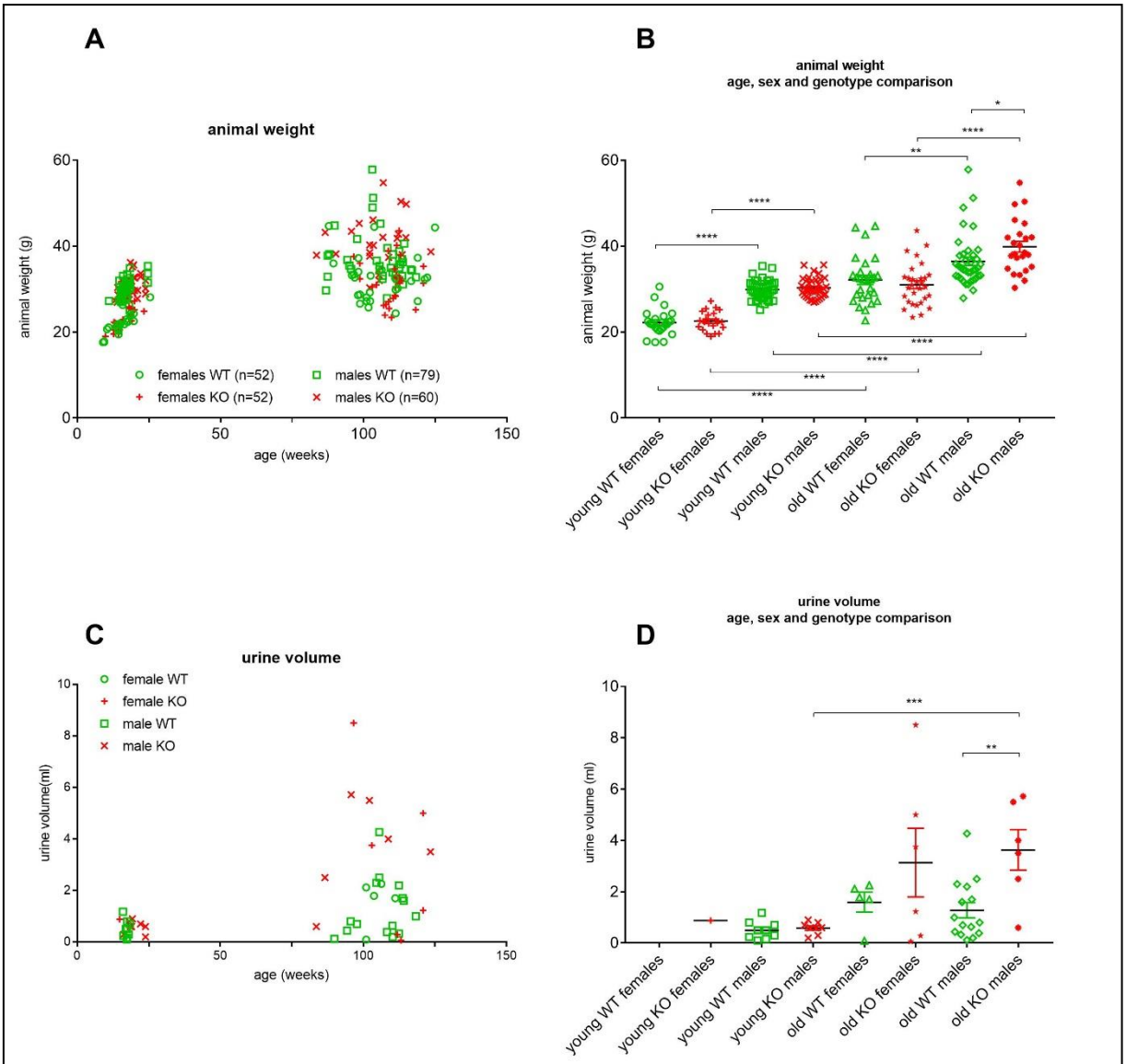

Figure 12: Animal weight and urine volume
(A): Body weight of animals. (B): Comparison of body weight between WT and KO genotypes for females and males in two age groups (17,2±3,2 weeks or 108±8,7; median ± SD). (C): Urine volume of all animals. (D): Comparison of urine volume between WT and KO genotypes of the two age groups. No enlarged urine volume was measured for young WT females. In aged telokin$^{-/-}$ mice urine volume was higher. The p values were obtained by unpaired, two-tailed students t-tests. All comparisons not depicted were not significantly different.

Bladder weight was higher in old animals (Figure 13 A). For young males and females as well as for old females, the bladder weight was significantly higher in KO compared to WT animals; old males showed no difference between the genotypes (Figure 13 B, Table 2).

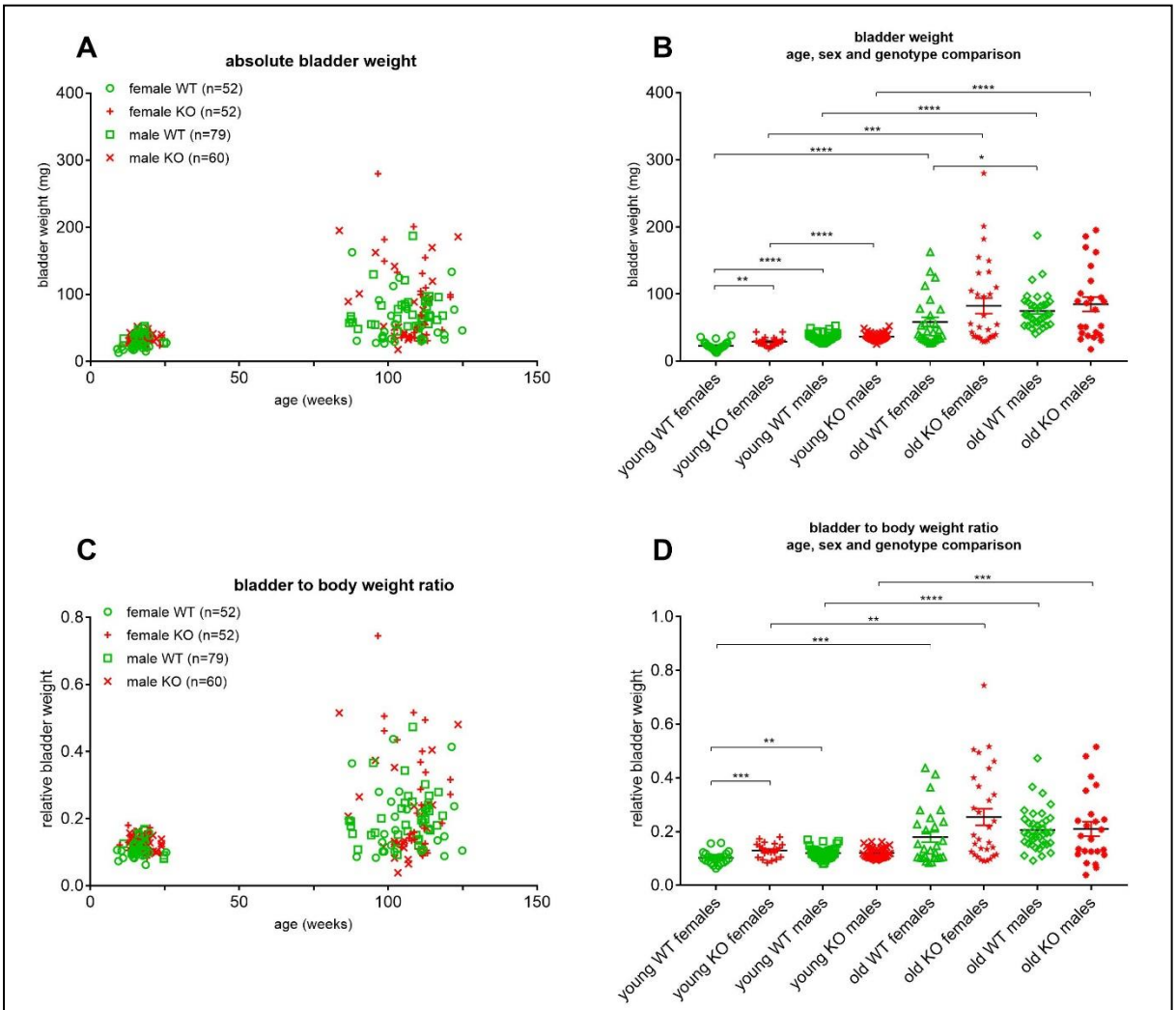

Figure 13: Bladder weight and bladder to body weight ratio
(A): Bladder weight of animals. (B): Comparison of bladder weight between WT and KO genotypes for females and males in two age groups (17,2±3,2 weeks or 108±8,7 weeks; median ± SD). (C): Bladder to body weight ratio. (D): Comparison of the bladder to body weight ratio between WT and KO genotypes for females and males in two age groups. P values were obtained by unpaired two-tailed students t-tests. All comparisons not depicted were not significantly different.

The bladder to body weight ratio (bladder weight in % of animal weight) was significantly higher in old compared to young WT of both sexes. Between genotypes, it was higher in female KO for both young and old female KO animals compared to WT. Telokin deficiency did not significantly affect the bladder to body weight ratio in males (Figure 13 C, D, Table 2).

Comparing the urethral contractile force during stimulation by 125 mM K^+, no significant difference was evident between telokin$^{-/-}$ and WT mice of either age or sex. Male mice exhibited a very significantly higher contractile force compared to female mice across all genotypes and ages ($p<0,0001$). Aged female mice displayed a significantly weaker contraction compared to young female mice ($p<0,01$), no such difference was seen in male mice however.

age, genotype, sex	animal weight (g)	urine volume (ml)	bladder weight (mg)	bladder weight in % of body weight	contractile force (mN) [K^+ 125 mM]	n	n*
young							
♀ WT	22,2±3	/	22,9±6,5**	0,102±0,023***	1,65±0,37	24	0
♀ KO	22,5±2,1	0,88	29,1±6,3	0,129±0,026	1,76±0,45	22	1
♂ WT	30±2,3****	0,4±0,3	35,6±6,2****	0,119±0,021§§	4,94±0,97****	41	9
♂ KO	30,4±2,4$^{$$$$}$	0,5±0,2	36,5±5,8$^{$$$$}$	0,12±0,02	4,75±1,23****	36	8
old	$$$$						
♀ WT	32,4±5,4	1,5±0,8	58,4±36,7*$^{$$$$}$	0,179±0,102$^{$$$}$	1,09±0,45§§	28	5
♀ KO	31,6±4,9	3,1±3,2	82,5±62,3***	0,254±0,168$^{&&}$	1,06±0,27$^{$$}$	30	6
♂ WT	36,9±5,9**$^{&}$	1,2±1,1**	74,8±27,3$^{&&&&}$	0,206±0,076$^{$$$$}$	4,59±1,11****	38	15
♂ KO	40,7±5,8****	3,6±1,9$^{$$$}$	85±52,9§§§§	0,209±0,13$^{&&&}$	4,37±1,32****	24	6

Table 2: Comparison between age, genotype and sex for animal and bladder weight and urine volume as well as urethral contractile force during K^+ stimulation

Effect of telokin deletion regarding animal weight, urine volume, bladder weight and the bladder body weight ratio, data are mean ± SD. Not every mouse urinated upon its demise or had residual urine in its bladder and therefore no data was measured for these animals. Only actually measured data is represented. n* corresponds to the number of animals for which urine volume was measured.

P values obtained by unpaired, two-tailed students t-tests: Animal weight: Young: **** WT females vs. WT males p<0,0001; $^{$$$$}$ KO males vs. KO females p<0,0001; Old: $^{$$$$}$ WT females, KO females, WT males, KO males vs. their corresponding young group p<0,0001; $^{&}$ old WT males vs. old KO males p<0,05; ** WT males vs. WT females p<0,01; **** KO males vs. KO females p<0,0001; urine volume: old: ** WT males vs. KO males p<0,01; $^{$$$}$ old KO males vs. young KO males p<0,001; bladder weight: young: ** WT females vs. KO females p<0,01; **** WT females vs. WT males p<0,0001; $^{$$$$}$ KO males vs. KO females p<0,0001; old: * WT females vs. WT males p<0,05; $^{$$$$}$ old WT females vs. young WT females p<0,0001; *** old KO females vs. young KO females p<0,001; $^{&&&&}$ old WT males vs. young WT males p<0,0001; §§§§ old KO males vs young KO males p<0,0001; bladder weight in % of body weight: young: *** WT females vs. KO females p <0,001; §§ WT females vs. WT males p<0,01; old: $^{$$$}$ old WT females vs. young WT females p<0,001; $^{&&}$ old KO females vs. young KO females p<0,01; $^{$$$$}$ old WT males vs young WT males p<0,0001; $^{&&&}$ old KO males vs young KO males p<0,001; contractile force: **** all male values vs. the corresponding female values p<0,0001; §§ old female WT vs. young female WT p<0,01; $^{$$}$ old female KO vs. young female KO p<0,001. All p values not mentioned were not significant.

4.3. Agonist-induced contractions

4.3.1. AVP-Concentration Response Curve

In this series of experiments, I tested the hypothesis, that deletion of telokin augments agonist-induced contraction. I further tested whether age and sex has a differential effect.

Application of AVP in cumulatively increasing concentrations ranging from 1 nM to 1 µM showed a concentration dependent increase in force. The peak force at each AVP concentration was determined, subtracted by the resting force, and was expressed relative to the maximum AVP induced contraction (Figure 15).

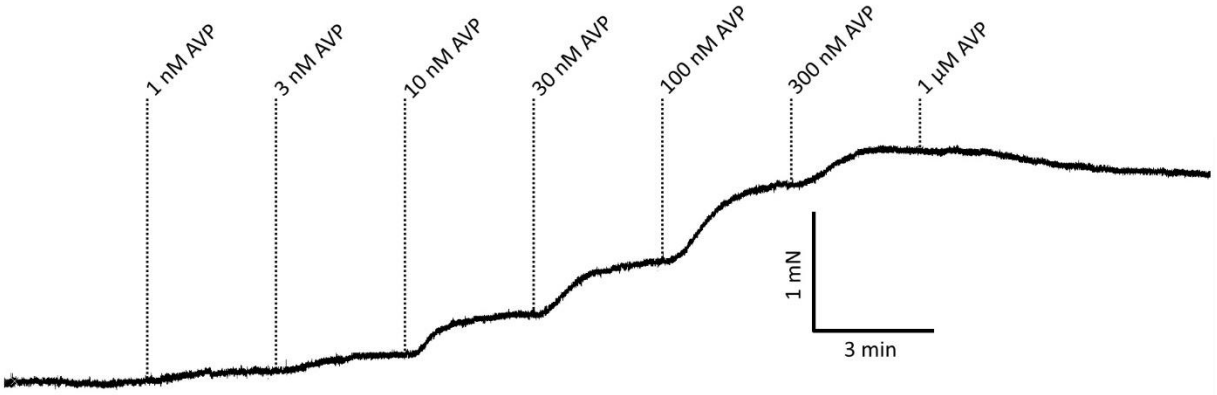

Figure 14: Typical AVP dose response curve
All specimens showed a concentration dependent increase in force in response to AVP. Peak force values were determined at each concentration. The resulting data were grouped (old WT females, young WT females, old KO females, young KO females, old WT males, young WT males, old KO males, young KO males; n=5 for each group) and a sigmoidal curve was fitted. The EC_{50}-values, maximum responses and Hill slopes were used to compare the curves (see Figure 15).

In females of both age groups and old males a leftward shift of the concentration response curves (CRC) of KO urethras compared to WT was observed (Figure 15 A, B, D). The young males is the only group not to display a difference among genotypes (Figure 15 C). The Hill slope was significantly steeper for KO animals compared to WT for young females (Table 3).

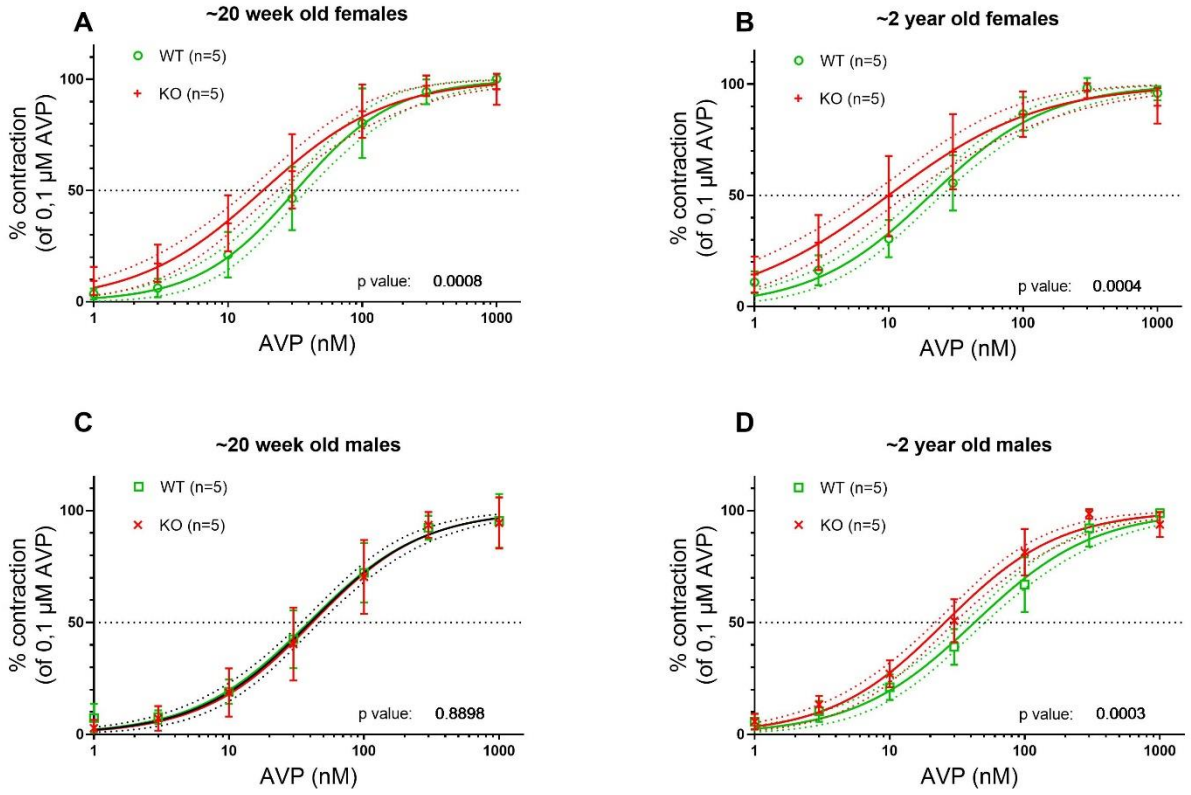

Figure 15: Effect of telokin deletion on AVP concentration response-curves of urethral ring preparations from young and old females and males
Concentration response relations were fitted by sigmoidal regression for contractions elicited by cumulatively increasing concentrations of AVP. The peak force value at each concentration was determined and the resting force was subtracted. The p values are derived from the comparisons between the curves using the extra sum-of-squares F test with the parameters Hill slope, EC_{50} and maximum response. In young and old females (A, B), and in old males (D) but not in young males (C), the concentration response curves to AVP were shifted to the left in KO urethras. Symbols and error bars represent means ± SD; the dotted lines represent 95% CI.

The effect of age was explored for each genotype and sex separately (Figure 16). It is worth noting, that old females of either genotype exhibited a leftward shift of the CRC. Such a shift was also observed in male KO but not in male WT urethras. The Hill slope was steeper in the young age group compared to the old in female and male WT animals (Table 3).

The CRC did not differ between young female and male WT mice whereas in old WT the CRC of AVP was to the left of female compared to male urethras. In telokin deficient mice the CRC of females was shifted to the left compared to males in both age groups (Figure 17).

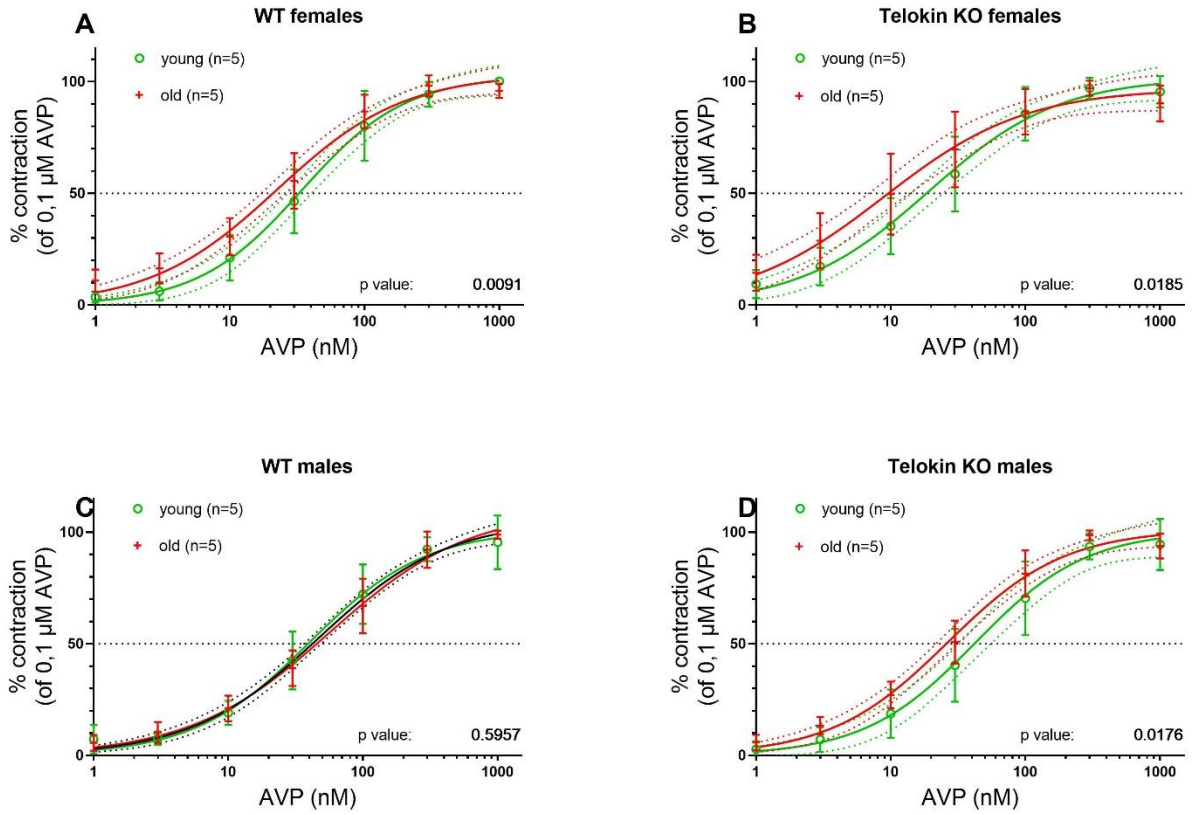

Figure 16: Effect of age on AVP concentration response curves of urethras from WT and telokin$^{-/-}$ male and female mice

Concentration response relations were fitted by sigmoidal regression for contractions elicited by cumulatively increasing concentrations of AVP in % of the maximal elicited force F_{MAX}. The p values are derived from the comparisons between the curves using the extra sum-of-squares F test with the parameters Hill slope, maximum value and EC_{50}. For WT females, KO females and KO males the AVP-force relationship was significantly shifted to the left for the older age group (A, B, D). WT males did not show a difference between the age groups (C). Symbols and error bars represent means ± SD; the dotted lines represent 95% CI. The bottom was constrained to 0.

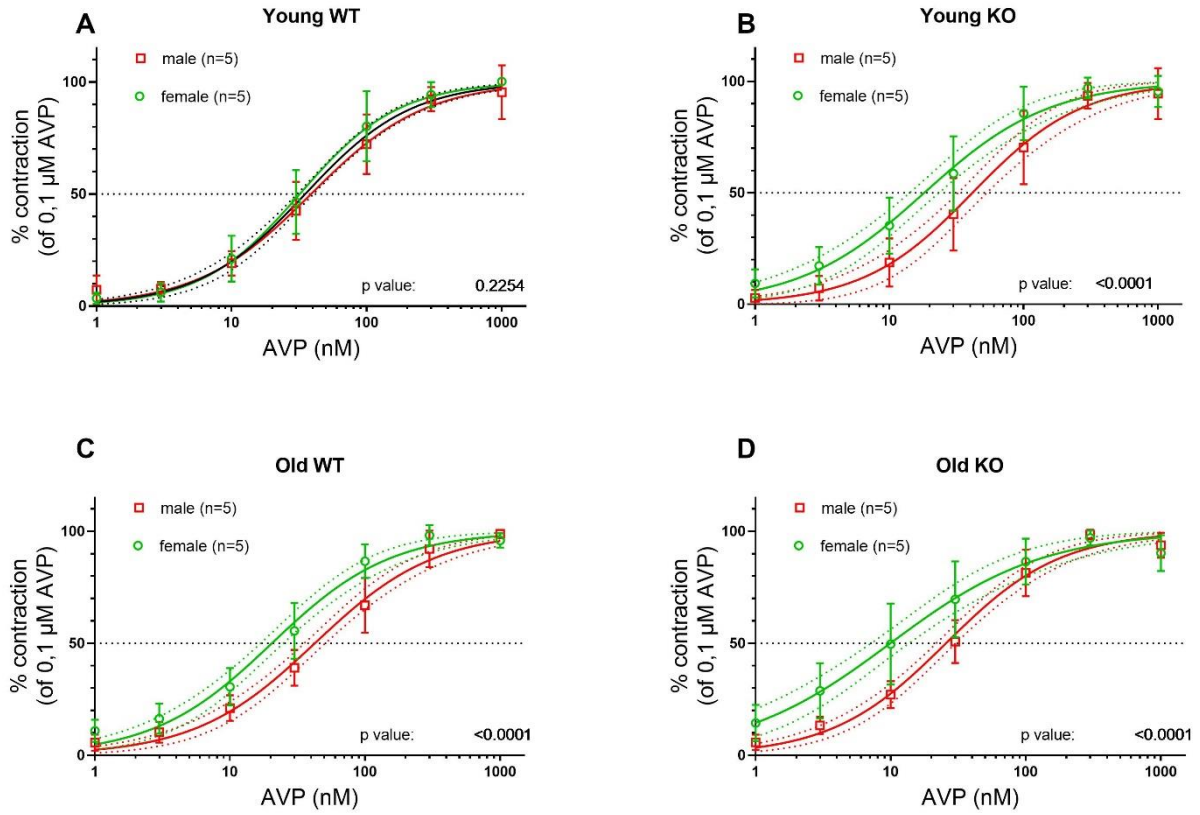

Figure 17: Effect of sex on AVP concentration response curves of urethras from WT and telokin$^{-/-}$ young and old mice

Concentration response relations were fitted by sigmoidal regression for contractions elicited by cumulatively increasing concentrations of AVP in % of the maximal elicited force F_{MAX}. The p values are derived from the comparisons between the curves using the extra sum-of-squares F test with the parameters Hill slope, maximum value and EC_{50}. For WT females, KO females and KO males the AVP-force relationship was significantly shifted to the left for the older age group (A, B, D). WT males did not show a difference between the age groups (C). Symbols and error bars represent means ± SD; the dotted lines represent 95% CI. The bottom was constrained to 0.

age, genotype, sex	contraction 0,1 µM AVP (mN)	pEC50	Hill slope	n
young				
WT females	2,66±0,59	7,48±0,21	1,26±0,06*	5
KO females	1,99±0,87	7,73±0,25	1,03±0,22	5
WT males	2,88±0,48	7,33±0,21	1,36±0,45	5
KO males	2,36±0,5	7,31±0,27	1,22±0,28	5
old				
WT females	2,06±0,44*	7,69±0,16$^{\$\$}$	1±0,24	5
KO females	1,31±0,23	7,88±0,44	1,04±0,15	5
WT males	3,54±0,72$^{\$\$}$	7,19±0,21	1,02±0,15	5
KO males	3,11±0,56$^{\$\$\$}$	7,49±0,16	1,27±0,26	5

Table 3: Response to AVP compared between WT and KO mice for different sexes and age groups

Values represented are mean ± SD. The p values correspond to the results of unpaired, two-tailed students t-tests. Contraction 0,1 µM AVP represents the maximum force after stimulation with AVP subtracted by passive tension. pEC_{50} represents the negative logarithm of the EC_{50}.

Contraction 0,1 µM AVP: old: * WT females vs. KO females $p<0,05$; $^{\$\$}$ WT females vs. WT males $p<0,01$; $^{\$\$\$}$ KO females vs. KO males $p<0,001$; pEC50: old: $^{\$\$}$ WT females vs. WT males $p<0,01$; Hill slope: * young WT females vs. old WT females $p<0,05$. All p values not mentioned were not significant.

4.3.2. Phenylephrine Concentration Response Curve

As females do not express the α1 adrenoreceptor in the urethra (Alexandre et al. 2017), the concentration response relationship of phenylephrine (PE), a selective α1 agonist, was investigated only in male mice of both age groups. Cumulative application of PE ranging from 0,1 µM to 30 µM showed a concentration dependent increase in force (Figure 18).

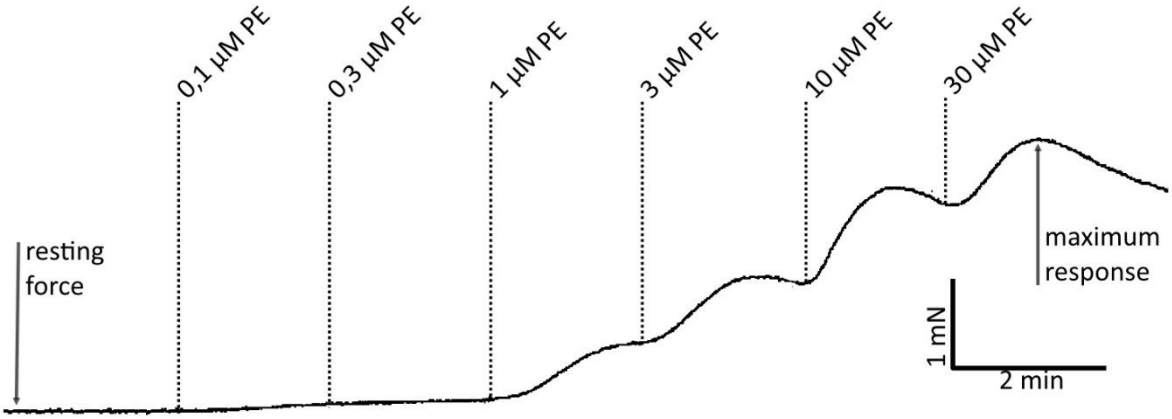

Figure 18: Original force tracing of a PE concentration response curve
All specimens showed a concentration dependent increase in force in response to PE. The peak force value at each concentration was determined and the resting force was subtracted. The resulting data were grouped (old WT males, young WT males, old KO males, young KO males; n=6-11, c.f. Figure 19). The concentration response relation was fitted by a sigmoidal non-linear regression. The EC_{50}, maximum response and Hill slope was used to compare the curves.

Peak force at each PE concentration was determined, the resting force was subtracted and the thus obtained force was expressed relative to the maximum PE elicited contraction at 30 µM PE (Fmax).

Urethras from KO animals of the ~ 2-year-old age group displayed a significantly higher Fmax (=maximum force minus the resting force) at 30 µM PE than those from WT animals. No significant difference was observed between WT and KO urethras from young mice (Table 4), although the pEC_{50} tended to be lower in the young age group.

The extra sum-of-squares F test, used to determine the goodness of fit, revealed that sigmoidal fits of the CRC for WT and KO urethras in the young and old age groups did not differ between, meaning all data can be expressed by the same fit, thus indicating that the sigmoidal fits of the CRC WT and KO animals do not differ.

In a separate analysis, I compared the effect of age in WT and telokin$^{-/-}$ urethra separately. In WT and telokin$^{-/-}$, the CRC of old compared to young urethras was shifted to the right. This shift was smaller in telokin deficient urethras as indicated by the smaller increase in the pEC_{50} value. The goodness of fit was significant when comparing young and old animals of both genotypes, indicating that age is a significant factor for PE response, with young animals displaying a stronger reaction.

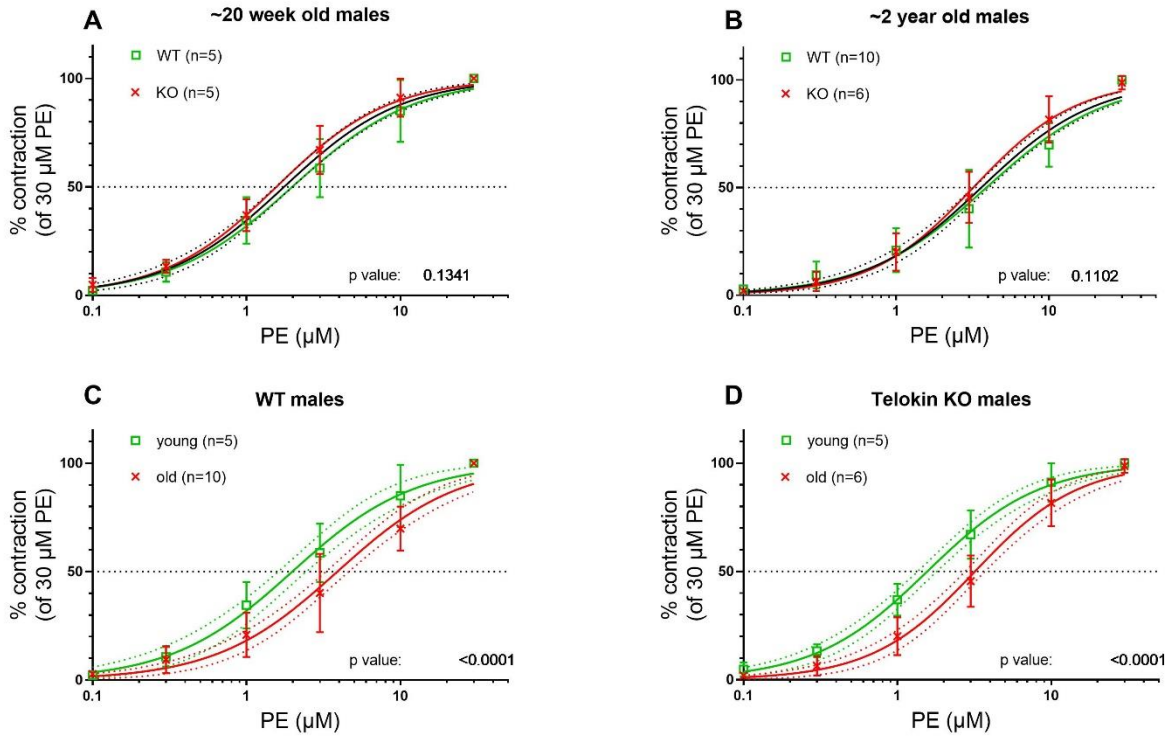

Figure 19: Effect of age and genotype on the PE concentration response curves
The concentration-contraction relations were fitted by sigmoidal regression (solid lines). Comparisons between the curves was done using the extra sum-of-squares F test with the parameters Hill slope, EC_{50} and maximum response. Symbols and error bars represent means ± SD; the dotted lines represent 95% CI.

age, genotype	contraction 30 µM PE (mN)	pEC50	Hill slope	n
young				
WT males	2,77±0,74	5,77±0,08**	0,94±0,18	5
KO males	2,54±0,69	5,71±0,15*	1,14±0,33	5
old				
WT males	3,19±0,67*	5,03±0,48	1,08±0,39	10
KO males	4,11±0,46§§	5,34±0,27	1,18±0,29	6
ANOVA				
genotype	n.s.	n.s.	n.s.	
age	0,0023	0,0023	n.s.	
interaction	n.s.	n.s.	n.s.	

Table 4: Response of males to PE compared between WT and KO and different age groups
Values represented are mean ± SD. The p values correspond the results of unpaired, two-tailed students t-tests. Contraction 30 µM PE represents the maximum force after stimulation with PE subtracted by passive tension. pEC_{50} represents the negative logarithm of the EC_{50}. n represents the number of animals. The significant p values from a 2-way ANOVA with no repeated measures are presented. Contraction 30 µM PE: * old WT males vs. old KO males p<0,05; §§ old KO males vs. young KO males p<0,01; pEC50: ** young WT males vs. old WT males p>0,01; * young KO males vs. old KO males p<0,05. All p values not mentioned were not significant.

4.4. NO mediated relaxations

4.4.1. Relaxations of AVP induced contractions by DEA-NO

The hypothesis was tested, that NO-induced relaxation was attenuated in telokin KO mice. For this, the NO donor 2-(N,N-diethylamino)-diazenolate-2-oxide (DEA-NO) was used. DEA-NO response was examined on urethral ring preparations from mice of young and old age of both sexes precontracted with 0,1 µM AVP. These concentration response relationship experiments were performed in the presence of 1 µM atropine, a competitive antagonist of muscarinic acetylcholine receptors M1-M5, and 100 µM N(G)-Nitro-L-arginine methyl ester (L-NAME), an inhibitor of the nitric oxide synthase. This was done to avoid cholinergic excitatory influences and inhibit the release of endogenous nitric oxide, respectively. The urethral ring preparations were precontracted with 0,1 µM AVP for five minutes. Then, after the contraction reached a plateau, DEA-NO was added in cumulatively increasing concentrations every 3 minutes, causing a concentration dependent relaxation.

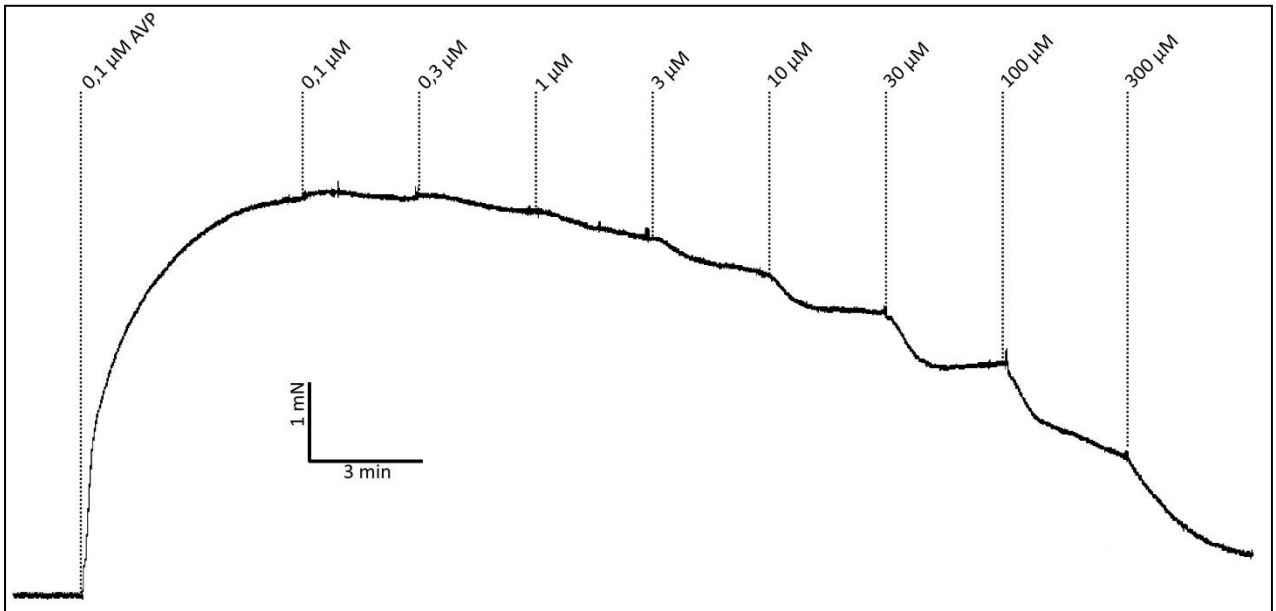

Figure 20: Original force tracing of a concentration dependent relaxation by DEA-NO. Experiments were performed in the presence of 1 µM atropine and 100 µM L-NAME. The preparation was precontracted with 0,1 µM AVP. 5 minutes after application of AVP, DEA-NO was added in cumulatively increasing concentrations every 3 minutes.

First, the effect of the genotype on DEA-NO elicited relaxation, separated for sex and age was analysed. Fmax (=maximum force minus the resting force) of the 0,1 µM AVP elicited contraction tended to be lower in WT males when compared to KO males of both age groups, but higher in WT females when compared to KO females, significantly so with young females (Table 5). Both young and old females showed a rightward shift of the concentration response curve of the KO animals compared to WT (Figure 21 A & B). Interestingly, in young but not in old males the concentration response curve was shifted to the left of the WT CRC in KO animals (Figure 21 C & D).

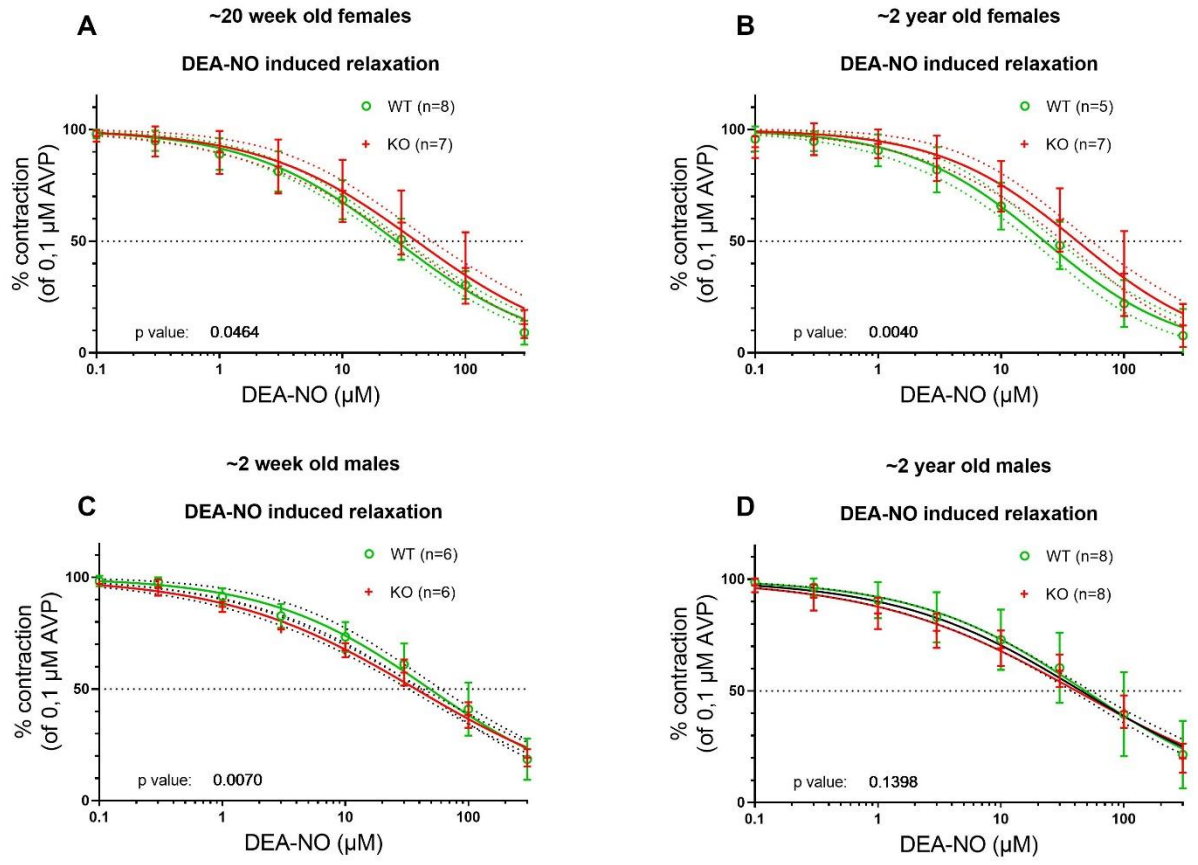

Figure 21: Effect of genotype on DEA-NO induced relaxation in urethras from young and old females and males
Curves fitted by non-linear regression (solid lines) for relaxations elicited by cumulatively increasing concentrations of DEA-NO. Comparisons between the curves was done using the extra sum-of-squares F test with the parameters Hill slope and IC_{50}. Symbols and error bars represent means ± SD; the dotted lines represent 95% CI.

In a second approach, the data was reevaluated to explore the effect of sex on DEA-NO mediated relaxation within the genotype and age groups. In urethras from old, but not young, WT animals, as well as from young and old KO animals, Fmax was significantly higher in males when compared to females. The pIC_{50} did not differ significantly between the sexes in any group. Young and old KO females had a significantly higher Hill slope when compared to males (Table 5). For both young and old WT animals, the concentration response curve was shifted to the left for females compared to males, and the extra sum-of-squares F test revealed a significant p value for the comparison of sigmoidal fits of the CRC (Figure 22 A & B). In young KO animals, not significant p value of the goodness of fit indicates, that the data can be expressed by the same fit (Figure 22 C). In old telokin$^{-/-}$ females, 3 and 10 µM DEA-NO induced a significantly weaker relaxation compared to males.

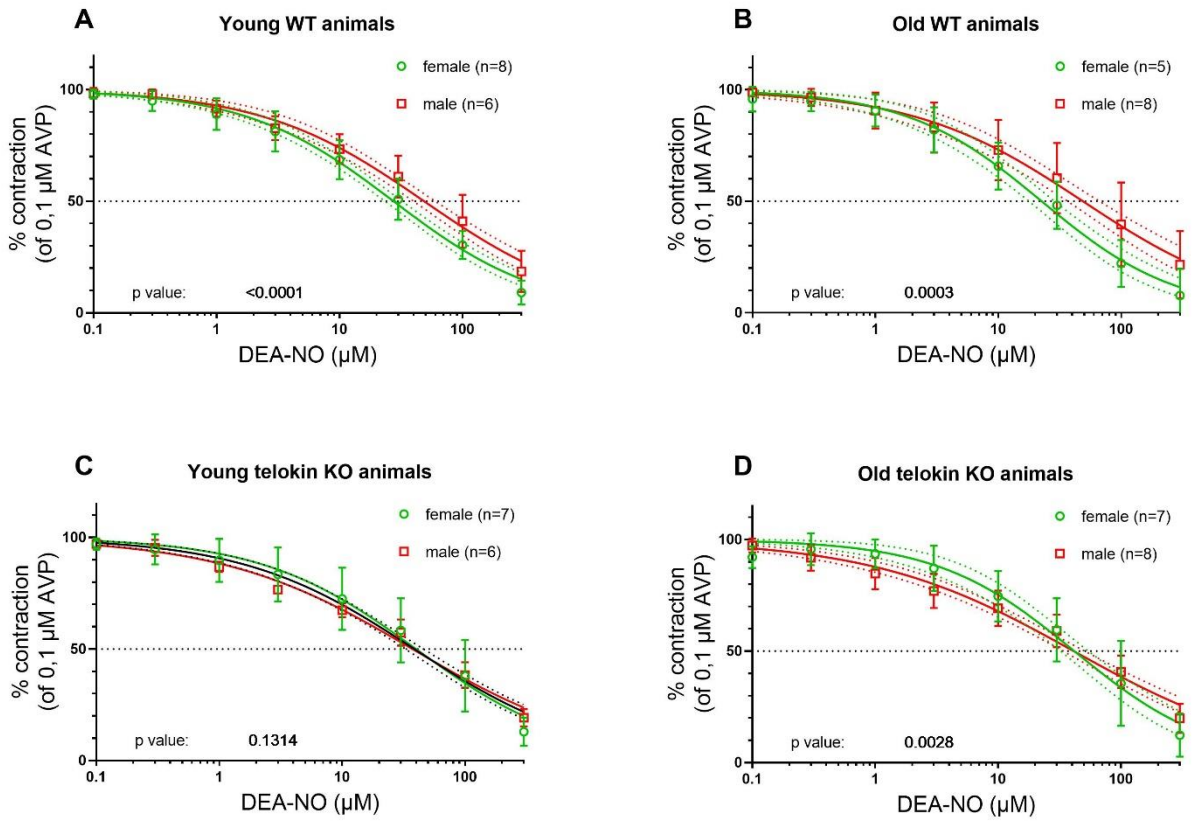

Figure 22: Effect of sex on DEA-NO mediated relaxation in WT and KO urethras
Curves fitted by non-linear regression for relaxations elicited by cumulatively increasing concentrations of DEA-NO. Comparisons between the curves was done using the extra sum-of-squares F test with the parameters Hill slope and IC_{50}. The IC_{50} values are presented in µM. Symbols and error bars represent means ± SD; the dotted lines represent 95 % CI.

Finally, the effect of age was investigated. Fmax at 0,1 µM AVP was significantly higher in young WT and telokin$^{-/-}$ females when compared to old animals (Table 5). Beyond that, no statistically significant differences relating to Fmax, pIC_{50}, Hill slope or goodness of fit were observed between young and old animals, irrespective of sex and genotype (Figure 23).

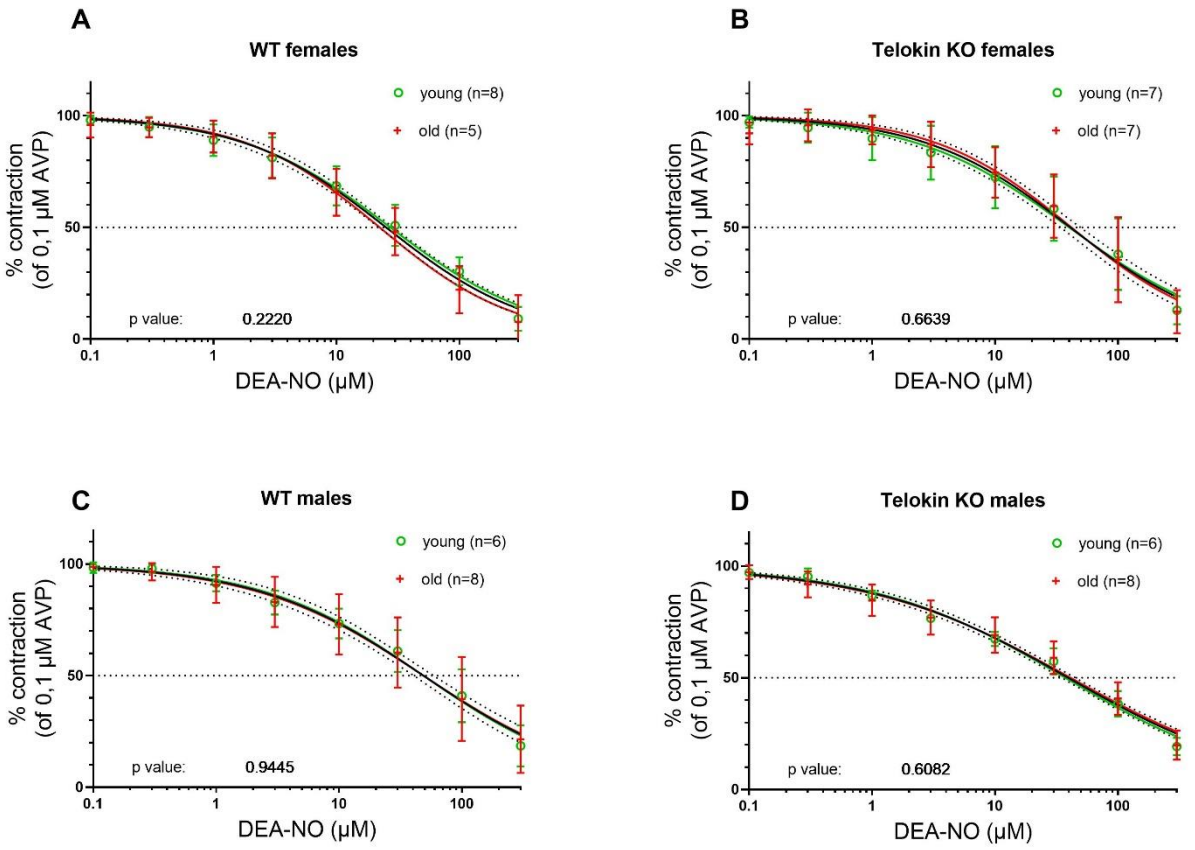

Figure 23: Effect of age on DEA-NO mediated relaxation
The preparations were pre-contracted with AVP. The concentration response relations of relaxations elicited by cumulatively increasing concentrations of DEA-NO were fitted by a sigmoidal regression curve (solid lines). Comparisons between the curves was done using the extra sum-of-squares F test with the parameters Hill slope, EC_{50} and maximum response. Symbol and error bars represent means ± SD; the dotted lines represent 95 % CI.

age, genotype, sex	contraction 0,1 µM AVP (mN)	pIC50	Hill slope	maximum relaxation (%)	n
young					
WT females	2,88±0,32*	4,57±0,21	0,76±0,15	90,9±4,98*	8
KO females	2,42±0,21§	4,43±0,37	0,77±0,19*	87,03±5,84	7
WT males	2,88±0,62	4,64±0,26	0,69±0,14	81,43±8,41	6
KO males	3,17±0,67	4,38±0,35	0,56±0,04	80,76±3,52	6
old					
WT females	2,06±0,47$^{\$\$\&\&}$	4,3±0,21	0,85±0,24	92,28±10,67	5
KO females	1,73±0,38$^{\$\$\$**}$	4,42±0,11	0,84±0,16**	87,66±8,91	7
WT males	2,99±0,48	4,32±0,43	0,72±0,16	78,51±14,11	8
KO males	3,66±0,89	4,39±0,15	0,57±0,15	80,13±6,11	8

Table 5: DEA-NO induced relaxation on AVP contraction
Values represented are mean ± SD. Statistical significance was tested using unpaired, two-tailed students t-tests. Contraction 0,1 µM AVP represents the maximum force after stimulation with AVP subtracted by passive tension. pIC_{50} represents the negative logarithm of the IC_{50}.

Contraction: Young: * WT females vs. KO females p<0,05; § KO females vs. KO males p<0,05; old: $^{\$\$}$ WT females vs. WT males p<0,01; $^{\$\$\$}$ KO females vs. KO males p<0,001; $^{\&\&}$ young WT females vs. old WT females p<0,01; ** young KO females vs. old KO females p<0,01. Hillslope: Young: * KO females vs. KO males p<0,05; old: KO females vs. KO males p<0,01. Maximum relaxation: *young WT females vs. young WT males p<0,05. All p values not mentioned were not significant.

4.4.2. DEA-NO induced relaxations of PE induced contractions

The DEA-NO induced relaxation was also assessed on urethral ring preparations precontracted with 10µM phenylephrine (PE) using ~20-week- and ~2-year-old male mice. Two DEA-NO concentrations (10µM and 310µM) were administered successively. The ensuing concentration dependent relaxation was maximal ~ 60 seconds after application, after which the preparations started to contract again (Figure 24).

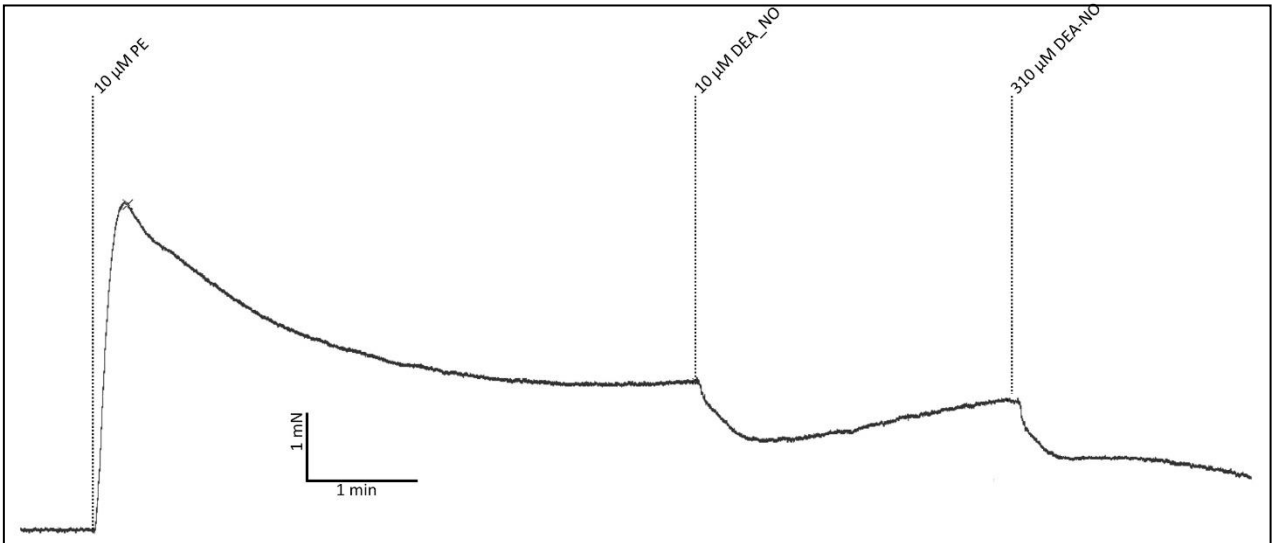

Figure 24: Original force tracing of DEA-NO elicited relaxation of urethral ring preparations precontracted by PE.
Contraction of urethra was elicited by 10 µM PE. After an initial contraction peak, a partial transient relaxation occurred with the preparation reaching a stable plateau after about 5 minutes. Then DEA-NO was added in two concentrations (10 and 310 µM) for 3 minutes each. The relaxation induced by 10 µM DEA-NO was followed by a gradual increase in force.

Maximal DEA-NO induced relaxation was expressed as percentage of the PE induced steady state force, just before application of 10 µM PE. DEA-NO had a stronger relaxing effect in the WT compared to KO mice in both age groups (Figure 25).

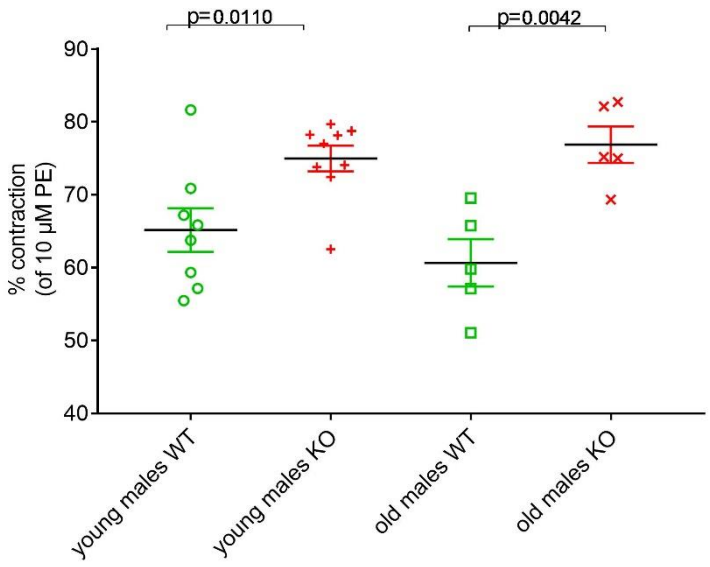

Figure 25: DEA-NO induced relaxation of PE precontracted urethral ring preparations.
Relaxation following stimulation by 10 µM DEA-NO of preparations precontracted with 10 µM PE. Contraction is expressed in percent of PE-induced force. For young and old animals, the experiments showed a significantly higher relaxation in WT urethras compared to KO. Symbols and error bars represent means ± SD. Statistical significance was tested using unpaired, two-tailed students t-tests.

4.4.2.1. DEA-NO mediated relaxation in combination with 80 mM K-PSS

To assess whether the observed difference in DEA-NO response present between the genotypes was mediated by activation of K^+-channels, DEA-NO was combined with high K-PSS and a reduced PE concentration of 1 µM in a new experiment. The influence of K^+-channels was abrogated by depolarization of smooth muscle by 80 mM K-PSS. Relaxation by DEA-NO was significantly smaller in KCl-precontracted urethral preparations. No significant difference in DEA-NO mediated relaxation between the genotypes was observed in the presence of high K-PSS.

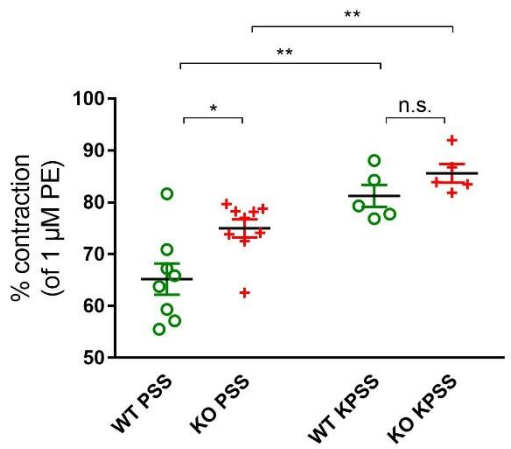

Figure 26: 10 µM DEA-NO induced relaxation of urethra precontracted with 1µM PE in 80 mM K-PSS

The relaxation induced by DEA-NO was significantly increased for WT compared to KO animals in the presence of PSS. This difference is abolished in a high K-PSS environment. WT and KO animals had a significantly reduced relaxation to DEA-NO in the high K-PSS when compared to the PSS. Contraction is expressed in percent of PE-induced force. Symbols and error bars represent means ± SD. Statistical significance was tested using unpaired, two-tailed students t-tests

4.4.3. The role of the soluble guanylyl cyclase

ODQ was used to test the hypothesis, that DEA-NO activates soluble guanylyl cyclase (sGC). ODQ is an inhibitor of guanylyl cyclase and was used in conjunction with DEA-NO on urethral rings precontracted with 0,1 µM AVP or 10 µM PE using ~20-week-old male mice. In preparations precontracted by AVP, 100 µM ODQ inhibited the DEA-NO induced relaxation at 30µM DEA-NO but not at > 100 µM DEA-NO (Figure 27 A). The effect of ODQ was more pronounced when the samples were precontracted with PE instead of AVP (Figure 27 B).

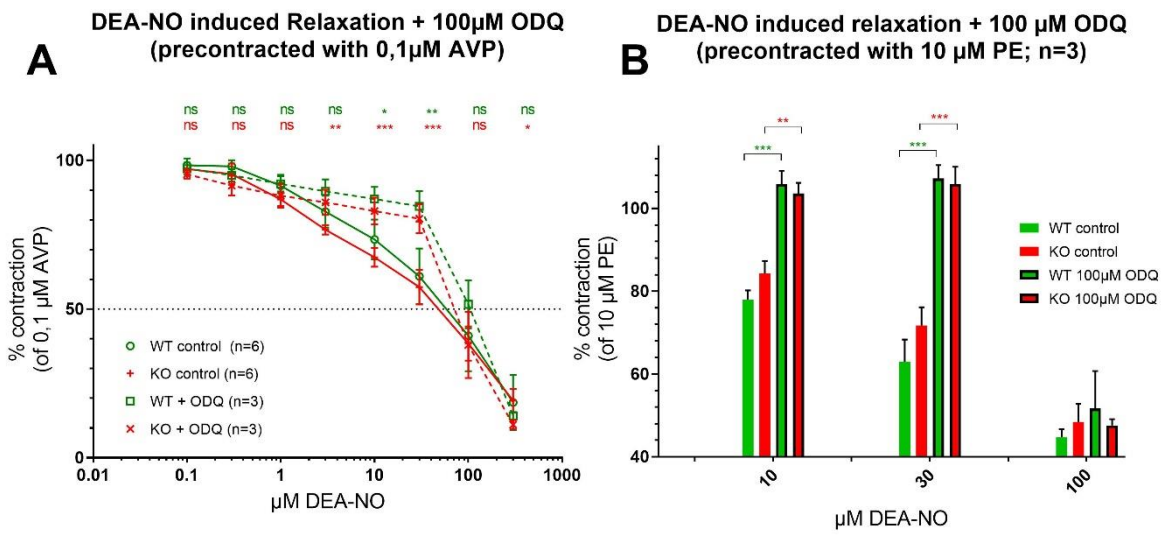

Figure 27: Effect of 100 µM ODQ on DEA-NO mediated relaxations of male urethras precontracted by either 0,1 µM AVP or 10 µM PE

(A): The urethral rings were precontracted with 0,1 µM AVP for 5 minutes, after which they were incubated with 100 µM ODQ for 10 minutes (control groups were not incubated with ODQ). All groups were then subjected to increasing concentrations of DEA-NO. Urethral ring preparations of the ODQ groups of both genotypes showed a significant attenuation of the relaxing effect of DEA-NO in concentrations > 100 µM for KO, and 10 µM for WT animals. (B): WT (n=3) and KO (n=3) mice were precontracted by 10 µM PE for 5 minutes, after which DEA-NO was cumulatively added every 3 minutes for concentrations of 10, 30 and 100 µM DEA-NO. After washing with PSS 3 times for 20 minutes, 100 µM ODQ was added and the procedure was repeated. Addition of ODQ caused a significant decrease of relaxation elicited by of 10 and 30 µM DEA-NO. Contraction is expressed in percent of AVP (A) or PE (B) induced force. Symbols and error bars represent means ± SD. Statistical significance was tested using unpaired, two-tailed students t-tests.

4.5. Relaxation induced by electric field stimulation

When working with NO donors, it is important to keep in mind that the NO concentrations released are not in the physiological range. Therefore, electrical field stimulation (EFS) was used to test the effect of endogenously released NO on precontracted urethral ring preparations. Atropine, phentolamine, indomethacin and propranolol (1µM each) were used to suppress adrenergic and cholinergic responses and to unmask the effects of NANC neurons. 0,1 µM AVP or 10 µM PE were used to precontract the preparations (Figure 28). In the latter case, phentolamine was omitted.

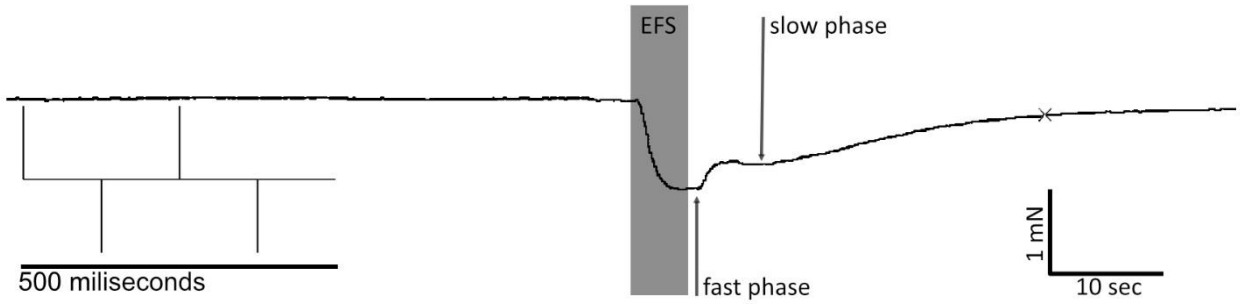

Figure 28: Typical EFS elicited relaxation
Original force tracing of 8 Hz bipolar pulses of 40 V and 5 second duration (0,5 ms pulse width). The urethral preparation was taken from a 112-week-old male WT mouse precontracted with 0,1 µM AVP. Insert: schematic view of the applied pulse at 8 Hz.

EFS induced relaxation exhibited two phases: A fast relaxation phase, that started ~1 second after onset of EFS reaching a plateau after ~3 seconds. Upon cessation of the stimulation the preparation remained relaxed for ~1 second, after which a fast partial tension recovery could be observed followed by a partial relaxation 10-15 seconds after onset of stimulation (slow phase), followed again by a gradual rise in force, approximately reaching initial values before EFS after 3 minutes (Figure 28).

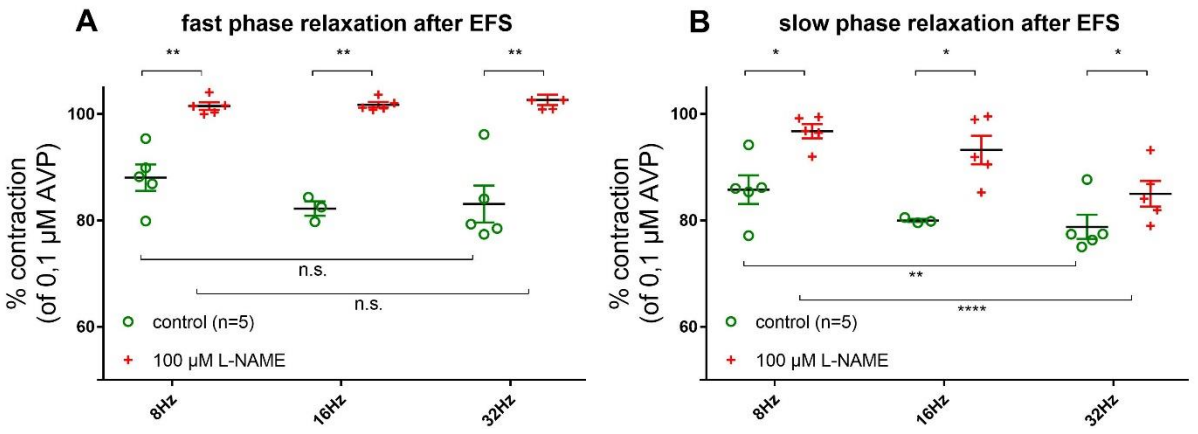

Figure 29: EFS-induced relaxation at increasing frequencies with and without L-NAME
Effect of L-NAME on fast and slow phase relaxation elicited by EFS (0,5 ms bipolar pulse width, 5 s duration, 40 V) of urethras of male WT animals of ~100 weeks of age. The urethras precontracted by 0,1 µM AVP in the presence of atropine, phentolamine, indomethacin and propranolol (1 µM each). The data are expressed in percent of the force immediately before the first EFS stimulation (mean ± SD, n=5).

The results show a frequency dependent relaxation in all preparations, with higher frequencies yielding a stronger relaxation. This increase in relaxation was significant regarding the slow, but not the fast relaxation phase (Figure 29).

To test the hypothesis, that EFS mediated relaxation involves release of NO, NOS was inhibited by the pan NOS inhibitor N^{ω}-nitro-L-arginine-methyl ester (L-NAME). L-NAME abolished the fast phase relaxation at all frequencies (Figure 29 A) and significantly attenuated the slow phase relaxation by 10,9±6,8 %, 16,8±4,7 % and 6,2±6,2 % at 8, 16 and 32 Hz, respectively (Figure 29 B).

I next tested the hypothesis, that EFS mediated relaxation involved activation of soluble guanylyl cyclase (sGC) using the sGC inhibitor ODQ. Inhibition of the soluble guanylyl cyclase (sGC) by ODQ suppressed the fast phase relaxation completely and significantly attenuated the slow relaxation phase by 4,6±1,7 %, 5,3±1,8 % and 8,1±2,1 % at 8, 16 and 32 Hz, respectively (Figure 30 B).

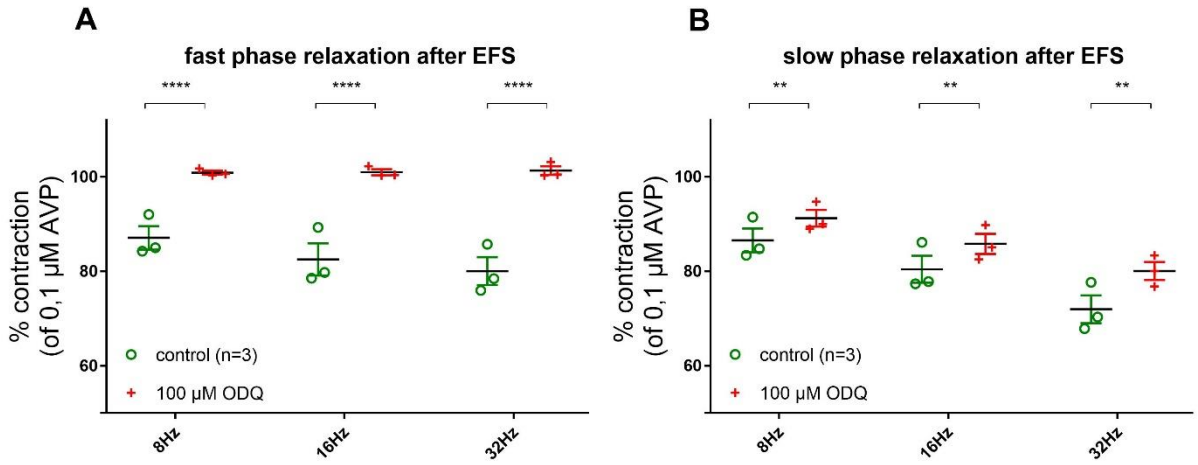

Figure 30: Effect of ODQ on EFS-induced relaxation of male urethras precontracted by AVP

Effect of ODQ on fast and slow phase relaxation elicited by EFS (0,5 ms bipolar pulse width, 5 s duration, 40 V) of urethras of male WT animals of ~ 20 weeks of age. The urethras were precontracted by 0,1 µM AVP in the presence of atropine, phentolamine, indomethacin and propranolol (1 µM each). The data are expressed relative to the force immediately before the first EFS stimulation (mean ± SD, n=3).

To verify that EFS-induced relaxations were mediated by stimulation of neurons, the sodium channel blocker tetrodotoxin (TTX) was used: Addition of 1 µM of TTX abolished the fast relaxation phase at 8 Hz completely and nearly completely at 16 and 32 Hz. TTX also significantly attenuated the slow relaxation phase compared to the control group (Figure 31 B).

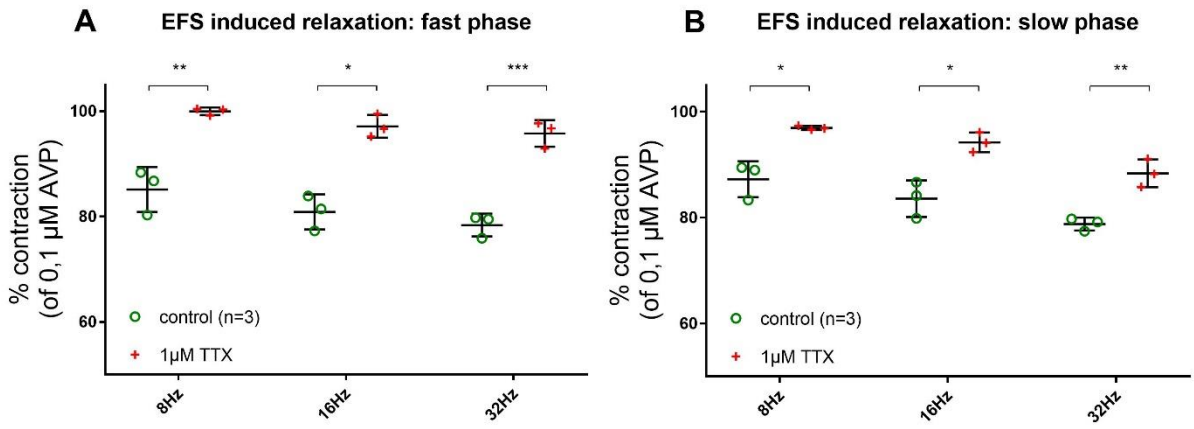

Figure 31: TTX inhibits EFS induced relaxation
Effect of TTX on the fast and slow relaxation phase of urethras from 3 ~100-week-old mice (1 WT male, 2 telokin-/- female) precontracted by 0,1 µM AVP in the presence of 1 µM each of atropine, phentolamine, indomethacin and propranolol. The data are represented relative to the contraction force immediately before the first EFS stimulation (mean ± SD, n=3).

Tubocurarine, a competitive nicotinic acetylcholine receptor antagonist, was used to assess the possibility that relaxation of the skeletal muscle sphincters contributes to the effect of EFS. 0,1 µM tubocurarine did not affect the fast relaxation phase at neither 8 or 32 Hz (Figure 32 A). It significantly attenuated the slow relaxation phase at 8 Hz but not at 32 Hz. (Figure 32 B).

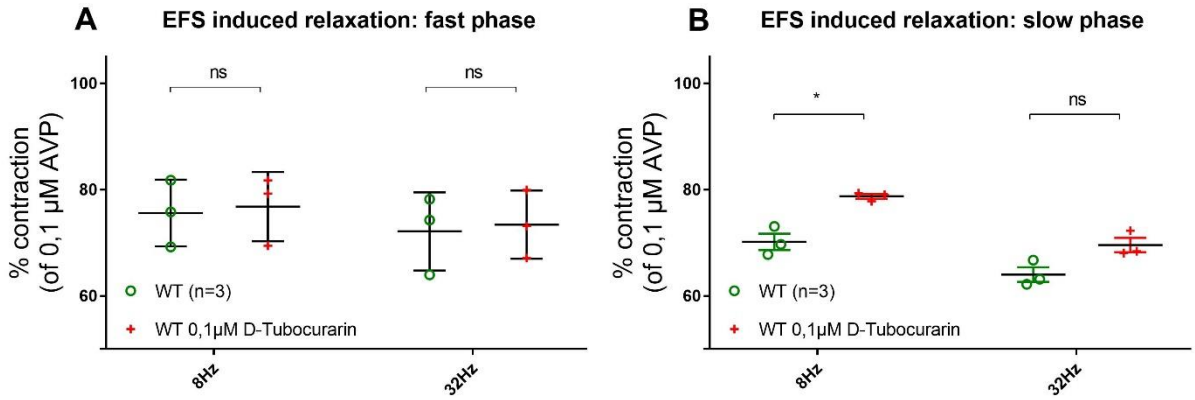

Figure 32: Effect of tubocurarine on EFS induced relaxation
Effect of tubocurarine on the fast and slow relaxation phase of urethras precontracted by 0,1 µM AVP in the presence of 1 µM each of atropine, phentolamine, indomethacin and propranolol. The data are expressed relative to the contraction force immediately before the first EFS stimulation (mean ± SD, n=3 urethral ring preparations from ~ 100-week-old female WT).

The competitive PKA inhibitor 8-(4-Chlorophenylthio)adenosine-3′,5′-cyclic monophosphorothioate (Rp-8-CPT-cAMPS) was used to test whether activation of PKA contributes to the EFS-induced relaxation. Rp-8-CPT-cAMPS significantly reduced the fast relaxation phase of urethras in KO urethras compared to WT animals (Figure 33 A). The slow relaxation phase remained unaffected (Figure 33 B).

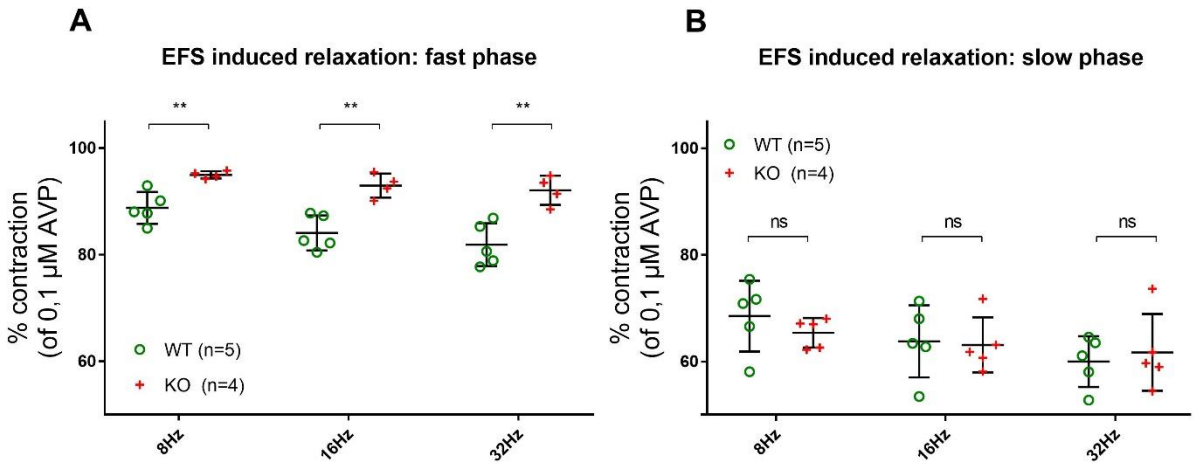

Figure 34: EFS-induced relaxation in the presence of Rp-8-CPT-cAMPS
EFS (0,5 ms bipolar pulse width, 5 s train duration, 40 V, frequency of 8, 16 and 32 Hz) induced relaxation of urethras precontracted by 0,1 µM AVP in the presence of 1 µM each of atropine, phentolamine, indomethacin and propranolol and 300 µM Rp-8-CPT-cAMPS. The data are expressed relative to the contractile force immediately before the first EFS stimulation (mean ± SD, n=4-5).

Subsequently the NO synthase inhibitor L-NAME was applied to test the contribution of NO and the cGMP pathway: 300 µM Rp-8-CPT-cAMPS was applied ~30 minutes before a contraction by 0,1 µM AVP was elicited. As the contraction force reached a plateau after ~ 5 minutes, a first series of EFS induced relaxations were induced. Then, after application of 100 µM L-NAME, followed by a 10-minute resting period, a second series of EFS was performed.

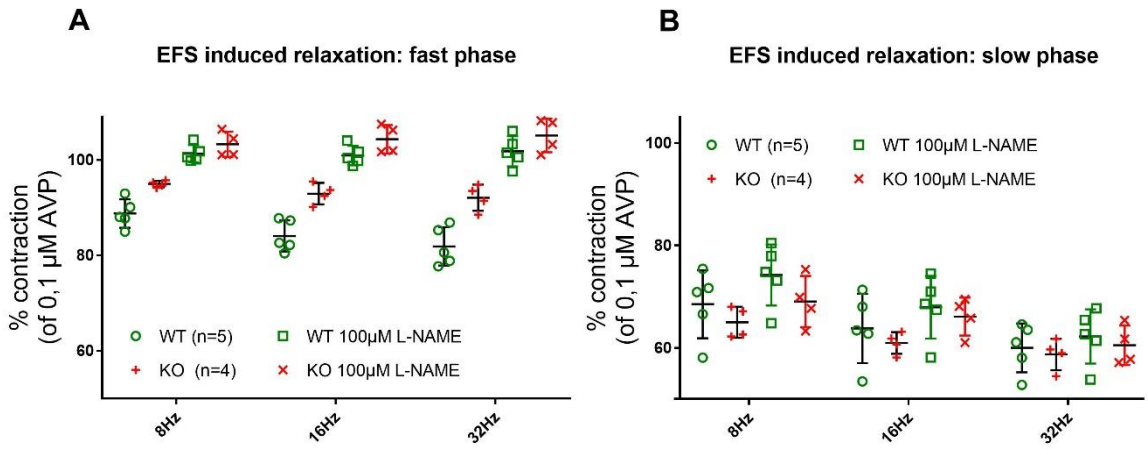

Figure 33: Combined inhibition of NOS and PKA
EFS (0,5 ms bipolar pulse width, 5 s duration, 40 V, frequency of 8, 16 and 32 Hz) induced relaxation of urethras precontracted by 0,1 µM AVP in the presence of 1 µM each of atropine, phentolamine, indomethacin and propranolol and 300 µM Rp-8-CPT-cAMPS. The data are expressed relative to the contraction force immediately before the first EFS stimulation (mean ± SD, n=4-5).

L-NAME further reduced the fast relaxation phase at all frequencies for urethras of both WT and KO animals (Figure 34 A) but had no effect on the slow relaxation phase (Figure 34 B). A three-way ANOVA test identified L-NAME, genotype and their combination as significant

factors for the fast relaxation phase. For the slow relaxation phase only the stimulation frequency and the presence of L-NAME were found to cause statistical significance (Table 6).

source of variation	p value	summary	p value	summary
	fast phase relaxation		slow phase relaxation	
Hertz	0,8529	ns	<0,0001	****
L-NAME	<0,0001	****	0,0222	*
genotype	<0,0001	****	0,318	ns
Hertz x L-NAME	0,4007	ns	0,3986	ns
Hertz x genotype	0,4866	ns	0,4908	ns
L-NAME x genotype	0,0249	*	0,6124	ns
Hertz x L-NAME x genotype	0,884	ns	0,8934	ns

Table 6: L-NAME influence on EFS-induced relaxation in the presence of a cAMP inhibitor
Results of a three way ANOVA test with the parameters genotype, Hertz and treatment with L-NAME. 5 WT and 4 KO male animals were used with an age of ~20 weeks.

In females, urethral ring preparations of WT mice responded stronger to EFS than KO mice: Specimens of both young and old mice showed a significant stronger relaxation after EFS for both the fast and slow phase relaxation at all frequencies (Figure 35).

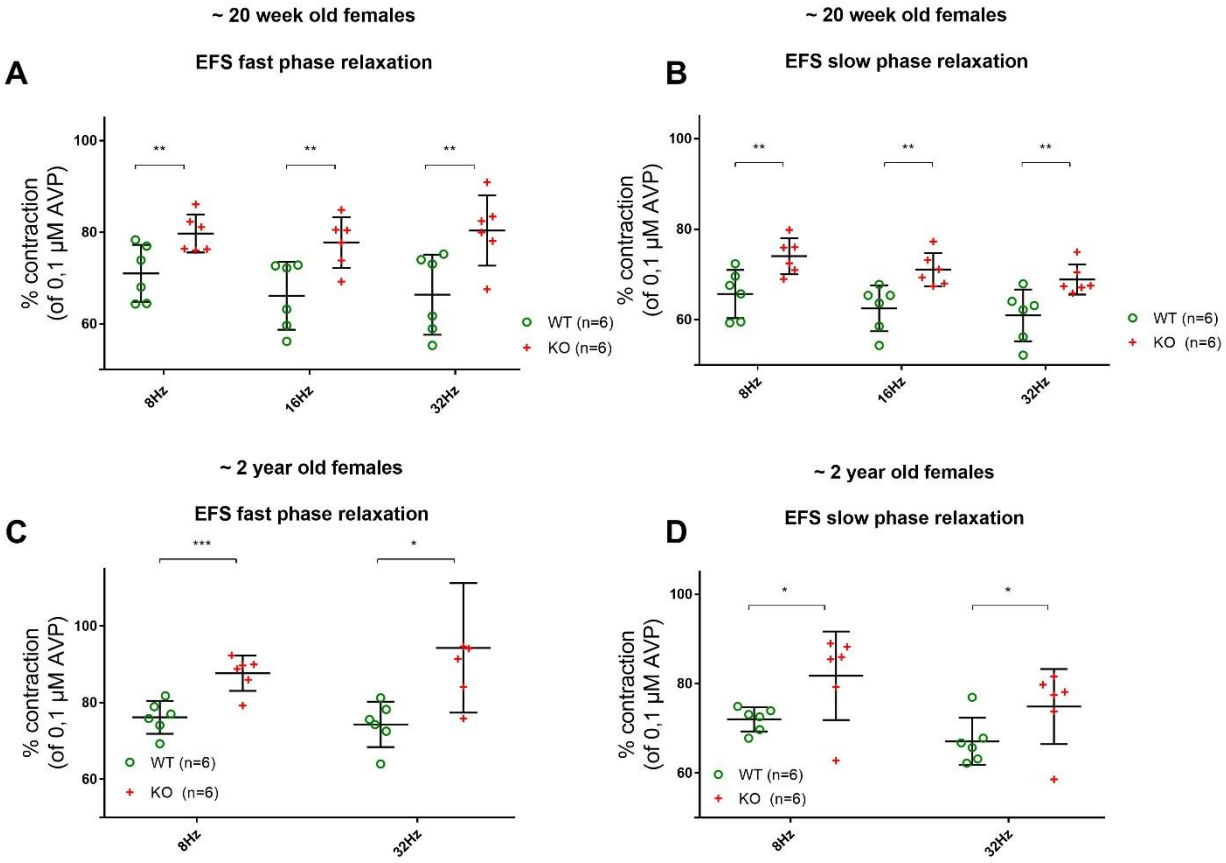

Figure 35: EFS induced relaxation of urethras from female mice
Fast and slow phase relaxation response elicited by EFS (0,5 ms bipolar pulse width, 5 s train duration, 40 V, frequency of 8, 16 and 32 Hz) of urethras precontracted by 0,1 µM AVP in the presence of atropine, phentolamine, indomethacin and propranolol (1 µM each). The data are expressed relative to the contraction force immediately before the first EFS stimulation (mean ± SD, n=6). The p values were calculated using paired, one-tailed students t-tests.

Deletion of telokin did not affect the male response to EFS of urethral preparations precontracted with 0,1 µM AVP: Neither age group showed a significant difference of the fast phase or slow relaxation phase at any frequency (Figure 36).

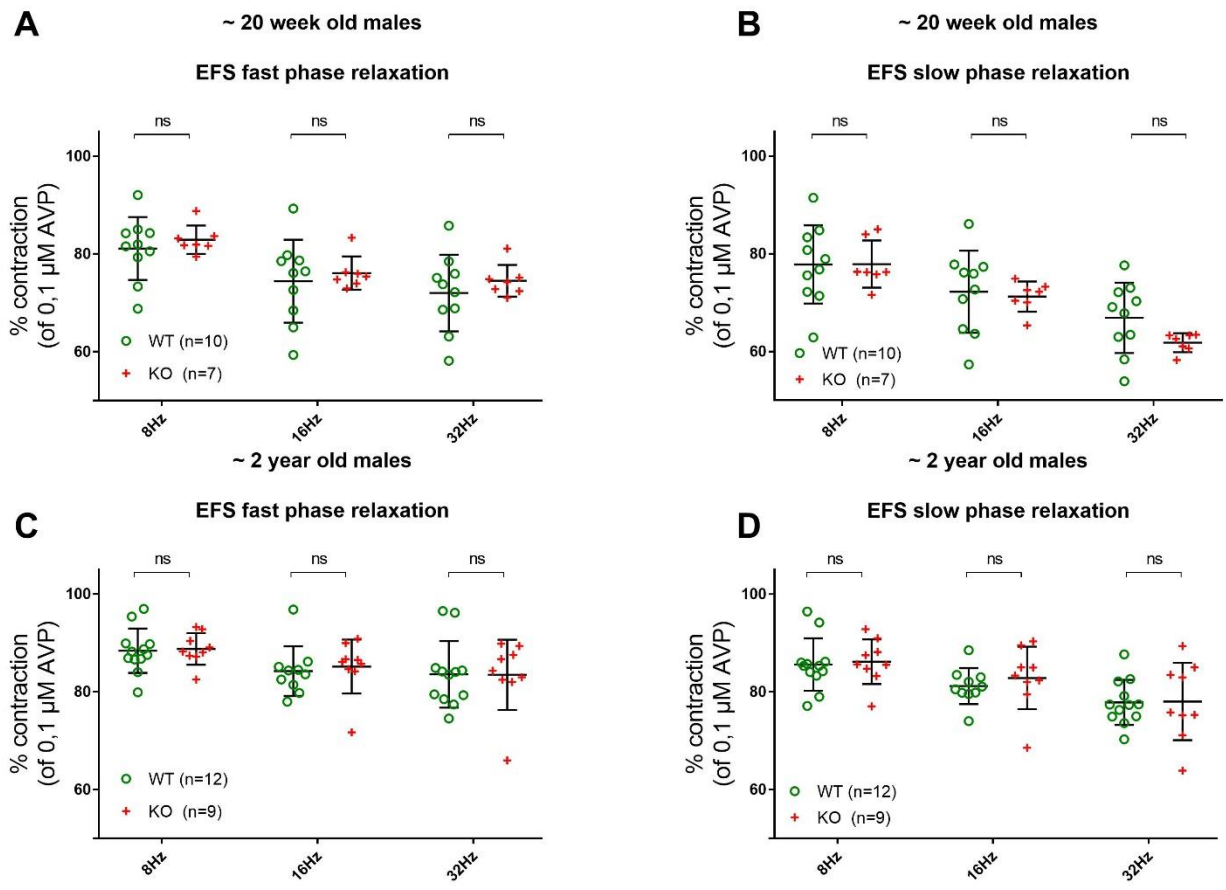

Figure 36: EFS induced relaxation of male mice
Fast and slow phase relaxation response elicited by EFS (0,5 ms bipolar pulse width, 5 s train duration, 40 V, frequency of 8, 16 and 32 Hz) of urethras precontracted by 0,1 µM AVP in the presence of 1 µM each of atropine, phentolamine, indomethacin and propranolol. The data are expressed relative to the contraction force immediately before the first EFS stimulation (mean ± SD, n=7-12).

4.5.1. Relaxing effect of EFS on PE precontracted preparations

EFS was also tested on preparations of young and old males precontracted by PE. These experiments were performed in accordance with the ones using AVP, albeit without the addition of phentolamine, as this would impair the PE induced contraction.

While the old age group did not show a difference between WT and KO, the young age group exhibited a significant stronger fast relaxation phase for WT compared to KO mice at 16 and 32 Hz (Figure 37).

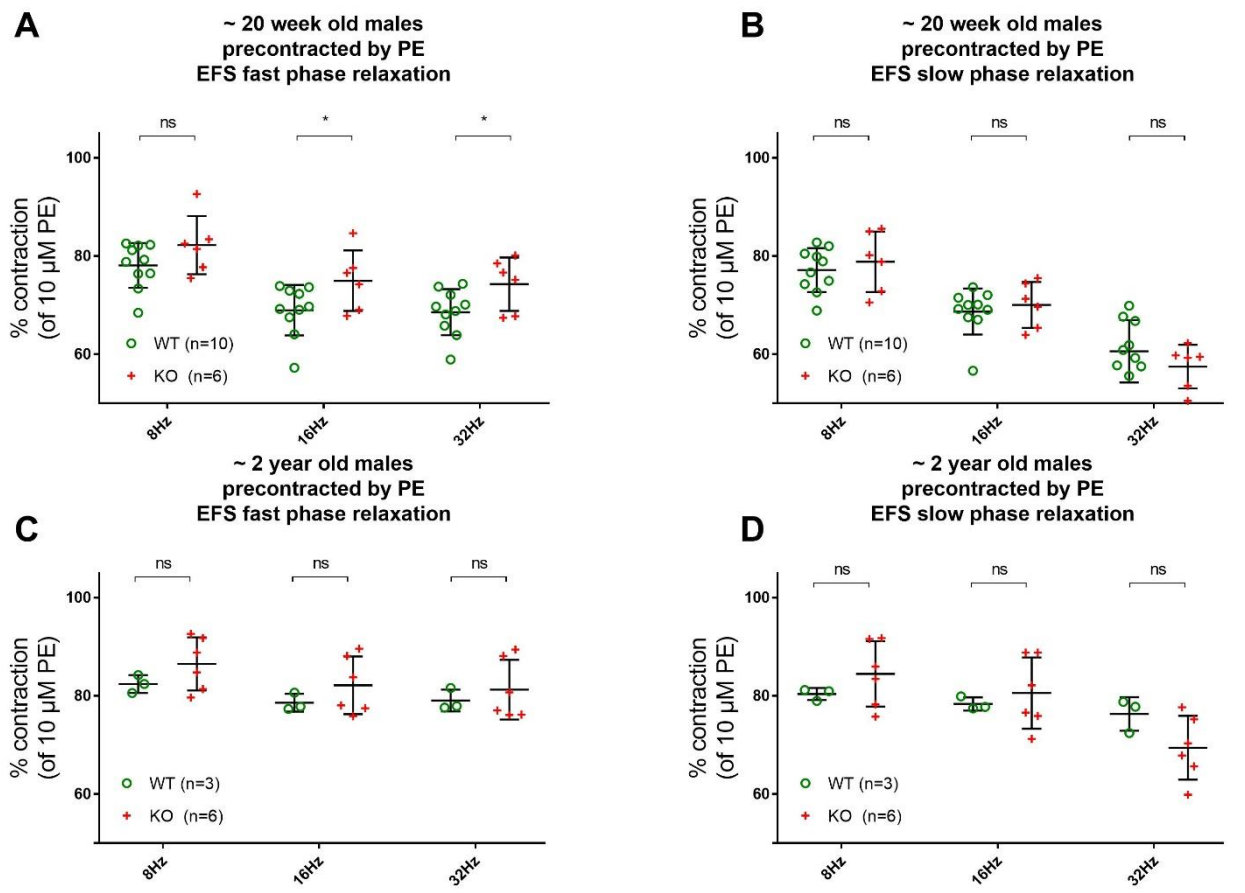

Figure 37: EFS induced relaxation of male mice on preparations precontracted by PE
Fast and slow phase relaxation response elicited by EFS (0,5 ms bipolar pulse width, 5 s duration, 40 V, frequency of 8, 16 and 32 Hz) of urethras precontracted by 10 µM PE in the presence of 1 µM each of atropine, indomethacin and propranolol. The data are expressed relative to the contraction force immediately before the first EFS stimulation (mean ± SD, n=3-10).

In two previous experiments, ODQ was used to inhibit the sGC to test the role of the cGMP pathway. The addition of ODQ yielded the same result as in preparations precontracted with AVP: The fast phase was abolished and the slow phase markedly attenuated (Figure 38).

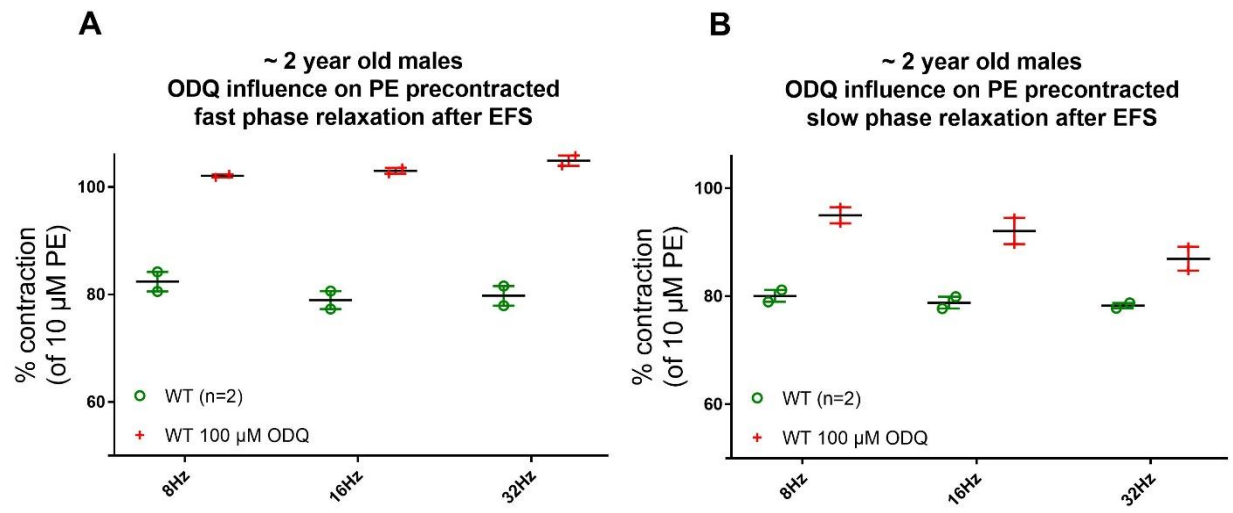

Figure 38: ODQ influence on EFS induced relaxation of preparations from male mice precontracted by PE
Fast and slow relaxation phases elicited by EFS (0,5 ms bipolar pulse width, 5 s duration, 40 V, frequency of 8, 16 and 32 Hz) of urethras precontracted by 10 µM PE in the presence of 1 µM each of atropine, indomethacin and propranolol. The data are expressed relative to the force immediately before the first EFS stimulation (mean ± SD, n=2).

5. Discussion

Filling, storing and voiding urine from the bladder requires a complex interplay between the detrusor smooth muscle of the bladder and the smooth and striated muscle of the urethra, the latter forming the internal and external urethral sphincters. Many systems and signalling cascades interact with each other, creating a delicate balance between contracting and relaxing activity. When this balance is disturbed, the patient may experience lower urinary tract symptoms (LUTS), ranging from urinary incontinence to overactive bladder syndrome. More than 70 % of subjects older than 40 years experience LUTS at least once in their lifetime (Coyne et al. 2009), making the research of the mechanisms of the lower urinary tract clinically relevant.

The mechanisms of urethral activity are intensely researched and many factors contributing to impaired function of the LUT were singled out: Studies showed that age contributes to urethral hyper-excitability and reduced relaxation (Triguero et al. 2014) and that different kinds of LUTS affect males more than females and vice versa (Irwin et al. 2006). An important signalling cascade in urethral contraction is the NO-PKG pathway. Consequences of PKG activation include lowering of the $[Ca^{2+}]_i$ and Ca^{2+}-desensitization. One of the targets of PKG is telokin, which disinhibits MLCP, thereby favouring relaxation. Based on previous studies on ileal and abdominal SM, it is a reasonable hypothesis that telokin is a mediator of urethral SM relaxation. In the present study I examined the effects of telokin, age and sex on contraction and relaxation ex vivo using urethral ring preparations. To my knowledge, no prior study has presented the combined effects of these three parameters on SM before. I tested the hypothesis that in telokin deficient urethras (1) contractile response is augmented and (2) relaxation is impaired. For this I conducted concentration response curve experiments with the contractile agonists AVP and PE and, in addition, I assayed their relaxations induced by DEA-NO and electric field stimulation in preparations precontracted by AVP and PE.

5.1. Experimental procedure

All animals were sacrificed by cervical dislocation and their urethras transferred into the myobath containing PSS at pH 7,4. After gradually heating the PSS up to 37 °C over the course of 60 minutes, the specimens were stretched to the optimal passive tension of ~ 1 mN. Every specimen was subjected to three control contractions elicited by K^+-PSS. The Myograph System 610A by Danish Myo Technology was used for isometric force recording.

Animal weight of WT mice was comparable with current literature using the C57BL/6 strain (e.g., weight of ~20 week old males: 30±2,3 g (my results) vs. 26.9±0,3 g (Aizawa et al 2012)). Vasopressin (AVP) and phenylephrine (PE) were used to assay the urethras contractile response. AVP, also called antidiuretic hormone, is released form the posterior pituitary gland and plays a key role in regulating blood pressure. There are four known receptors for AVP,

V1a receptors, V1b receptors, V2 receptors and oxytocin receptors. In the murine urethra, AVP induced contractions are mediated by the V1a receptor, which is coupled to Gq (Zeng et al. 2015). Its two main functions are increasing the amount of water reabsorption into the kidneys and contraction of vascular walls, both of which increase blood pressure (Cuzzo et al. 2023).
In addition, the contractile response to PE on urethras from male mice was tested. PE is an α_1-adrenoceptor agonist, which is coupled to G_q. Expression of adrenoceptors is abundant in male urethras, while in female urethras α_1-receptor mediated contraction seems to be of less importance (Alexandre et al. 2017).
NO-induced relaxation was tested using the NO-donor DEA-NO on specimens precontracted by either AVP or PE. In addition, EFS experiments were performed to assay the effects of neuronally released NO.

5.2. Outflow obstruction and bladder hypertrophy

In rats, mild or severe obstruction of the urethra led to a significant increase in bladder weight after 7-14 days (Saito et al. 1993). In my studies, young telokin$^{-/-}$ females had a significantly heavier bladder compared to WT mice, and old females showed a trend towards higher bladder weight (p=0,0606). The bladder weight to body weight ratio was also significantly higher in female telokin$^{-/-}$ mice.
This leads to the notion, that the impaired relaxation due to lack of telokin is, in females, severe enough to cause partial outflow obstruction and consequently hypertrophy of the bladder, e.g., increased bladder weight. Males, however, which did not show any effect of telokin deletion in EFS induced relaxation, did not exhibit a significantly increased bladder weight. It stands to reason, that telokin deletion did impair relaxation of female urethras, causing outflow obstruction leading to hypertrophy of the bladder, while male response to deletion of telokin was, if at all, much milder and did not cause outflow obstruction.
Mice deficient in PKG exhibited no difference in animal weight or ratio of bladder to body weight when compared to WT (Persson et al. 2000).

5.3. Influence of age on body weight and bladder weight

In my studies I found that body weight of ~2-year-old WT and telokin$^{-/-}$ mice was significantly (p<0,0001) increased compared to their ~20-week-old male and female counterparts. A significant increase in body weight with age in mice was also reported by Oliviera (de Oliviera et al. 2019). In rats, middle-aged animals (12-15 months old) exhibited a significantly higher body weight when compared to 3-month-old animals (Kimura et al. 2018).
In senescence-accelerated mice, body weight was significantly decreased when compared to the control group, made up of senescent-accelerated mouse resistant mice (Triguero et al. 2014). The mice used were 36-38 weeks old at the time of death, which is equivalent to over

“middle-aged” in non-senescence-accelerated mice (Kang et al. 2014). The senescence-accelerated mouse prone strains (SAMP) have been created to simulate accelerated aging (Takeda et al. 1981). When compared to mice from the same genetic background but with a normal life expectancy (senescence-accelerated resistant, SAMR), these models can be utilized to investigate the impact of aging on various systems, including the nervous, cardiovascular, and endocrine systems.

In my studies, bladder weight, both in absolute values and in relation to body weight, of mice of both genotypes and sexes was also significantly ($p<0,0001$) increased with ageing. It is worth noting, that, compared to young animals, the variability of bladder weights (absolute and normalized to body weight) is higher in old animals.

The mice in my experiments had a median age of 4±0,7 and 25,1±2 months in young and old animals, respectively. When comparing female mice of 3 and 18 months of age, the significance in bladder weight, but not the bladder to body weight ratio, was reported (de Oliviera et al. 2019).

5.4. Influence of age on function

In the present study, aged female mice (both telokin$^{-/-}$ and WT) displayed a significantly weaker contraction in response to stimulation by 125 mM K^+ compared to young mice ($p<0,01$). Such a difference was not observed in 80 mM K^+ induced urethral contractions between 3- and 18-month-old female mice (de Oliviera et al. 2019). Likewise, no difference in urethral contractions induced by high K^+ concentrations was observed in both the SAMR1 and SAMP8 strains (Triguero et al. 2014).

I observed a leftward shift of old mice in the concentration response curve (CRC) for AVP: Old WT and telokin$^{-/-}$ females as well as telokin$^{-/-}$ males exhibited a significantly stronger reaction to AVP compared to young animals. A possible explanation for the increased sensitivity with age is an increase of the receptor density.

Interestingly, I observed the opposite effect in the CRC experiments for PE: Old males (telokin$^{-/-}$ and WT) displayed a rightward shift compared to young mice ($p<0,0001$). In my research, I limited my experiments involving PE on male mice, as the density of α_1-adrenoceptors is lower in female urethras compared to males (Alexandre et al. 2017).

Further, I performed CRC experiments of DEA-NO on urethras precontracted by AVP as well as PE. I observed no differences between the age groups in neither sex or genotype. This is in accordance to studies comparing CRC of DEA-NO in urethras precontracted by 0,1 µM AVP in senescence accelerated and senescence resistant mice (Triguero et al. 2014).

Higher contraction force in aged mice was also reported in senescent murine femoral arteries (Lubomirov et al. 2021) and basilar arteries (Lubomirov et al. 2016). In both cases the basal phosphorylation levels of RMLC were significantly increased. Such experiments in murine

urethra were not published so far to the best of my knowledge. A similar effect could be possible in the urethra.

5.5. Influence of sex

In my results, males exhibited a significantly higher body weight compared to females across both age groups and genotypes (telokin$^{-/-}$ and WT). In his paper, Triguero also reported a higher body weight in male mice compared to female, although this result was not significant. Further, the bladder weight of young females (both telokin-/- and WT) and aged WT females was significantly lower when compared to males. Aged telokin deficient mice do not express a significant difference in bladder weight. Young WT males showed a significantly higher bladder weight to body weight ratio compared to females. This was also reported in both the SAMR1 and the SAMP8 strains (Triguero et al. 2014).

In my studies, males of both ages and genotypes displayed a significantly stronger contractile force in response to stimulation by 125 mM K^+ ($p<0,0001$) when compared to females. This is in accordance with findings by other researchers (Triguero et al. 2014).

Reports of sex difference in the physiology of the lower urinary have been numerous and include studies on many different species (Patra 2013). In humans, the level of muscarinic receptors expressed in the trigone was found to significantly differ between sexes, as males showed a higher amount of the M2 and M5 subtypes when compared to females (Sigala et al. 2002) In addition, α_1-adrenergic receptors were reported to be more widely expressed in the trigone of females (Sigala et al. 2004). Further, the urinary ratio of ATP to creatinine was 4-fold higher in females compared to males (Sugaya et al. 2009).

In rabbits, EFS induced urethral relaxation was significantly higher in males compared to females (Lee et al. 1994). In addition, females exhibited a significantly higher density of α_2 adrenoceptors in the urethra (Morita et al. 1987), and of β adrenoceptors in the bladder (Morita et al. 1998).

Urethras from female dogs are reported to contain higher proportion of collagen and lower proportion of muscle tissue compared to males (Ponglowhapan et al. 2008). Further, COX2 expression was higher in females compared to males (Ponglowhapan et al. 2009).

In rats, a substantial body of work was done regarding differences between sexes in LUT pharmacology. The external urethral sphincter (EUS) of females was described as poorly developed, whereas the male EUS is reported to be extensive and thick (Cruz et al. 2005).

It was reported, that the detrusor from female rats was more sensitive to carbachol compared to males (Longhurst et al. 2000). Further, EFS induced contractions of male urethras were reported to have a significantly higher purinergic component compared to females (Creed et al. 2010).

It was reported that there exists a distinction in the expression and biological activity of phosphodiesterase type 5 (PDE5) in the male and female bladders of rats. Specifically, PDE5 activity is more evident in males compared to females (Vignozzi et al. 2012).

5.6. Influence of telokin on contraction and relaxation

As detailed in the introduction, it was reported that telokin affects relaxation and contraction, possibly by increasing the activity of MLCP in the contractile machinery, thus decreasing Ca^{2+} sensitivity.

In permeabilized murine ileum, telokin$^{-/-}$ animals exhibit a significant left shift of the pCa-force relationship compared to WT (Khromov et al. 2006). Permeabilization allows for direct study of the contractile machinery without interference of Ca^{2+} fluxes. The same study also showed significantly attenuated relaxation by 8-Br-cGMP of Ca^{2+}-induced force in murine telokin$^{-/-}$ ileal SM compared to WT mice.

In non-permeabilized fundus SM of 6–8-week-old male mice, contractile responses of telokin$^{-/-}$ SM to 1µM CCh and KCl were significantly larger compared to WT mice. Relaxation of fundus preparations of telokin$^{-/-}$, precontracted by either CCh or KCl, was significantly attenuated in response to an NO donor (sodium nitroprusside, SNP) as well as in response to EFS (An et al. 2015).

In my own studies, I was in part able to corroborate the increased contractile response of telokin deficient mice compared to WT: Young and old females as well as old males had a significantly increased urethral contraction force in response to AVP. However, in young male mice of ~20 weeks of age I did not observe a significant difference in urethral contractile force between telokin$^{-/-}$ and WT mice in response to AVP, PE or KCl stimulation.

The reduced relaxation of telokin$^{-/-}$ mice reported by An is, in part, in accordance with my own findings: In urethras precontracted with AVP, female WT showed a significantly larger relaxation to DEA-NO compared to telokin$^{-/-}$ mice. No difference between the genotypes was found in old males however, and young males even showed a greater relaxation in KO mice compared to WT. This is in contrast to NO-induced relaxation of male urethras both young and aged precontracted by PE: Both age groups exhibited a significantly stronger relaxation for WT compared to telokin$^{-/-}$ mice.

The reduced relaxing effect of EFS of telokin$^{-/-}$ mice on precontracted smooth muscle described by An was, in part, seen in my experiments: Females of both age groups exhibited significantly attenuated EFS induced relaxation of AVP-precontracted urethras in KO compared to WT mice. Both young and old females displayed a significantly attenuated relaxation in telokin$^{-/-}$ urethras compared to WT in both the fast and slow relaxation phase and across all frequencies (8, 16 and 32 Hz). In males however, no such difference between telokin deficient mice and WT was observed in neither age group, when precontracted by AVP. When precontracted by

PE, there was a significant attenuation of urethral relaxation in young telokin$^{-/-}$ males during the fast relaxation phase at 16 and 32 Hz compared to WT.

5.7. Mechanisms of NO-mediated relaxation

Relaxation of the urethra is mainly mediated by the NO-sGC-cGMP-PKG pathway. This was demonstrated in a series of elegant experiments by different researchers:

Neuronal nitric oxide synthase (nNOS) deficient mice displayed significantly larger bladders with substantial muscular hypertrophy compared to WT (Burnett et al. 1997). Low frequency EFS induced relaxation of urethral preparations was present in WT, but absent in nNOS^{-} animals. The nitric oxide synthase inhibitor L-NAME was able to inhibit the relaxation in WT animals. SNP, an NO donor, induced urethral relaxation in both WT and nNOS^{-} animals to the same extent, which were both inhibited by the soluble guanylyl cyclase (sGC) inhibitor ODQ. These findings indicate, that the nNOS is critical for urethral relaxation. My own results corroborate this conclusion, as L-NAME was able to abolish the EFS induced fast relaxation phase on AVP-urethras.

NO activates sGC, the deletion of it abrogated DEA-NO-induced relaxation in murine urethral SM, indicating that sGC is a downstream target of nNOS (Lies et al. 2013). This is in accordance with my experiments, where the guanylyl cyclase inhibitor ODQ significantly attenuated DEA-NO induced relaxation and abolished EFS induced relaxation in urethras precontracted by AVP or PE.

Given the high amount of NO an NO-donor allocates, it is not surprising, that ODQ was not able to completely abolish DEA-NO induced relaxation. NO release from nitrergic nerve endings induced by EFS is a much more physiological approach, with NO levels more akin to the ones in vivo, and more emphasis should be given the EFS experiments rather than the ones with an NO donor.

Activation of adenylate cyclase and guanylate cyclase by dibutyryl camp and 8-Br-cGMP, respectively, resulted in elevation of cAMP and cGMP levels in on SM strips of urethra and bladder from rabbits (Morita et al. 1992). This also led to a dose dependent relaxation. While bladder SM reacted more strongly to cAMP than to cGMP, urethras reacted more strongly to cGMP than to cAMP.

Deletion of PKG significantly impaired relaxation induced by an NO donor, a cGMP analog and a cAMP activator in murine urethras precontracted by AVP. Further, EFS induced relaxation was practically abolished in PKG$^{-/-}$ mice (Persson et al. 2000). The NOS inhibitor LNNA did inhibit EFS induced relaxation of WT, but had no effect in PKG $^{-/-}$ mice. The findings from immunohistochemical investigations revealed no variation in the location of nerves rich in NO in mice deficient in PKG, thereby indicating that the source of NO production remained unaffected (Persson et al. 2000).

All these findings, implicating the importance of the NO-sGC-cGMP-PKG pathway in urethral relaxation, are consistent with the results of my studies. Further, I was able to additionally show, that telokin is downstream component of the signalling cascade.

		Contraction					Relaxation		
WT vs KO		AVP Fmax	AVP pEC50	PE Fmax	PE pEC50	KCl Fmax	DEANO pIC50	EFS fast % relaxation	EFS slow % relaxation
young	♀	=	=			=	=	>	>
	♂	=	=	=	=	=	=	=	=
old	♀	>	=			=	=	>	>
	♂	=	=	<	=	=	=	=	=
young vs old									
WT	♀	=	=			<	=	=	>
	♂	=	=	=	<	<	=	=	=
KO	♀	=	=			<	=	>	>
	♂	=	=	<	<	<	=	=	=
female vs male									
WT	young	=	=			>	=	=	=
	old	<	<			>	=	=	=
KO	young	=	=			=	=	=	=
	old	<	=			=	=	=	=

Table 7: Overview of results
An overview of the obtained results, comparing age and sex. The = symbol indicates no significant difference between the groups. When a significance difference was present, the symbols < and > show, which group had a higher value. Blue colored cells represent a significant outcome of the extra sum-of-squares F test, indicating that the concentration response curves differ between data sets. The EFS values represent the results at 8 Hz.

5.8. Telokin deletion attenuates EFS-induced relaxation only of SM of female mice

Electric field stimulation was used to test the effect of endogenously released NO. When applied to precontracted urethral ring preparations, a frequency dependent relaxation could be observed: A first, fast relaxation phase occurred for the duration of the stimulation (500 ms), beginning immediately after onset. After cessation, a temporary tension recovery could be observed. 10-15 seconds after the initial onset of the stimulation, a second, slow relaxation phase took place, which was generally weaker than the first.

EFS induces release of neurotransmitters from neurons (Ponce 2014) and also excites skeletal (Forrest and Briskey 1967) and smooth muscle (Paton 1975). Being interested only in relaxation caused by neuronal release of NO, thus activating the NO-sGC-cGMP-PKG

pathway, I took certain measures and conducted a series of experiments to rule out interference of other targets of EFS:

Firstly, the experiments were performed in the presence of 1 µM each of atropine (competitive antagonist of M1-M5), phentolamine (unspecific α antagonist), indomethacin (inhibitor of cyclooxygenase 1 & 2) and propranolol (nonselective β blocker). This cocktail was used to suppress the effects of adrenergic and cholinergic neurons (Yano et al. 1995), thereby preventing contractile responses to EFS, as well as possible artifacts by cyclooxygenases (Fornai 2005).

The voltage gated sodium channel blocker tetrodotoxin abolished the fast relaxation phase at all applied frequencies, and significantly attenuated the slow relaxation phase. This suggests, that the EFS induced fast relaxation phase was neuronally mediated.

Influence of striated muscles was tested using the nicotinic acetylcholine receptor antagonist tubocurarine: Although tubocurarine had no influence on the EFS-induced fast relaxation phase, it did attenuate the slow relaxation phase at 8 Hz (p=0,0169) and 32 Hz (p=0,0671). This suggests, that probably only the fast relaxation phase is entirely mediated by the NO-sGC-cGMP-PKG pathway.

Further, I tested the hypothesis, that the EFS induced relaxations were due to NO release by NANC neurons. Both the NOS inhibitor L-NAME and the sGC inhibitor ODQ abolished the fast relaxation phase at 8 Hz and significantly decreased it at 16 and 32 Hz. Interestingly, EFS still induced frequency dependent relaxation of the slow type in the presence of L-NAME and ODQ, albeit significantly attenuated. This suggests, that the slow relaxation phase is, in part, mediated by a non-nitrergic NANC mechanism. In future research, it would be of interest to study the combined effects of tubocurarine and TTX, especially how this would affect the slow relaxation phase. As it stands, both reduce the EFS-induced slow relaxation phase. It could either be possible, that their effects are mediated by the same mechanism. Or their effects could be additive, implying a different mechanism of action.

EFS mediated relaxation was significantly decreased in AVP-precontracted urethras from telokin$^{-/-}$ females. Both the fast and slow relaxation phases were significantly attenuated in KO mice in young as well as in the old age group when compared to WT. Urethras from male specimens did not show this difference between genotypes for neither relaxation phase for any frequency or age group, when precontracted by AVP.

Interestingly, when precontracted by PE, young males did exhibit a difference between the genotypes: Urethras from telokin deficient mice showed a trend towards impaired relaxation at 8 Hz (p=0,0695), and relaxation was significantly attenuated at 16 Hz (p=0,0269) and 32 Hz (p=0,0219) when compared to WT. The fact that young males only showed attenuated relaxation when precontracted by PE is puzzling, given that PE and AVP receptors both couple to the same type of GPCR, namely G_q (Zeng et al. 2015). A possible explanation lies in the

fact, that the PE experiments were conducted without the presence of phentolamine. The absence of this α_1 receptor antagonist may influence the contractility of the SM.
My results indicate, that relaxation is partially mediated by non-nitrergic NANC-mechanisms.

5.9. Non-nitrergic NANC mechanisms

A possible candidate as an inhibitory non-nitrergic NANC neurotransmitter is vasoactive intestinal polypeptide (VIP). VIP is one of the neurotransmitters responsible for EFS mediated relaxation of the female pig urethra (Hosokawa and Kaseda 1993). Rabbit urethra SM show a distribution of VIP-fibres throughout the smooth muscle layers, as well as a concentration dependent VIP induced relaxations (Waldeck et al. 1998). VIP relaxations are mediated by the cAMP-PKA pathway (Hernandez et al. 2006).
In my studies, inhibiting PKA with the Rp-8-CPT-cAMPS resulted in significantly weaker EFS-induced relaxations of the fast phase in urethras taken from KO animals compared to WT. However, the slow relaxation phase was unaffected by deletion of telokin in the presence of Rp-8-CPT-cAMPS.
Further, it may be possible, that β_3 receptors take part in the relaxation response seen in murine urethral experiments. The significance of the β_3 receptor was initially highlighted in urethras of rats, dogs, and guinea pigs, as β_3 agonists could induce relaxations (Takeda et al. 1999, Yamaguchi 2002). In human corpus cavernosum tissues, β_3 induced relaxations were independent from NO (Cirino et al. 2003). Also, because cGMP levels were significantly increased but cAMP levels remained unaffected by β_3 stimulation, it may suggest, that cGMP, rather than cAMP was involved in mediating the relaxant response to β_3 stimulation. Further, β_3 relaxant response may require inactivation of the ROK pathway.
In murine urethra, stimulation of β_3 receptors induced a significant increase in cAMP levels (Alexandre et al. 2017). In addition, ODQ failed to affect the relaxation induced by mirabegron, indicating no involvement of the cGMP pathway.
The β blocker propranolol I used in my experiments has a low affinity towards the β_3 subtype (Bylund et al. 2007). This makes it impossible to rule out a possible involvement in the results obtained in the present study.
ATP signalling, i.e., purinergic transmission, might be another possible mediator of NANC relaxation. In the rabbit bladder, purinergic transmission accounts for almost the entirety of detrusor contraction (Sibley 1984). In the urethra, ATP is reported to cause relaxations in pigs, guinea pigs, rabbits and hamsters (Burnstock 2013). The exact mechanism by which these relaxations occur are not yet fully understood. In one proposed mechanism, ATP acts through degradation to adenosine. This is unlikely, as the ecto-ATPase inhibitor ARL 67156 did not affect electrically evoked relaxations in the female pig urethra (Werkström et al. 2005).

5.10. Limitations of my studies and outlook

My results of this study relied on ex vivo experiments. Although many interesting results could be obtained by this approach, they are all limited to studying a tissue sample in a single point of time. Alterations of the phenotype based on sex, age or genotype, like for example an enlarged bladder, can only be studied at the time of dissection. In vivo experiments, however, would allow the researchers to study the animals over a long period of time and in their natural, physiologic conditions. Future research may be done on living animals. Non-invasive tests like the frequency volume chart and voiding spot assay allows the accurate measurement of micturition behaviour. To my knowledge, no research so far published results about the micturition behaviour of telokin deficient mice. Investigation of the storage and voiding phases using filling cystometry and pressure-flow studies, respectively, are well developed, invasive testing methods. Parameters assessed using these methods include bladder capacity and compliance, number of non-voiding contractions, maximum detrusor pressure, maximum flow rate and post voided residual volume (Ito et al. 2017). Together with conventional techniques used in ex vivo experiments, new questions could be pursued: Is there a relation between enlarged bladder and detrusor pressure? Are there many non-voiding contractions in mice with enlarged bladder? Is there a correlation between telokin deficiency and urethral flow rate? Mice developing lower urinary tract symptoms like overactive bladder syndrome or urine retention could be identified, monitoring the onset and progression of the symptoms.

Further, study of levels of expression and phosphorylation of telokin, PKG, MLCP, RMLC would be attractive aspects of future research.

In conclusion, more research is needed to further elucidate the role of age, sex and telokin in murine urethral relaxation.

6. References

Aizawa, N., Homma, Y., & Igawa, Y. (2012). Influence of High Fat Diet Feeding for 20 Weeks on Lower Urinary Tract Function in Mice. *LUTS: Lower Urinary Tract Symptoms, 5*, 101–108. doi:10.1111/j.1757-5672.2012.00172.x

Alexandre, E. C., de Oliveira, M. G., Campos, R., Kiguti, L. R., Calmasini, F. B., Silva, F. H., . . . Antunes, E. (2017). How important is the α1-adrenoceptor in primate and rodent proximal urethra? Sex differences in the contribution of α1-adrenoceptor to urethral contractility. *American Journal of Physiology-Renal Physiology, 312*, F1026–F1034. doi:10.1152/ajprenal.00013.2017

Alexandre, E. C., Kiguti, L. R., Calmasini, F. B., Silva, F. H., da Silva, K. P., Ferreira, R., . . . Antunes, E. (2016). Mirabegron relaxes urethral smooth muscle by a dual mechanism involving β3-adrenoceptor activation and α1-adrenoceptor blockade. *British Journal of Pharmacology, 173*, 415–428. doi:10.1111/bph.13367

An, C., Bhetwal, B. P., Sanders, K. M., Somlyo, A. V., & Perrino, B. A. (2015). Role of Telokin in Regulating Murine Gastric Fundus Smooth Muscle Tension. (A. Guerrero-Hernandez, Ed.) *PLOS ONE, 10*, e0134876. doi:10.1371/journal.pone.0134876

Andersson, K.-E. (2015). Purinergic signalling in the urinary bladder. *Autonomic Neuroscience, 191*, 78–81. doi:10.1016/j.autneu.2015.04.012

Andersson, K.-E., Pascual, A. G., Persson, K., Forman, A., & Tøttrup, A. (1992). Electrically-Induced, Nerve-Mediated Relaxation of Rabbit Urethra Involves Nitric Oxide. *Journal of Urology, 147*, 253–259. doi:10.1016/s0022-5347(17)37208-7

Ashton, F. T., Somlyo, A. V., & Somlyo, A. P. (1975). The contractile apparatus of vascular smooth muscle: Intermediate high voltage stereo electron microscopy. *Journal of Molecular Biology, 98*, 17–29. doi:10.1016/s0022-2836(75)80098-2

Bolla, S. R., Hoare, B. S., & Varacallo, M. (2023). Anatomy, Abdomen and Pelvis: Deep Perineal Space. *Anatomy, Abdomen and Pelvis: Deep Perineal Space.* Treasure Island (FL).

Bortolini, M. A., Bilhar, A. P., & Castro, R. A. (2014). Neural control of lower urinary tract and targets for pharmacological therapy. *International Urogynecology Journal, 25*, 1453–1462. doi:10.1007/s00192-014-2452-4

Brandes, R., Lang, F., & Schmidt, R. F. (2019). *Physiologie des Menschen mit Pathophysiologie.* Springer.

Burnett, A. L., Calvin, D. C., Chamness, S. L., Liu, J.-X., Nelson, R. J., Klein, S. L., . . . Snyder, S. H. (1997). Urinary bladder-urethral sphincter dysfunction in mice with targeted disruption of neuronal nitric oxide synthase models idiopathic voiding disorders in humans. *Nature Medicine, 3*, 571–574. doi:10.1038/nm0597-571

Burnstock, G. (1972). Purinergic nerves. *Pharmacological reviews, 24*(3), 509-81.

Burnstock, G. (1976). Purinergic receptors. *Journal of Theoretical Biology, 62*, 491–503. doi:10.1016/0022-5193(76)90133-8

Burnstock, G. (2007). Physiology and Pathophysiology of Purinergic Neurotransmission. *Physiological Reviews, 87*, 659–797. doi:10.1152/physrev.00043.2006

Burnstock, G. (2013). Purinergic signalling in the urinary tract in health and disease. *Purinergic Signalling, 10*, 103–155. doi:10.1007/s11302-013-9395-y

Bylund, D. B., & Gruetter, C. A. (2007). Propranolol. In *xPharm: The Comprehensive Pharmacology Reference* (pp. 1–9). Elsevier. doi:10.1016/b978-008055232-3.62481-x

Carlile, A., Davies, I., Faragher, E., & Brocklehurst, J. C. (1987). The Epithelium in the Female Urethra: A Quantitative Study. *Journal of Urology, 138*, 775–777. doi:10.1016/s0022-5347(17)43369-6

Chess-Williams, R. (2002). Muscarinic receptors of the urinary bladder: detrusor, urothelial and prejunctional. *Autonomic and Autacoid Pharmacology, 22*, 133–145. doi:10.1046/j.1474-8673.2002.00258.x

Ciccarelli, M., Sorriento, D., Coscioni, E., Iaccarino, G., & Santulli, G. (2017). Adrenergic Receptors. In *Endocrinology of the Heart in Health and Disease* (pp. 285–315). Elsevier. doi:10.1016/b978-0-12-803111-7.00011-7

Cirino, G., Sorrentino, R., di Villa Bianca, R. d., Popolo, A., Palmieri, A., Imbimbo, C., . . . Mirone, V. (2003). Involvement of β 3 -adrenergic receptor activation via cyclic GMP- but not NO-dependent mechanisms in human corpus cavernosum function. *Proceedings of the National Academy of Sciences, 100*, 5531–5536. doi:10.1073/pnas.0931347100

Coyne, K. S., Sexton, C. C., Thompson, C. L., Milsom, I., Irwin, D., Kopp, Z. S., . . . Wein, A. J. (2009). The prevalence of lower urinary tract symptoms (LUTS) in the USA, the UK and Sweden: results from the Epidemiology of LUTS (EpiLUTS) study. *BJU International, 104*, 352–360. doi:10.1111/j.1464-410x.2009.08427.x

Creed, K. E., Loxley, R. A., & Phillips, J. K. (2010). Functional expression of muscarinic and purinoceptors in the urinary bladder of male and female rats and guinea pigs. *Journal of Smooth Muscle Research, 46*, 201–215. doi:10.1540/jsmr.46.201

Cruz, Y., & Downie, J. W. (2005). Sexually dimorphic micturition in rats: relationship of perineal muscle activity to voiding pattern. *American Journal of Physiology-Regulatory, Integrative and Comparative Physiology, 289*, R1307–R1318. doi:10.1152/ajpregu.00088.2005

Cuzzo, B., Padala, S. A., & Lappin, S. L. (2023). Physiology, Vasopressin. *Physiology, Vasopressin.* Treasure Island (FL).

Dalghi, M. G., Montalbetti, N., Carattino, M. D., & Apodaca, G. (2020). The Urothelium: Life in a Liquid Environment. *Physiological Reviews, 100*, 1621–1705. doi:10.1152/physrev.00041.2019

de Oliveira, M. G., Alexandre, E. C., Bonilla-Becerra, S. M., Bertollotto, G. M., Justo, A. F., Mónica, F. Z., & Antunes, E. (2019). Autonomic dysregulation at multiple sites is implicated in age-associated underactive bladder in female mice. *Neurourology and Urodynamics, 38*, 1212–1221. doi:10.1002/nau.23990

Ferreira, A., & Duarte Cruz, C. (2021). The urethra in continence and sensation: Neural aspects of urethral function. *Neurourology and Urodynamics, 40*, 744–752. doi:10.1002/nau.24632

Fornai, M. (2005). Role of cyclooxygenases 1 and 2 in the modulation of neuromuscular functions in the distal colon of humans and mice. *Gut, 54*, 608–616. doi:10.1136/gut.2004.053322

Forrest, J. C., & Briskey, E. J. (1967). Response of Striated Muscle to Electrical Stimulation. *Journal of Food Science, 32*, 483–488. doi:10.1111/j.1365-2621.1967.tb00816.x

Förstermann, U., & Sessa, W. C. (2011). Nitric oxide synthases: regulation and function. *European Heart Journal, 33*, 829–837. doi:10.1093/eurheartj/ehr304

Fry, C. H., Meng, E., & Young, J. S. (2010). The physiological function of lower urinary tract smooth muscle. *Autonomic Neuroscience, 154*, 3–13. doi:10.1016/j.autneu.2009.10.006

Griffiths, K., & Madhani, M. (2022). The Use of Wire Myography to Investigate Vascular Tone and Function. In *Atherosclerosis* (pp. 361–376). Springer US. doi:10.1007/978-1-0716-1924-7_23

Hai, C. M., & Murphy, R. A. (1988). Cross-bridge phosphorylation and regulation of latch state in smooth muscle. *American Journal of Physiology-Cell Physiology, 254*, C99–C106. doi:10.1152/ajpcell.1988.254.1.c99

Hernández, M., Barahona, M. V., Recio, P., Benedito, S., Martínez, A. C., Rivera, L., . . . Orensanz, L. M. (2006). Neuronal and smooth muscle receptors involved in the PACAP- and VIP-induced relaxations of the pig urinary bladder neck. *British Journal of Pharmacology, 149*, 100–109. doi:10.1038/sj.bjp.0706832

Holstein, A. F., Davidoff, M. S., Breucker, H., Countouris, N., & Orlandini, G. (1991). Different epithelia in the distal human male urethra. *Cell and Tissue Research, 264*, 23–32. doi:10.1007/bf00305719

Hosokawa, H., & Kaseda, M. (1993). EXPERIMENTAL STUDIES ON VIP AS NON-CHOLINERGIC AND NON-ADRENERGIC NEUROTRANSMITTER IN BLADDER NECK AND POSTERIOR URETHRA. *The Japanese Journal of Urology, 84*, 440–449. doi:10.5980/jpnjurol1989.84.440

Irwin, D. E., Milsom, I., Hunskaar, S., Reilly, K., Kopp, Z., Herschorn, S., . . . Abrams, P. (2006). Population-Based Survey of Urinary Incontinence, Overactive Bladder, and Other Lower Urinary Tract Symptoms in Five Countries: Results of the EPIC Study. *European Urology, 50*, 1306–1315. doi:10.1016/j.eururo.2006.09.019

Ito, H., Pickering, A. E., Igawa, Y., Kanai, A. J., Fry, C. H., & Drake, M. J. (2017). Muro-Neuro-Urodynamics; a Review of the Functional Assessment of Mouse Lower Urinary Tract Function. *Frontiers in Physiology, 8*. doi:10.3389/fphys.2017.00049

Ito, M., Dabrowska, R., Guerriero, V., & Hartshorne, D. J. (1989). Identification in Turkey Gizzard of an Acidic Protein Related to the C-terminal Portion of Smooth Muscle Myosin Light Chain Kinase. *Journal of Biological Chemistry, 264*, 13971–13974. doi:10.1016/s0021-9258(18)71627-x

Jung, J., Ahn, H. K., & Huh, Y. (2012). Clinical and Functional Anatomy of the Urethral Sphincter. *International Neurourology Journal, 16*, 102. doi:10.5213/inj.2012.16.3.102

Kang, L., Li, S., Xing, Z., Li, J., Su, Y., Fan, P., . . . Cui, H. (2014). Dihydrotestosterone treatment delays the conversion from mild cognitive impairment to Alzheimer's disease in SAMP8 mice. *Hormones and Behavior, 65*, 505–515. doi:10.1016/j.yhbeh.2014.03.017

Keller, J. A., Chen, J., Simpson, S., Wang, E. H.-J., Lilascharoen, V., George, O., . . . Stowers, L. (2018). Voluntary urination control by brainstem neurons that relax the urethral sphincter. *Nature Neuroscience, 21*, 1229–1238. doi:10.1038/s41593-018-0204-3

Khromov, A. S., Momotani, K., Jin, L., Artamonov, M. V., Shannon, J., Eto, M., & Somlyo, A. V. (2012). Molecular Mechanism of Telokin-mediated Disinhibition of Myosin Light Chain Phosphatase and cAMP/cGMP-induced Relaxation of Gastrointestinal Smooth Muscle. *Journal of Biological Chemistry, 287*, 20975–20985. doi:10.1074/jbc.m112.341479

Khromov, A. S., Wang, H., Choudhury, N., McDuffie, M., Herring, B. P., Nakamoto, R., . . . Somlyo, A. V. (2006). Smooth muscle of telokin-deficient mice exhibits increased sensitivity to Ca 2+ and decreased cGMP-induced relaxation. *Proceedings of the National Academy of Sciences, 103*, 2440–2445. doi:10.1073/pnas.0508566103

Kimura, R., Miyazato, M., Ashikari, A., Oshiro, T., & Saito, S. (2018). Age-associated urethral dysfunction in urethane-anesthetized rats. *Neurourology and Urodynamics, 37*, 1313–1319. doi:10.1002/nau.23481

Lee, C. L., Lee, J., Park, J. M., Na, H. S., Shin, J. H., Na, Y. G., & Kim, K. H. (2021). Sophisticated regulation of micturition: review of basic neurourology. *Journal of Exercise Rehabilitation, 17*, 295–307. doi:10.12965/jer.2142594.297

Lee, J. G., Wein, A. J., & Levin, R. M. (1994). Comparative Pharmacology of the Male and Female Rabbit Bladder Neck and Urethra: Involvement of Nitric Oxide. *Pharmacology, 48*, 250–259. doi:10.1159/000139187

Lies, B., Groneberg, D., & Friebe, A. (2013). Correlation of cellular expression with function of NO-sensitive guanylyl cyclase in the murine lower urinary tract. *The Journal of Physiology, 591*, 5365–5375. doi:10.1113/jphysiol.2013.262410

Longhurst, P. A., & Levendusky, M. (2000). Influence of gender and the oestrous cycle on in vitro contractile responses of the rat urinary bladder to cholinergic stimulation. *British Journal of Pharmacology, 131*, 177–184. doi:10.1038/sj.bjp.0703551

Lubomirov, L. T., Jänsch, M. H., Papadopoulos, S., Schroeter, M. M., Metzler, D., Bust, M., . . . Pfitzer, G. (2021). Senescent murine femoral arteries undergo vascular remodelling associated with accelerated stress-induced contractility and reactivity to nitric oxide. *Basic & Clinical Pharmacology & Toxicology, 130*, 70–83. doi:10.1111/bcpt.13675

Lubomirov, L. T., Papadopoulos, S., Pütz, S., Welter, J., Klöckener, T., Weckmüller, K., . . . Pfitzer, G. (2016). Aging-related alterations in eNOS and nNOS responsiveness and smooth muscle reactivity of murine basilar arteries are modulated by apocynin and phosphorylation of myosin phosphatase targeting subunit-1. *Journal of Cerebral Blood Flow & Metabolism, 37*, 1014–1029. doi:10.1177/0271678x16649402

Matsui, M., Motomura, D., Karasawa, H., Fujikawa, T., Jiang, J., Komiya, Y., . . . Taketo, M. M. (2000). Multiple functional defects in peripheral autonomic organs in mice lacking muscarinic acetylcholine receptor gene for the M 3 subtype. *Proceedings of the National Academy of Sciences, 97*, 9579–9584. doi:10.1073/pnas.97.17.9579

Michel, M. C., & Vrydag, W. (2006). α1-, α2- and β-adrenoceptors in the urinary bladder, urethra and prostate. *British Journal of Pharmacology, 147*. doi:10.1038/sj.bjp.0706619

Morita, T., Latifpour, J., O'Hollaren, B., Wheeler, M. A., & Weiss, R. M. (1987). Sex differences in function and distribution of alpha 1- and alpha 2-adrenoceptors in rabbit urethra. *American Journal of Physiology-Renal Physiology, 252*, F1124–F1128. doi:10.1152/ajprenal.1987.252.6.f1124

Morita, T., Masuda, H., Tosaka, A., Ishizaka, K., Tsujii, T., & Kondo, S. (1998). SEX DIFFERENCES IN FUNCTION AND DISTRIBUTION OF beta-ADRENOCEPTORS IN RABBIT URINARY BLADDER. *Journal of Urology, 159*, 555–558. doi:10.1016/s0022-5347(01)63982-x

Morita, T., Tsujii, T., & Dokita, S. (1992). Regional Difference in Functional Roles of cAMP and cGMP in Lower Urinary Tract Smooth Muscle Contractility. *Urologia Internationalis, 49*, 191–195. doi:10.1159/000282424

Murphy, R. A., Herlihy, J. T., & Megerman, J. (1974). Force-Generating Capacity and Contractile Protein Content of Arterial Smooth Muscle. *The Journal of General Physiology, 64*, 691–705. doi:10.1085/jgp.64.6.691

Paton, D. (1975). *Methods in Pharmacology; volume 3; Smooth Muscle.*

Patra, P. B., & Patra, S. (2013). Sex Differences in the Physiology and Pharmacology of the Lower Urinary Tract. *Current Urology, 6*, 179–188. doi:10.1159/000343536

Persson, K., Pandita, R. K., Aszòdi, A., Ahmad, M., Pfeifer, A., Fässler, R., & Andersson, K.-E. (2000). Functional characteristics of urinary tract smooth muscles in mice lacking cGMP protein kinase type I. *American Journal of Physiology-Regulatory, Integrative and Comparative Physiology, 279*, R1112–R1120. doi:10.1152/ajpregu.2000.279.3.r1112

Pfitzer, G. (2001). Invited Review: Regulation of myosin phosphorylation in smooth muscle. *Journal of Applied Physiology, 91*, 497–503. doi:10.1152/jappl.2001.91.1.497

Pfitzer, G. (2014). Die glatte Muskulatur. In *Löffler/Petrides Biochemie und Pathobiochemie* (pp. 805–816). Springer Berlin Heidelberg. doi:10.1007/978-3-642-17972-3_64

Ponce, F. A. (2014). Electrostimulation. In *Encyclopedia of the Neurological Sciences* (pp. 1110–1111). Elsevier. doi:10.1016/b978-0-12-385157-4.00743-0

Ponglowhapan, S., Church, D. B., & Khalid, M. (2008). Differences in the proportion of collagen and muscle in the canine lower urinary tract with regard to gonadal status and gender. *Theriogenology, 70*, 1516–1524. doi:10.1016/j.theriogenology.2008.06.099

Ponglowhapan, S., Church, D. B., & Khalid, M. (2009). Expression of cyclooxygenase-2 in the canine lower urinary tract with regard to the effects of gonadal status and gender. *Theriogenology, 71*, 1276–1288. doi:10.1016/j.theriogenology.2008.12.021

Prince, M. J., Wu, F., Guo, Y., Gutierrez Robledo, L. M., O'Donnell, M., Sullivan, R., & Yusuf, S. (2015). The burden of disease in older people and implications for health policy and practice. *The Lancet, 385*, 549–562. doi:10.1016/s0140-6736(14)61347-7

Pütz, S., Barthel, L. S., Frohn, M., Metzler, D., Barham, M., Pryymachuk, G., . . . Pfitzer, G. (2021). Caldesmon ablation in mice causes umbilical herniation and alters

contractility of fetal urinary bladder smooth muscle. *Journal of General Physiology, 153*. doi:10.1085/jgp.202012776

Pütz, S., Lubomirov, L. T., & Pfitzer, G. (2009). Regulation of Smooth Muscle Contraction by Small GTPases. *Physiology, 24*, 342–356. doi:10.1152/physiol.00023.2009

Rand, M. J. (1992). NITRERGIC TRANSMISSION: NITRIC OXIDE AS A MEDIATOR OF NON-ADRENERGIC, NON-CHOLINERGIC NEURO-EFFECTOR TRANSMISSION. *Clinical and Experimental Pharmacology and Physiology, 19*, 147–169. doi:10.1111/j.1440-1681.1992.tb00433.x

Saito, M., Wein, A. J., & Levin, R. M. (1993). Effect of partial outlet obstruction on contractility: Comparison between severe and mild obstruction. *Neurourology and Urodynamics, 12*, 573–583. doi:10.1002/nau.1930120610

Sancho, M., Ferrero, J. J., Triguero, D., Torres, M., & Garcia-Pascual, A. (2014). Altered neuronal and endothelial nitric oxide synthase expression in the bladder and urethra of cyclophosphamide-treated rats. *Nitric Oxide, 39*, 8–19. doi:10.1016/j.niox.2014.04.002

Shadrin, I. Y., Khodabukus, A., & Bursac, N. (2016). Striated muscle function, regeneration, and repair. *Cellular and Molecular Life Sciences, 73*, 4175–4202. doi:10.1007/s00018-016-2285-z

Shcherbakova, O., Serebryanaya, D., Postnikov, A., Schroeter, M., Zittrich, S., Noegel, A., . . . Pfitzer, G. (2010). Kinase-related protein/telokin inhibits Ca2+-independent contraction in Triton-skinned guinea pig taenia coli. *Biochemical Journal, 429*, 291–302. doi:10.1042/bj20090819

Shermadou, E. S., Rahman, S., & Leslie, S. W. (2023). Anatomy, Abdomen and Pelvis: Bladder. *Anatomy, Abdomen and Pelvis: Bladder.* Treasure Island (FL).

Sibley, G. N. (1984). A comparison of spontaneous and nerve-mediated activity in bladder muscle from man, pig and rabbit. *The Journal of Physiology, 354*, 431–443. doi:10.1113/jphysiol.1984.sp015386

Sigala, S., Mirabella, G., Peroni, A., Pezzotti, G., Simeone, C., Spano, P., & Cunico, S. C. (2002). Differential gene expression of cholinergic muscarinic receptor subtypes in male and female normal human urinary bladder. *Urology, 60*, 719–725. doi:10.1016/s0090-4295(02)01819-8

Sigala, S., Peroni, A., Mirabella, G., Fornari, S., Palazzolo, F., Pezzotti, G., . . . Spano, P. (2004). Alpha1 adrenoceptor subtypes in human urinary bladder: Sex and regional comparison. *Life Sciences, 76*, 417–427. doi:10.1016/j.lfs.2004.09.008

Somlyo, A. V., & Siegman, M. J. (2012). Smooth Muscle Myocyte Ultrastructure and Contractility. In *Muscle* (pp. 1117–1132). Elsevier. doi:10.1016/b978-0-12-381510-1.00083-1

Sugaya, K., Nishijima, S., Kadekawa, K., Miyazato, M., & Mukouyama, H. (2009). Relationship between lower urinary tract symptoms and urinary ATP in patients with benign prostatic hyperplasia or overactive bladder. *Biomedical Research, 30*, 287–294. doi:10.2220/biomedres.30.287

Takeda, M., Obara, K., Mizusawa, T., Tomita, Y., Arai, K., Tsutsui, T., . . . Nomura, S. (1999). Evidence for beta3-adrenoceptor subtypes in relaxation of the human urinary bladder detrusor: analysis by molecular biological and pharmacological methods. *The Journal of pharmacology and experimental therapeutics, 288*(3), 1367-73.

TAKEDA, T., HOSOKAWA, M., TAKESHITA, S., IRINO, M., HIGUCHI, K., MATSUSHITA, T., . . . SHIMIZU, K. (1981). A new murine model of accelerated senescence. *Mechanisms of Ageing and Development, 17*, 183–194. doi:10.1016/0047-6374(81)90084-1

Tang, D. D. (2008). Intermediate filaments in smooth muscle. *American Journal of Physiology-Cell Physiology, 294*, C869–C878. doi:10.1152/ajpcell.00154.2007

Triguero, D., Lafuente-Sanchis, A., & Garcia-Pascual, A. (2014). Changes in nerve-mediated contractility of the lower urinary tract in a mouse model of premature ageing. *British Journal of Pharmacology, 171*, 1687–1705. doi:10.1111/bph.12567

Unwin, N. (2013). Nicotinic acetylcholine receptor and the structural basis of neuromuscular transmission: insights fromTorpedopostsynaptic membranes. *Quarterly Reviews of Biophysics, 46*, 283–322. doi:10.1017/s0033583513000061

VanBuren, P., Work, S. S., & Warshaw, D. M. (1994). Enhanced force generation by smooth muscle myosin in vitro. *Proceedings of the National Academy of Sciences of the United States of America, 91*(1), 202-5.

Vetterkind, S., & Morgan, K. G. (2012). Regulation of Smooth Muscle Contraction. In *Muscle* (pp. 1173–1180). Elsevier. doi:10.1016/b978-0-12-381510-1.00087-9

Vial, C., & Evans, R. J. (2000). P2X receptor expression in mouse urinary bladder and the requirement of P2X1 receptors for functional P2X receptor responses in the mouse urinary bladder smooth muscle. *British Journal of Pharmacology, 131*, 1489–1495. doi:10.1038/sj.bjp.0703720

Vignozzi, L., Filippi, S., Morelli, A., Comeglio, P., Cellai, I., Sarchielli, E., . . . Maggi, M. (2012). Testosterone/Estradiol Ratio Regulates NO-Induced Bladder Relaxation and Responsiveness to PDE5 Inhibitors. *The Journal of Sexual Medicine, 9*, 3028–3040. doi:10.1111/j.1743-6109.2012.02946.x

Waldeck, K., Ny, L., Persson, K., & Andersson, K.-E. (1998). Mediators and mechanisms of relaxation in rabbit urethral smooth muscle. *British Journal of Pharmacology, 123*, 617–624. doi:10.1038/sj.bjp.0701645

Wang, R., Li, Q., & Tang, D. D. (2006). Role of vimentin in smooth muscle force development. *American Journal of Physiology-Cell Physiology, 291*, C483–C489. doi:10.1152/ajpcell.00097.2006

Waxenbaum, J. A., Reddy, V., & Varacallo, M. (2023). Anatomy, Autonomic Nervous System. *Anatomy, Autonomic Nervous System.* Treasure Island (FL).

Webb, R. C. (2003). SMOOTH MUSCLE CONTRACTION AND RELAXATION. *Advances in Physiology Education, 27*, 201–206. doi:10.1152/advan.00025.2003

Werkström, V., & Andersson, K.-E. (2005). ATP- and adenosine-induced relaxation of the smooth muscle of the pig urethra. *BJU International, 96*, 1386–1391. doi:10.1111/j.1464-410x.2005.05853.x

Winder, M., Tobin, G., Zupančič, D., & Romih, R. (2014). Signalling Molecules in the Urothelium. *BioMed Research International, 2014*, 1–14. doi:10.1155/2014/297295

Wirth, A., & Offermanns, S. (2012). G-Protein-Coupled Receptors in Smooth Muscle. In *Muscle* (pp. 1145–1153). Elsevier. doi:10.1016/b978-0-12-381510-1.00085-5

Wu, X., Haystead, T. A., Nakamoto, R. K., Somlyo, A. V., & Somlyo, A. P. (1998). Acceleration of Myosin Light Chain Dephosphorylation and Relaxation of Smooth Muscle by Telokin. *Journal of Biological Chemistry, 273*, 11362–11369. doi:10.1074/jbc.273.18.11362

Wu, Y., Qi, J., Wu, C., & Rong, W. (2020). Emerging roles of the TRPV4 channel in bladder physiology and dysfunction. *The Journal of Physiology, 599*, 39–47. doi:10.1113/jp279776

Yamaguchi, O. (2002). β3-adrenoceptors in human detrusor muscle. *Urology, 59*, 25–29. doi:10.1016/s0090-4295(01)01635-1

Yang, C. C. (2003). Micturition. In *Encyclopedia of the Neurological Sciences* (pp. 150–152). Elsevier. doi:10.1016/b0-12-226870-9/00226-4

Yano, S., Kiyota, Y., Yamamoto, M., & Watanabe, K. (1995). Pharmacological Features of Non-adrenergic Non-cholinergic (NANC) Relaxation Induced by Electrical Vagal Stimulation in Isolated Mouse Stomach. *Japanese Journal of Pharmacology, 69*, 9–15. doi:10.1254/jjp.69.9

Zeng, J., Ekman, M., Grossi, M., Svensson, D., Nilsson, B.-O., Jiang, C., . . . Swärd, K. (2015). Vasopressin-induced mouse urethral contraction is modulated by caveolin-1. *European Journal of Pharmacology, 750*, 59–65. doi:10.1016/j.ejphar.2015.01.029

7. Appendix

7.1. Table of Figures

7.2. Table of Tables